STUDIES ON ROTATING PACKED DISC BIOREACTOR

THESIS

Submitted in partial fulfillment of the requirements for the degree of

DOCTOR OF PHILOSOPHY

by

ROHIT P KALNAKE

Register No. 155024CH15F09

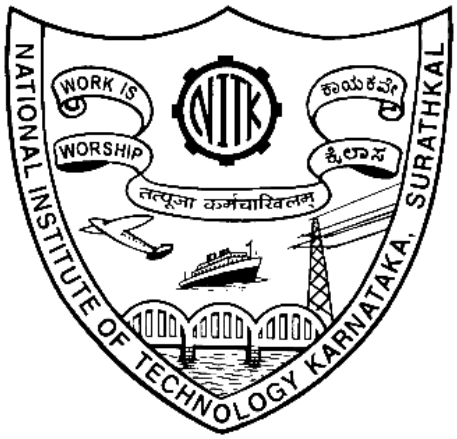

DEPARTMENT OF CHEMICAL ENGINEERING

NATIONAL INSTITUTE OF TECHNOLOGY KARNATAKA,

SURATHKAL, MANGALORE - 575 025

JULY, 2021

D E C L A R A T I O N

I hereby *declare* that the Research Thesis entitled **"STUDIES ON ROTATING PACKED DISC BIOREACTOR"** which is being submitted to the **National Institute of Technology Karnataka, Surathkal** in partial fulfillment of the requirements for the award of the Degree of **Doctor of Philosophy** in Chemical Engineering is a *bonafide report of the research work carried out by me*. The material contained in this Research Thesis has not been submitted to any University or Institution for the award of any degree.

Name: Rohit P Kalnake

Register number: 155024CH15F09

Department of Chemical Engineering

Place: Surathkal

Date: 04-01-2021

C E R T I F I C A T E

This is to *certify* that the Research Thesis entitled **"STUDIES ON ROTATING PACKED DISC BIOREACTOR"** submitted by **ROHIT P KALNAKE (Register Number: 155024CH15F09)** as the record of the research work carried out by him, *is accepted as the Research Thesis submission* in partial fulfillment of the requirements for the award of degree of **Doctor of Philosophy**.

Research Guides

Dr. Keyur Raval
Associate Professor
Department of Chemical Engineering
NITK, Surathkal

Dr. D.V.R. Murthy
Professor (Retd.)
Department of Chemical Engineering
NITK, Surathkal

Chairman- DRPC

A C K N O W L E D G M E N T S

This thesis is developed in years of research that has been undertaken since I came to this prestigious institute, NITK. By that time, I had an opportunity to work with a number of people whose contribution in different ways to the research and the making of the thesis deserves a special mention. It is a pleasure to convey my gratitude to all of them in my humble acknowledgment.

First and foremost, I wish to express my sincere gratitude to my Research Guide, Dr. D.V.R. Murthy, Professor and Dr. Keyur Raval, Associate Professor, Department of Chemical Engineering, NITK Surathkal. Without their valuable guidance, support, enthusiasm and encouragement, I could never finish my Doctoral work. His vast knowledge of chemical engineering and logical way of thinking has been great value for me. I thank him for graciously taking the time to read and offer the required improvements to the manuscripts and thesis. It is not sufficient to express my gratitude with only a few words.

I am extremely thankful to the RPAC committee members, Dr. Arun, M., Associate Professor, Department of Mechanical Engineering and Dr. Vidya Shetty K., Professor, Department of Chemical Engineering, for their valuable advice and suggestions which enabled me to notice the flaws in my research work and make necessary improvements according to their reviews and comments.

I humbly express my sincere gratitude to The Director, NITK Surathkal. I wish to thank our former H.O.D.s Dr. Vidya Shetty K., Professor, Dr. Rajmohan B, Professor, Dr. Hari Mahalingam, Associate professor, and present H. O. D., Dr. Prasanna B.D., Associate Professor, Department of Chemical Engineering, NITK Surathkal for providing me necessary facilities, funding, and support during the phase of this research work. I would also like to thank all the faculty members of the Department of Chemical Engineering, NITK Surathkal for their valuable support and encouragement. I would as well like to express my sincere thanks to Mr. Suresh, Mr. Ramesh, Mr. Harish, Mr. Sukesh, Mrs. Shashikala Mohan, Mr. Sadashiva, Mrs. Thrithila, Mrs. Bhavyashree, and Mrs. Vijetha and all other non-teaching staffs for their helpful suggestions and timely maintenance of the laboratory equipment.

I gratefully acknowledge to my friends Mrs. Amruta S. Shet, Mr. Lister H. Falleiro, Dr. Suman Das, Dr. Sushma Havanur, Mr. Akash Anand, Dr. Rajshekhar, Dr. Kunal, Dr. Harsha, Dr. Vishnu, Mr. Basavaraj S. Nainegali, Mrs. Archana, Mrs. Vrushali Kadam, Mr. Ritesh Sambhare, Miss Priyanka Bhat, Mrs. Diksha Sharma, Mr. Omkar, for their care, support and encouragement.

Rohit P. Kalnake

DEDICATED

TO

MY PARENTS

A B S T R A C T

A novel rotating packed disc bioreactor (RPDB) with the maximum working volume of 65 liter is designed for biological waste water treatment. A hollow disc with radial vanes mounted on the disc was a novel design of this contactor. Stimulus-response experiments were conducted in the contactor to understand liquid mixing behavior under different operating conditions. The recycle stream was also used in the operation of the contactor. The disc design and recycle ratio had marked influence on the mixing behavior. A mathematical model was developed for the flow behavior under recycle and a good agreement was found between the model and experimental results. Moreover, the surface area available in the RPDB was about 4 times more than the surface area available in a standard rotating biological contactor (RBC) operating at similar conditions. The modified design characterized in terms of oxygen volumetric mass transfer coefficient (k_La), in the physical gas–liquid system. The oxygen volumetric mass transfer coefficients (k_La) obtained in this bioreactor are about eight times higher than the similar size of the conventional rotating biological contactors at similar operating conditions. The dimensionless empirical model is developed, by incorporating the operating parameters.

In RPDB, mixed cultures of white-rot fungi (WRF), namely, *P.chrysosporium* and *T.versicolor* are used to degrade reactive black-5 (RB-5) under different rotational speeds as well as recycle ratios. Degradation mechanism of Reactive Black -5 is critically discussed and intermediate products following *P.chrysosporium* and *T.versicolor* are identified using LC-MS. The decolourization efficiency of more than 90% and chemical oxygen demand (COD) reduction of more than 85% was achieved in continuous operation. The recycle stream improved COD reduction by about 15% as compared to that without recycle. The rate of COD removal was 737.9 mg/L/h at 30 rpm and 9.75 recycle ratio in the continuous operation, which is the highest removal rate reported for a synthetic RB-5 effluent in a continuous bioreactor of size 65 liter so far in the literature.

Keywords: Rotating biological contactor (RBC), recycle reactor, stimulus-response experiments, COD

T A B L E O F C O N T E N T

CHAPTER NO.	TITLE	PAGE NO.
	ABSTRACT	i
	TABLE OF CONTENT	iii
	LIST OF FIGURES	vii
	LIST OF TABLES	xi
	LIST OFABBREVATIONS	xiii
	NOMENCLATURE	xv
1	**INTRODUCTION**	1
2	**LITERAURE REVIEW**	7
	2.1. Introduction	7
	2.2. Rotating biological contactor (RBC)	7
	2.3. Characterization of the RBC	8
	2.3.1. Residence time distribution in bioreactor	8
	2.3.2. Oxygen mass transfer	11
	2.3.2.1. Available models for physical oxygen transfer	11
	2.4. Biodegradation in RBCs	14
	2.5. Factor affecting the performance of RBC	15
	2.5.1. Effect of rotation speed	15
	2.5.2. Effect of Hydraulic retention time (HRT)	15
	2.5.3. Effect of Organic and hydraulic loading rates	15
	2.5.4. Effect of recycle ratio	16
	2.5.5. Effect of staging	21
	2.5.6. Effect of disc submergence	22
	2.5.7. Effect of dissolved oxygen content	22
	2.6. Selection of microorganism	23
	2.6.1. Microorganisms degrading Azo dyes	23
	2.6.1.1. Lignin modifying enzymes (LMEs)	27
	2.6.2. Immobilization of microorganisms	28
	2.6.2.1. Dye decolorization by immobilized fungi	34
3	**SCOPE AND OBJECTIVES**	35
4	**RESEARCH METHODOLOGY**	37
	4.1. Materials	37
	4.2. Contractor specifications	37
	4.2.1. Description of the experimental setup	37
	4.3. Mathematical model	42
	4.3.1. Estimation of model parameters	46
	4.4. Oxygen mass transfer studies	47
	4.5. Microorganisms, medium and subculturing	48

CHAPTER NO.	TITLE	PAGE NO.
	4.5.1. Growth and degradation on agar plates	49
	4.5.2. Acclimatization of fungal culture	50
	4.6. Shake flask studies	50
	4.6.1. Dye degradation studies	50
	4.6.2. Acclimatization of fungal culture for bioreactor studies	51
	4.7. Rotating packed disc bioreactor (RPDB) studies	52
	4.8. Qualitative and quantitative analysis	53
	4.8.1. Spectrophotometric analysis	53
	4.8.2. Chemical oxygen demand estimation	54
	4.8.3. Total organic carbon estimation	55
	4.8.4. Adsorbed dye estimation	55
	4.8.5. Biomass (dry weight) estimation	55
	4.8.6. Determination of order of degradation kinetics	55
	4.8.7. Enzyme assay	56
	4.8.7.1. Manganese peroxidase	56
	4.8.7.2. Lignin peroxidase	56
	4.8.7.3. Laccase	57
	4.9. Statistical analysis	57
5	**RESULTS AND DISSCUSSION**	59
	5.1. Introduction	59
	5.1.1. Influence of the number of discs	62
	5.1.2. Influence of rotational speed of discs	64
	5.1.3. Influence of recycle ratio	64
	5.2. Oxygen transfer rate studies	68
	5.2.1. Effect of rotational speed on k_La and oxygen transfer rate	68
	5.2.2. Effect of number of discs on k_La	68
	5.2.3. Effect of recycle feed on the k_La	70
	5.3. Biodegradation of Reactive Black 5	75
	5.3.1. Growth and dye degradation on solid media	75
	5.3.2. Growth and dye degradation in liquid media	76
	5.3.3. Degradation in the shake flask	78
	5.3.3.1. Comparative study of the decolorization of RB-5 by using individual fungal culture *(P.chrysosporium and T.visicolour)* and mixed fungal culture	78
	5.3.3.2. Effect of initial dye degradation	79

CHAPTER NO.	TITLE	PAGE NO.
	5.3.3.3. Degradation pathway of RB-5 by using LC-MS/MS	81
	5.3.3.4. Determination of reaction order for RB-5 degradation	82
	5.3.4. Bioreactor studies	83
	5.3.4.1. Biodegradation studies in batch operation	84
	5.3.4.1.1. Effect of rotational speed	84
	5.3.4.1.2. Effect of recycle stream	85
	5.3.4.2. Continuous treatment of synthetic wastewater in RPDB	88
6	**CONCLUSIONS AND FUTURE SCOPE**	91
	REFERENCES	93
	APPENDICES	119
	RESEARCH PUBLICATIONS	127
	BIO-DATA	129

L I S T O F F I G U R E S

FIGURE NO.	TITLE	PAGE NO
2.1	Schematic representation of film, boundary layer and liquid mixing region within the liquid.	9
2.2	The catalytic cycle of peroxidases	27
2.3	The catalytic cycle of Laccase	28
4.1	Schematic diagram (a) hollow circular disc, (b) horizontal trough with a semi-circular bottom (c) Schematic line diagram of rotating packed disc bioreactor experiment setup.	39, 40
4.2	Shows the diagram of the RTD model system for each stage in the contactor	44
4.3:	The model for estimating the model parameters followed step by step iterative procedure	46
4.4	Schematic representation of the oxygen concentration for the static gassing out method to determine the k_La value	47
4.5	Flow chart of the shake flask studies	51
4.6	Flow chart of the reactor studies	52
5.1	Comparison between model and experimental exit age distributions at varied conditions: a, b) for 32.5L; c, d) for 65L.	60
5.2	Influence of a number of discs on exit age distribution: (a) for 32.5 L; (b) for 65 L.	63
5.3	Influence of rotational speed of discs on exit age distribution: (a) for 32.5 L; (b) for 65 L.	65
5.4	Influence of recycle ratio (R) on exit age distribution: a) for 32.5 L; b) for 65 L.	67

5.5	Effluence of rotational speed and Number of the disc on k_La and oxygen transfer rate (OTR) value for volume 32.5L (a) and 65L (b).	69
5.6	Effluence of recycle stream on k_La value for volume 32.5L (a)and 65L (b). Solid symbols indicate RPDB operation with recycle (58.5 (L/h)) and Open symbols indicate RPDB operation without recycle.	71
5.7	Parity part showing experiment and model predicated value of oxygen volumetric mass transfer coefficient (kLa) with two different recycle ratios. Solid symbols indicate, 58.5 (L/h) recycle stream (■ (10rpm),● (20rpm),▲ (30rpm),▼ (40rpm),◆(50 rpm), and ◀ (60 rpm)), Open symbols indicate, 6 (L/h) recycle ratio (□(10 rpm),○(20 rpm),△(30 rpm),▽(40 rpm),◇(50 rpm), and◁(60 rpm)) and symbols for without recycle (+(10 rpm),×(20 rpm),✳(30 rpm),✯(40 rpm),⊠(50 rpm), and ⊗(60 rpm)).	74
5.8	Dye (30mg/L) degradation by *T. versicolor*, day 1(A) and day 7 (B); *P.chrysosporium* day 1(C) and day 7(D), Mixed culture day 1(E) and day 7(F)	76
5.9	Degradation of dye by *P. chrysosporium* and *T. versicolor* (day 5) (inoculation by discs).	77
5.10	Degradation of RB-5 studies in shake flask: (a) decolorization of RB-5 dye (30,60 and 100mg/L) by using *P. chrysosporium, T. versicolor, and mixed culture.* (b) TOC removal efficiency for different dye concentration (30,60 and 100mg/L) by using *P. chrysosporium, T. versicolor,* and mixed culture.	79
5.11	LiP enzyme activity in the presence of RB-5 dye at 100mg/L	80
5.12	Mass/charge ratios detected for a degraded (by Mixed culture) RB5 sample, post-extraction	82
5.13	Effect of rotational speed on the COD removal (a), DO(b), LiP activity (c), and TOC removal efficiency (d) by using immobilized mixed culture in a batch operation.	86
5.14	Effect of recycle feed and compared without recycle on the COD removal (a), DO (b), LiP activity (c), and TOC removal	87

efficiency(d) by using immobilized mixed culture in a batch operation.

5.15 SEM of immobilized cells on granular activated carbon, the sample from 65 liters, after being fed with 30 mg/L RB-5 dye over a period of 7 days. 88

5.16 Degradation of RB-5 dye: COD removal efficiency and dissolved oxygen concentration for "with recycle" and "without recycle" stream in the continuous operation by using immobilized mixed culture in the RPDB. 89

5.17 Enzymatic activity during continuous experiments in the RPDB with and without recycle stream 90

L I S T O F T A B L E S

TABLE NO.	TITLE	PAGE NO.
1.1	Various treatment methods for dye degradation	2
1.2	Various biofilm processes used for dye wastewater treatment	4
2.1	The effect of rotational speed in the performance of RBC systems for different studies	17
2.2	Presents HRT used for different effluents using RBCs	21
2.3	Bacterial strain used for azo dye degradation	24
2.4	White rot fungus strain used for azo dye degradation	29
2.5	Summarizes the azo dye decolorization by fungi immobilized on different supports	32
4.1	The contractor has the following specifications	38
4.2	Experimental conditions used in this work	42
4.3	Media composition for fungus culture	49
5.1	Experimental parameter for RTD analysis for contactor 32.5 L and 65 L	61
5.2	Comparison of the k_La values reported by different researchers	72
5.3	Kinetics of decolorization of RB-5 under the various concentration	83

A B B R I V A T I O N S

COD	Chemical oxygen demand
DO	Dissolved oxygen
GAC	Granular activated carbon
LC-MS	Liquid chromatography-mass spectrometry
LiP	Lignin Peroxidase
MnP	Manganese Peroxidase
RBC	Rotating Biological Contactor
RMSE	Root mean square error
RTD	Residence time distribution
RPDB	Rotating Packed Disc Bioreactor
SS	Stainless steel
TOC	Total organic carbon

N O M E N C L U A T U R E

A	Total area of gas-liquid interface in the system (m^2)
A_d	Exposed surface area of disc (m^2)
A_t	Surface area of trough (m^2)
C'	Tracer outlet concentration, mg/L
Co	Initial tracer concentration, mg/L
Cm	Tracer concentration at the inlet to first stage, mg/L
Ce	Tracer concentration at the exit of cascade, mg/L
Cn	Tracer concentration from n^{th} stage, mg/L
C	Concentration of species
C^*	Saturation concentration of dissolved oxygen in water (mg-O_2/l)
C_0	Oxygen concentration at equilibrium in water (mg-O_2/l)
D	Diameter of disc (m)
D_L	Diffusivity of oxygen in water (m^2/min)
$E(\theta)$	The distribution function for a residence time
N	Number of discs.
n	Number of discs (Model)
R	Recycle ratio
t	Time, (h)
V	Volume of the trough (m^3)
V_1	Total volume of liquid hold, (m^3)

V	Volume of each stage in the cascade, (m^3)
V_0	Volume of mixing compartment at inlet, (m^3)
Ve	Volume of splitting compartment at outlet, (m^3)
w	Mass of tracer injected as pulse, (mg)
X	Conductivity of tracer, µS/cm
k_L	Overall liquid phase mass transfer coefficient (m./min)
k_La	Oxygen volumetric mass transfer coefficient
v_c	Peripheral velocity of disc (m./min)
v_0	Fresh feed flow rate (m^3/min)
v_m	Volumetric flow rate of mixed feed, l/h
v_r	Recycled feed rate(m^3/min)
v_e	Exit flow rate (m^3/min)
σ^2	Variance or square of the standard deviation (min^2)
ω	Rotational speed of disc (RPM)
δ	Thickness of water film on the disc (m)
μ	Viscosity of water (m^3/s)
ρ	Density of water (kg/m^3)
ϕ	Constant having the dimesions of mass concentration
τ	Ratio of upper region stage volume to the feed flow rate, V/υ_0
τ_0	Ratio of stage volume to the feed flow rate, V_0/υ_0
θ	Dimensionless time, $t/\bar{t}$
$\bar{t}$	Mean residence time of exit age distribution, (1/ min).

α	Fraction of upper mixing volume in each stage in the model.
β	Fraction of cross flow between upper and lower mixing volumes in each stage in the model.

CHAPTER - 1
INTRODUCTION

CHAPTER 1

1. INTRODUCTION

The quality of water, soil, and air are prime issues in the present scenario. Chemicals, which pollute water, soil, and air, create a potential health hazard for any living organism and affect the environment. Pollutants bring about an undesirable change in the atmosphere. (Grover, 2006). The fast depletion of fresh water and a steep increase in the world population, and rapid industrialization has increased the demand for clean drinking water, a prime concern today.

It is practically difficult to dispose of industrial wastewater effluents, especially from the food, pharmaceutical, and textile industries. In addition to the environmental problem, they are consuming a large amount of fresh water in the textile industry's finishing and dyeing operations. Hence, wastewater recycling has been recommended to decrease freshwater intake and its impact on the environment. Approximately 100,000 commercial dyes and dyestuff are used as a coloring agent (cosmetic, leather, textile) industry. Out of which, 10 to 20% of the dyes are discharged in the wastewater (Anliker, 1979; Sarkar et al., 2017). Azo dyes are commonly used dyes in pharmaceutical, textile, cosmetic and food industries (Yamjala et al. 2016; Brüschweiler and Merlot 2017; Šuleková et al. 2017; Guerra et al. 2018;). About 70% of the dyes used are azo dyes, which are toxic and carcinogenic to micro and macro-organisms and their habitats in aquatic and terrestrial ecosystems (Saratale et al., 2009; Ayed et al., 2011; Singh 2014; Sarkar et al., 2017). The degradation of wastewaters from textile industries are technically challenging because of the high chemical stability and toxic nature of the azo dye (Soares et al., 2004; Arregui et al., 2019; Allegre et al., 2006)

Dawood and Sen (2014) discussed (Table 1.1) the advantages and disadvantages of various physical and chemical treatment approaches for dye degradation, such as photocatalyst, membrane filtration, ozonation, adsorption, and ion exchange. Usually, the existing techniques of dye effluent treatments involve an integration of chemical, physical, and biological methods such as coagulation-flocculation, adsorption, chemical oxidation,

microfiltration, electrochemical and membrane filtration followed by activated sludge process (Hai et al. 2007; Sima et al. 2016).

Table 1.1. Various treatment methods for dye degradation (Dawood and Sen, 2014)

Separation Technique	**Advantages**	**Disadvantages**
Physiochemical		
Adsorption	High adsorption capacity for all dyes	The high cost of adsorbents. Need to dispose of adsorbents. Low surface area for some adsorbents
Ion exchange	loss of sorbents less	limited for dispersing dyes.
Membrane filtration	Useful for all dyes with high quality effluent.	Suitable for treating low volume and production of sludge.
Chemical		
Ozonation	No production of sludge.	Half-life is very short (20 min) and operational cost is high.
Photocatalyst	Economically feasible and low operational cost	Produce toxic byproducts after degradation of photocatalyst
Biological		
Aerobic degradation	Efficient in the removal of azo dyes and low operational cost	Prolonged process and provide a suitable environment for the growth of microorganisms
Anaerobic degradation	By-products used as energy sources	Need further treatment under aerobic conditions and yield of methane and hydrogen sulfide

It is challenging to have a single type of effluent treatment method for complete removal of the dye since it is uneconomical and may generate toxic or hazardous by-products. The final biological wastewater treatment of effluent dye is the critical step because the microorganisms used to treat the dye effluent in the final stage are most susceptible to the inhibitory or toxic effects of dyes. There are two basic categories of biological treatment: aerobic and anaerobic. In the anaerobic method, azo dyes biodegrade in aromatic amines and other contaminants, which require further aerobic treatment process.

Aerobic treatment processes are classified into two major types: activated sludge processes and biofilm processes (Wang et al., 2011). In the activated sludge process, microorganisms are freely suspended, which leads to operational problems such as bulking sludge, rising sludge, and foam, which affects the effluent treatment (Metcalf. 2003). Moreover, the activated sludge process is susceptible to washout if there is a variation in hydraulic loading or organic loading in influent. Contrary to the activated sludge process, the biofilm processes anchor the microorganisms on the support matrix. Since a matrix supports microorganisms, the biofilm processes use a small plant footprint and are not as susceptible to variations in effluent quality as the activated sludge process (Wang et al. 2011; Ogugbue et al. 2012).

Rotating biological contactors, fluidized beds, and packed beds are examples of biofilm processes. The advantages and limitations of various biofilm processes are given in **Table 1.2.** It is evident from **Table 1.2** that packed bed and rotating biological contactors are preferred choices because of few disadvantages and relatively low operating costs. Moreover, the comparison between the packed bed and rotating biological contactors indicates that rotating biological contactors are more advantageous in mixing and mass transfer aspects. However, their commercial use is limited to a municipal water treatment facility and effluent treatment where effluent is less hazardous or toxic to microorganisms. Since an active biofilm is only a few mm thick over the rotating disc, arrangements are made to increase the rotating disc's surface area.

Table 1.2. Various biofilm processes used for dye wastewater treatment

Type of reactor	Advantages	Limitations	References
Packed-bed reactor (Size: 300 mL-32 L)	Ease of operation Additional contact between solid and liquid, which increased the high residence time of liquid, High yields are formed due to increased solid/liquid contact. The operation and maintenance, Effective for the removal of pollutants present in very low concentration.	Irregular contact of the mycelium with the effluent, thus the growth of the microorganisms is irregular poor mixing as in packed beds are susceptible to channeling Development of ineffective regions in the reactor over the time course.	(Priya Ak et al. 2001; Senan et al. 2003; Manikandan et al. 2009; Kapdan et al. 2010; Park et al. 1998; Mielgo et al. 2001a)
Fluidized bed reactor (FBR) (Size: 1.5-20 L)	Uniform Particle Mixing and enhances solid and liquid contact interfacial area, which increases its adsorption capacity. Reduction of sludge production give adequate mass and oxygen transfer. Ability to operate a reactor in continuous State, lack of clogging of the biomass	It increased the plant footprint. Pumping Requirements, Particle Entrainment and foaming Difficult to calculate the complex mass and heat flows.	(Zahmatkesh et al. 2010; Balaji and Poongothai 2012; Qiu et al. 2014; Tisa et al. 2014; Aghdasinia et al. 2016)

Type of reactor	Advantages	Limitations	References
	Elimination of limit on liquid flow rates due to decoupling of the residence time of liquid phase and microbial cells		
Rotating Biological Contactors (Size: 1 - 43 L)	Resistance to high hydraulic and organic loadings Provide a large surface area for the development of fixed biological culture Short contact periods are required because of the large active surface They are capable of handling a wide range of flows Well drainable excess sludge collected in the clarifier Short retention time Low power requirements Low sludge production and excellent process control	Frequent maintenance of bio-drum/ biofilm, Oxygen which is supplied into the system by moving the bio-drum is limited The active biofilm layer is only of few millimeters on the matrix surface Difficult replacement of the disc	(Paolini, 1986;Banerjee 1997a; Kapdan et al. 2000; Srikattanaprom, 2000; Ak et al. 2001; Abraham et al. 2003; Patwardhan, 2005; Guimaraes et al. 2005; Sirianuntapiboon, 2006; Di Palma and Verdone, 2009; Pakshirajan et al. 2011; Novotny et al. 2012; Pakshirajan and Kheria, 2012; Mansouri et al. 2012; Hassard et al. 2015; Mathure and Sima et al. 2016; Cortez et al. 2008b).

Furthermore, the active biofilm over the rotating matrix's topmost surface may wash out due to insufficient anchoring on the matrix. Therefore, these contactors are still susceptible to variations in organic/hydraulic loading. These limitations are overcome by improving the design aspects of the rotating contactor. For the above analysis, a novel rotating contactor is designed in this research work that combines the advantages of the packed bed and rotating biological contactors.

CHAPTER - 2
LITERATURE REVIEW

CHAPTER 2:

2. LITERATURE REVIEW

2.1 Introduction

This chapter deals with the extensive discussion on published literature in the field of azo dye degradation in Rotating biological contactor (RBC). The biodegradation pathway of azo dyes and different microorganisms are available for degradation of azo dyes are reported. The degradation of metabolites and kinetics of azo dye is explained. The other solids used for immobilization and different techniques for immobilizations are discussed. As granular activated carbon was used to immobilization the microorganism cells, the dye adsorption equilibrium and kinetic study are reported. In a bioreactor, the substrate is contacted with the microorganisms and designed favorable conditions for the microorganism to grow and remains in the contactor. The different bioreactor is reviewed with their advantages and disadvantages. In this study, a novel bioreactor called "Rotating packed disc contactor" is introduced for its use as a bioreactor.

2.2 Rotating biological contactor:

The rotating biological contactors (RBCs) are more advantageous over the mixing and mass transfer aspects in this introduction. The RBCs are used as a secondary treatment system in wastewater treatment plants, which are vigorous and capable of withstanding at high flow rates in organic loading (Franzini 1980). The rotating disc supports the development of microorganism growth. However, the pilot plant systems used in a later stage for process development; for example, the culture's growth and optimize the operating condition should be scalable. For this reason, it is important to know the established 'rule of thumb' methods used frequently to scale-up and scale-down (Leon et al., 2014; Mansouri et al., 2012). These established methods include scaling based on hydrodynamic characteristics and gas-liquid mass transfer in the reactor (Leon et al., 2013). The use of a particular scale-up method for a specific bioprocess depends on the maximum growth rate, and the process condition of the bioreactor is the question. Because some of the organisms are fast-growing such as *Escherichia coli* and *Vibrio natriegens* (Pei and

Schmidt 2018), which may face oxygen limitation; therefore, scale-up of such bioprocess can be designed based on maximum oxygen transfer rate (OTR) (Patwardhan 2008). Some microorganisms exhibit a very slow growth rate, such as *M. tuberculosis*, *M. leprae*, and *M. smegmatis* (Pei and Schmidt 2018), which are susceptible to shear force (Zhan et al. 2019; Mathure and Patwardhan 2005).

2.3 Characterization of the rotating biological contactors

2.3.1 Residence time distribution (RTD) in bioreactors

The hydrodynamic characteristics in the bioreactors are important for estimating the efficiency of cell cultivation and productivity of results. Mixing plays a very important role in the growth of fungus by controlling the unfavorable pH, temperature, nutrient, and toxin gradients within the bioreactor. Mixing also plays a major role in the distribution of oxygen to all parts of the bioreactor. The poor mixing can affect respiration rate and cell viability due to the formation of dead volume and short-circuiting streams in the reactor (Mansouri et al., 2012; Patwardhan, 2008). For a high-density cell medium, sufficient mixing is required to prevent the cells from settling at the bottom of the reactor, which leads to oxygen and nutrient starvation from limiting cell growth (Fogler 2010; Levenspiel 1999; Metcalf 2003).

The hydrodynamic characteristics of a reactor measured by the tracer method assess the degree to which bioreactor design has been achieved as expected (Fogler 2010; Levenspiel 1999). Several authors determined the hydrodynamic characteristics of the RBC using the residence time distribution (RTD) (Kim et al. 1984; Leon et al. 2014; Raghuraman and Varma 1974; Sima et al. 2012; Banerjee 1997b; Bintaja et al. 1975; Sassi et al. 1996; Taylor et al. 1985). In RBC systems, the liquid film is formed on the disc surface due to its rotation. Further, this liquid film mixes with the bulk of the liquid, thereby generates turbulence in the bulk liquid. The authors reported the critical parameters that affect an RBC's hydrodynamics: flow velocity, point velocity, film thickness, mixing of the film with the bulk liquid, etc. (Leon et al. 2013; Sima et al. 2012). The RTD studies on the RBC identified operating conditions in which the dead volume, channeling of fluid, recycling of fluid, and poor hydraulic loading were observed (Leon et al. 2014; Patwardhan 2003;

Raghuraman and Varma 1974; Mansouri et al., 2012; Šíma et al., 2012a). Various models have been used to describe the extent of the mixing, flow behavior, film thickness, and liquid back-mixing in the RBC(Kim et al. 1984; Leon et al. 2014; Mansouri et al. 2012; Raghuraman and Varma 1974; Šíma et al. 2012a; Zeevalkink et al. 1978).

The single parameter dispersion number, Paclet, and Morrill dispersion index (MDI) were used to explain the flow behavior (Fogler 2010; Levenspiel 1999; Metcalf 2003). According to this model, the axial dispersion affected the ideal plug flow behavior. In this case, flow behavior changed from ideal plug flow (dispersion number = 0) to the ideal mixed flow (dispersion number = ∞). In the biofilm reactor, the diffusion of tracer into and out of the liquid film can affect the RTD experiment curve. As the tracer concentration is high, diffusion occurs into the film and, when it is low, the diffusion occurs out of the film.

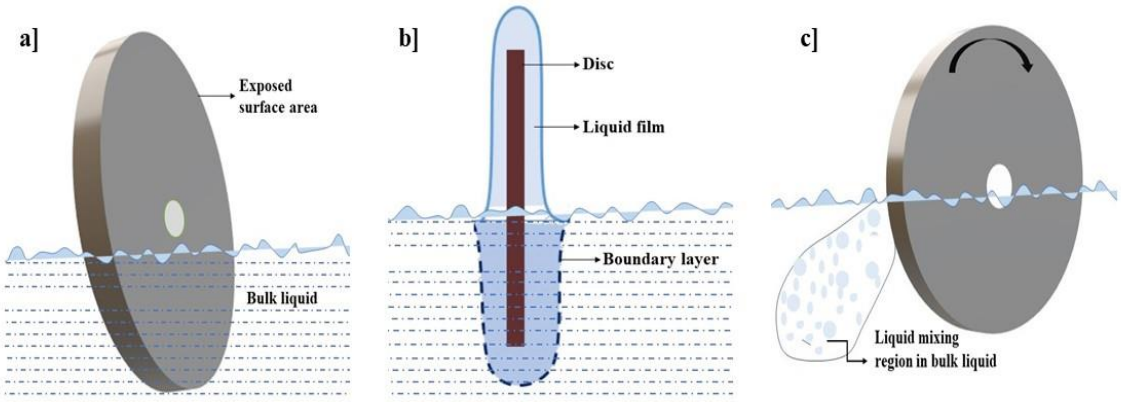

Figure 2.1. Schematic representation of the film, boundary layer, and liquid mixing region within the liquid (Suga and Boongorsrang 1983).

This phenomenon explains the tracer output, introducing the long tail (Kim et al. 1984; Teixeira et al. 2001). The tracer's diffusion characteristics into and out of the liquid film defined by (Bintaja et al. 1975; Suga and Boongorsrang 1983; Taylor et al. 1985; Yamane and Yoshida 1972; Zeevalkink et al. 1978). Bintaja et al. (1975) and Yamane and Yoshida (1972) demonstrated that as the disc moves upward, the liquid film form on the disc surface and is stripped off and mixes with the bulk liquid as soon as the disc re-enters the bulk liquid. Zeevalkink et al. (1978) developed a correlation between liquid and solid called

average film thickness (δ) considering the above phenomenon. Suga and Boongorsrang (1983) assumed that when the disc re-enters into the bulk liquid, a boundary layer is formed on the disc surface by mixing the film with the bulk liquid. The film thickness and boundary layer formation on the disc surface is shown schematically in Figure 2.1. Taylor et al. 1985 suggested that the film thickness variation is due to some forces such as centrifugal forces, gravitational forces, shear force, and surface tension. Some authors suggested that both the discs behave as a centrifuge. The liquid rotates between the boundary layer at a constant angular velocity, and radial and axial flow results outside the boundary layer.

Kim et al. (1984a) used the four-parameter model to explain the degree of axial mixing in the rector. The model considered two mixed regions (upper and lower mixing region with their volume fraction), the crossflow between them, and a dead volume. Mansouri et al. (2012) analyzed hydraulic residence time distribution using a central composite face-centered design with four parameters. The four parameters considered were a deviation from ideal retention time ($\Delta\tau$), dead volume percentage, dispersion index (Morrill dispersion index (MDI), and dispersion number, which were computed as a response by changing the hydraulic retention time and rotational speed. They concluded that as the rotational speed increased dispersion number increased as a result RBC behaved more like a mixed regime with axial dispersion rather than being the plug flow regimes. Šíma et al. (2012a) investigated the mean residence time distribution and the parameter of the gamma distribution model and the model of a stirred tank in series with the back-flow. Their results indicated that the gamma distribution model with the number of the stirred tank in series as a parameter showed a well-mixed regime in the reactor. Leon et al. (2014) describe the reactor model based on single-phase RTD measurement in a multistage horizontal rotating foam stirrer reactor. The model consisted of the stirred tank in series with back-flow and dead volume. The parameters showed that the reactor behaved like a plug flow when six stages were used. All the above authors suggested further improvement in the reactor design to reduce the dead volume and improve mixing in the reactor in terms of residence time distribution studies.

2.3.2 Oxygen mass transfer

In anaerobic bioprocess, the overall rate of substrate conversion is controlled by the biochemical reactions' kinetics. Oxygen the least soluble of all medium components used in a bioprocess, and microorganisms use it for growth, maintenance, metabolite production, and shortage of oxygen, affect performance (Garcia-Ochoa and Gomez 2009; Mathure and Patwardhan 2005).

In a rotating biological contactor (RBC), the disc rotates upward direction; it carries the liquid and forms a liquid film on the disc surface. This liquid film comes in contact with the atmosphere while rotation and oxygen transfer occurs into the film through diffusion (Matias et al., 2017; Di Palma and Verdone 2009). In the presence of biofilm, oxygen further diffuses into the biofilm, where it is used to degrade toxic chemicals from the wastewater (Li et al., 2019; Patwardhan 2003). However, excess attached biomass blocked the transmission pores between oxygen and substrate, resulting in low mass transfer rate, low biological activity, and high effluent suspended biomass that affects the process's performance (Chern et al. 2001; Hassard et al. 2015). This limitation can be overcome by renewing the liquid film so that oxygen transfer is more efficient in the bulk liquid. Thus, it is important to understand the hydrodynamic parameters that affect the water's liquid film thickness on the disc. The mass transfer rate or overall mass transfer coefficient (k_L) in various RBCs have been investigated, and empirical and theoretical models are proposed for estimation (Kim and Molof 1982; Kubsad et al. 2004a; Zeevalkink et al. 1979; Chavan and Mukherji 2008; Monayerie et al. 2012).

2.3.2.1 Available models for oxygen transfer

Yamane and Yoshida (1972) used a theoretical approach to solve the differential oxygen diffusion equation applied to a liquid film covering a disc. As the fully theoretical approach is very complex, the other authors relied on other empirical and dimensional data interpretation analyses. Friedman et al. (1979) considering the rotational speed (ω) of the disc to develop a simple empirical model given in equation 2.1.

$$\ln k_L = 1.31 \ln\omega + 14.78 \qquad (2.1)$$

Where k_L was represented as 10^{-6} m/s, and that of ω was represented RPM.

Ouano (1978) introduced Reynold's number as a dimensional group, which is well known for the scale-up parameter. It is well recognized that oxygen mass transfer is a function of the turbulence generated by the operating parameter. Further, the dimensional analysis model to estimate overall oxygen mass transfer coefficient (k_L) in RBCs was performed, and the following model has proposed equation. 2.2.

$$k_L = \frac{V/A}{DL} = k\left(\frac{A}{A_p}\right)^a \left(\frac{D^2}{u}\omega \cdot \rho\right)^b \quad (2.2)$$

Where *k* was proportionality constant, *V* was reactor working volume; A was a total area of the gas-liquid interface in the system, D_L was molecular diffusion coefficient, density of the liquid (ρ), absolute viscosity of the liquid (*m*), area of the disc (*Ap*) and is $D^2*\omega*\rho/\mu$ corresponding to Reynolds number. Sant' Anna (1980) proposed a modified version of the Ouano model discussed in equation 2.3. In this model, additional dimensional groups were included for better agreement with the experimental values of the mass transfer coefficient,

$$k_L \frac{D}{D_L} = s_h = k\left(\frac{w \cdot D^2 \rho}{u}\right)^a \left(\frac{w^2 D}{g}\right)^b \left(\frac{D - D_0}{D}\right)^C \quad (2.3)$$

$Sh = k.Re^a\ Fr^b\ YI^c$;

Where *Sh*, *Re*, and *Fr* were dimensional groups, and *YI* was the immersion factor. The parameter (*k*, *a*, *b*, and *c*) obtain by Sant' Anna (1980) are different from Boumansour and Vasel (1998) estimated using Sant' Anna model by using their experimental data and they concluded that the values were obtained from Sant'Anna (1980) were not significant.

Some researchers have considered the liquid film formed on the surface of disc to be mainly responsible for oxygen transfer in RBCs. Therefore, in the model of mass transfer coefficient proposed by Bintanja et al. (1975), it was expected that the discs enter a water film of uniform thickness *(δ)* that was combined with the bulk of water in the trough after the end of the revolution. For the contact between air and the water film during one revolution, a mean contact time, t_R, was defined, which depends on the angular velocity and immersion depth. The velocity of the film was presumed the same as the velocity of

the disc. Further, Zeevalkink et al. (1979) explained Bintanja et al. (1975) model, considering the film thickness *(δ)* as a function of the vertical component of peripheral velocity (V_c) of the disc for proper mixing in the trough.

Zeevalkink et al. (1978) obtained the liquid film thickness *(δ)* on a disc of RBC by solving the Navier–Stokes equation and gives the following equation 2.4.

$$\delta = 1.2\ (V_c)^{1.5}\ (10^{-4}\text{m}) \qquad (2.4)$$

Equation. 2.4 was further used to determine the volume renewal number used in the Kim and molof (1982) empirical model. Kim and Molof (1982) Suggested that the mass transfer coefficient was significantly affected by the volume renewal number (*Nv*, 1/min) dependent on the rotational speed *(ω),* disc diameter *(D),* and spacing between the discs (ϕ/2) given in equation 2.5. Later on, this number redefined by Kubsad et al. (2004) by adding parameters such as a number of discs *(n),* working volume *(V),* and total disc surface area exposed to air to incorporating with volume renewal number (*Nv*) was shown in equation 2.6.

$$\text{Nv} = 1.697\text{A n } \omega^{1.5} \phi^{0.5}/\text{V} \qquad (2.5)$$

$$k_L a = 0.02\ (\text{Nv})^{0.36} \qquad (2.6)$$

Chavan and Mukherji (2008), Proposed two dimensionless models for the prediction of oxygen transfer coefficient in RBCs. One of the proposed model expressions estimates the mass transfer coefficient ($k_L a$) due to turbulence shown in equation 2.7. That was correlated with design and operating parameters such as diameter of the disc (*D*), exposed surface area of discs (A_d), rotational speed (ω), cross-sectional area of the tank (*At*), density (ρ), and viscosity (μ) of water. In contrast, another model expression was correlated with all the above parameters along with the thickness of the water film (δ) and a working volume of the reactor (*V*), as showed in equation 2.8.

$$\left(\frac{k_L a\ \rho A_d}{\mu}\right) = \left(\frac{D}{A_d^{0.5}}\right)^a \left(\frac{\rho\ A_d \omega}{\mu}\right)^b \left(\frac{A_d}{A_t}\right)^c \text{.....(2.7)}$$

$$\left(\frac{k_L a\ \rho A_d}{\mu}\right) = \left(\frac{D}{A_d^{0.5}}\right)^a \left(\frac{\rho\ A_d \omega}{\mu}\right)^b \left(\frac{A_d}{A_t}\right)^c \left(\frac{\delta}{V^{\frac{1}{3}}}\right)^d \text{.....(2.8)}$$

All the above model studies reported that formed different groups of variables by using various design and operating parameters. Analyzed these groups' effect to obtain the best agreement between the experimental and model-projected values of k_La.

2.4 Biodegradation in RBCs:

Doman first used the rotating biological contactor in 1929. He used a series of partially submerged discs rotating at 0.5 rpm. The effluent's retention time was 2.4 h, and the maximum film thickness was less than 0.8 mm. The author achieved maximum BOD_5 removal of 28%. The first commercialization report of RBC for municipal water treatment came from Germany in 1959. Extensive research is done on the application and design aspects of RBCs in the past fifty years for municipal water treatment and high BOD containing effluents such as dairy waste. Recently, (Patwardhan 2003; Cortez et al. 2008b, Hassard et al. 2015b) critically analyzed RBCs in their review article and reported the following important aspects.

- Discs submergence is optimum at 40- 45% level. Submergence above 50% decreased the oxygen transfers in the bioreactor.
- Optimum rotational speeds should be 1–10 rpm for discs with 1–4 m diameter mounted on shafts around 5–10 m long.
- Space between discs was advisable.
- The optimum staging was recommended for maximizing removal.

The major factors affecting RBC's performance are speed of rotation, dissolved oxygen level, hydraulic loading rates, hydraulic retention time (HRT), and disc submergence. Each factor is discussed in detail below.

2.5 Factor affecting the performance of RBC

2.5.1 Effect of rotation speed

The disc's rotational speed is a critical operational parameter for the reactor hydrodynamics' efficiency, oxygen mass transfers from air to the liquid inside the trough. Tables 2.1 demonstrate the influence of the rotational speed of the RBC on water treatment. Leon et al. (2014) reported that the exchange rate increases in the stagnant region within the RPM

limiting up to 450 rpm. As a result, the dead volume decreased. Kim et al. (1984) suggested that disc edge, trough wall, and free surface in a vessel contributed the majority in mixing behaviors for the change in disc speed. Patwardhan (2003), Hassard et al. (2015), and Di Palma and Verdone (2009) reported on oxygen transfer rate with increases in the rotation speed of the discs. However, for discs attached to the biofilm, rotational speed beyond critical point was detrimental as reported by Ramsay et al. (2006); as the biofilm is washed out, this effluent's degradation rate reduces. Similarly, studies were reported by (Gupta and Gupta 2001; Israni et al. 2002; Malachova et al. 2013; Nahid et al. 2001; Najafpour et al. 2005), for biodegradation of effluent waste.

2.5.2 Effect of hydraulic retention time (HRT)

Studies reported that increasing the HRT, improve the diffusion of the substrate into the biofilm, followed by its subsequent degradation (Hanhan et al. 2005; Najafpour et al. 2005). Raghuraman and Varma (1974) reported that the liquid interconnected zones' flow rates created turbulence and improved degradation. Pakshirajan et al. (2011) studied the performance of a RBC for azo dye-containing effluent. They reported complete decolorization within 48 h of HRT for wastewater containing dye concentration of 25–200 mg/L. For an above 200 mg/L dye concentration, efficiency marginally reduced to 85% for the same HRT.

2.5.3 Effect of organic and hydraulic loading rates

Alemzadeh and Vossoughi (2001) and Cortez et al. (2008b) explained that in RBC, increasing the organic and hydraulic loading caused the problems like excessive biofilm production, reduction of dissolved oxygen, and reduction in liquid retention time. Similarly, (Hassard et al. 2015; Patwardhan 2003) reported that as the hydraulic loads increased at a constant HRT, there was a reduction in COD removal rates, BOD, and nitrogen due to less time of contact with the biofilm as shown in Table 2.1. Banerjee (1997a) investigated the degradation of phenol in an RBC system and observed that an increase in the hydraulic loading lead to an increase in the phenol removal rate, but phenol removal efficiency decreased.

2.5.4 Effect of recycle ratio

Recirculation in the RBC system is used to improve overall efficiency. It gives the extra aeration that influences the DO concentration and hydraulic loading rate of the system. Studied the effect of recirculation in the RBC system to treat various wastewaters. (Confer and Logan 1998) suggested that the recirculation helps to returned settled solid aid bacteria and other associate biomass which carried extracellular enzymes that could help break down complex polymers. (Ayoub and Saikaly 2004) showed that the Positive effect of recirculation was attributed to the dilution of influent organic concentration to the RBC system or used to improve overall performance in removing COD and BOD and improving effluent DO concentration in the system. Klees (1992) reported that, with increasing recirculation ratio improved removal efficiencies in COD, BOD, and NH_3–N. A recent study investigated the changes in the mode of recirculation seemed not a marked effect on the overall removal (Calvin. P.C.Poon, 1979; G.M.Ayaub et al. 2004).

Table 2.1.: The effect of rotational speed in the performance of RBC systems for different studies

Reactor specifications			Type of wastewater	Rotational speed	Performance	References
Type of material	**Dimensions**	**Submergence (%)**				
Stainless steel discs covered with cloth	Diameter - 0.09 m	50	Synthetic phenolic wastewater	40 - 175 rpm	At 40 rpm - 30.9 mg phenol removed/dm^3. At 150 rpm - 114 mg phenol removed/dm^3	(Israni et al. 2002)
Lightweight clear plastic discs	Diameter - 0.35 m	54	Food cannery wastewater	3 and 11 rpm	At 3 rpm - 62.67% SCOD removed At 11 rpm - 93.70% SCOD removed	(Najafpour et al. 2005)
Propylene Pall rings	Diameter - 2.54 cm	40	Baker's yeast wastewater	15 and 17 rpm	At 15 rpm - 77% COD removed. At 17 rpm - 78% COD removed	(Nahid et al. 2001)

Reactor specifications			Type of wastewater	Rotational speed	Performance	References
Type of material	**Dimensions**	**Submergence (%)**				
Acrylic discs	Diameter - 0.25 m	32	Municipal wastewater	5 rpm	At HRT = 24 h and At hydraulic liquid rate = 20 dm^3/ m^2 d, Initial feed 20 g COD/ m^2 d and 2.2 g N/m2 d, Out of which, 19.4 g COD/ m^2 d removed in the 1st stage and 1.1 g N/m^2 d,	(Gupta and Gupta 2001)
Propylene square rings	Diameter - 68 mm	40	Synthetic wastewater (food industry)	3 rpm	Initial feed rate 2.04 g BOD_5/ m^2 d and 0.6 g BOD_5/dm^3d After treatment 92.5% BOD_5 removal achieved;	(Sirianuntapiboon 2006

Reactor specifications			Type of wastewater	Rotational speed	Performance	References
Type of material	**Dimensions**	**Submergence (%)**				
Rigid polyethylene discs	Diameter - 0.5 m	37	Industrial wastewater	8 and 11 rpm	At 11 rpm OLR of 5.3 ± 2.9 mg $SBOD_5$/ m^2 d, with an $SBOD_5$ removal efficiency was 76, 75 and 85% for COD, BOD_5 and $SBOD_5$ respectively.	(Ayoob Torkian, K. Alinejad 2015)
Wood disc	----	------	Synthetic dye	20 rpm	For 50 and 100 mg/L concentration 96% decolourization. At: 200mg/L, 81% is the highest decolourization	(Axelsson et al. 2006)
Mild steel	2-5 mm in thickness, 30 cm in diameter	28 %	Industrial dye wastewater	1-2 rpm	At: lower feed concentration (0.51-36 mg/L), more than 70% degradation. (HRT various from 1 to 73 hr)	(Abraham et al. 2003)

Reactor specifications			Type of wastewater	Rotational speed	Performance	References
Type of material	**Dimensions**	**Submergence (%)**				
Polyurethane foam (PUF)	8 cm in diameter, 1cm thick	40%	Industrial dye wastewater	2 rpm	At 150 mg/L, complete degradation within 20 days	(Malachova et al. 2013)
Plastic	0.1 m	60,50 and 40 %	sugar effluent and dairy effluent	6 rpm	For 0.0083 kg COD/ m^2/day, 91.66% removal sugar effluent 0.0025 kg COD/ m^2/day, 87.57% removal dairy effluent.	(Selvakumar and Kumar 2007)
stainless steel	21 cm in diameter and 3 mm in thickness	40%	artificial wastewater	15 rpm	For 1.56 to 10.6 g COD/m^2/day From 1.56 to 4.05 g COD/m^2/day removal efficiency increases. 4.05 to 10.6 g COD/m^2/day removal efficiency reduces.	(Alemzadeh and Vossoughi 2001)
polyurethane foam	--------	50%	synthetic Polycyclic aromatic hydrocarbons (PAH)	5 to 30 rpm	PAH removal was greater than 90% after 60 h	(Zheng and Obbard 2002)

These studies indicate that rotational speed has a marked influence on the degradation rate.

Table.2.2.: Presents HRT used for different effluents using RBCs (Hassard et al. 2015)

Organic pollutant	Initial pollutant concentration, mg L^{-1}	Degrading species/consortia	Removal efficiency (%)	HRT (d)
Benzene	1193	Pseudomonas sp., Bacillus, Enterococcus sp.	97.7	1.23
Xylene	1226	Pseudomonas sp., Bacillus, Enterococcus sp.	98.5	1.23
Phenol	250	Exiguobacterium aurantiacum	48.4	1.00
Pyridine	280	E. aurantiacum	34.2	0.50
Quinoline	280	E. aurantiacum	48.9	0.50
Benzol(α)pyrene	0.21	Phanerochaete chrysosporium	96.9	11.72
Trichloroethylene	30	Mixed culture (MC) augmented with Thiosphaera pantotropha	98.7	2
Mn	45	Ulothrix sp.	36.7	1
Cu	100	Ulothrix sp.	38	1
Cu	100	Activated sludge consortium enriched by metal spiking	59	1
Zn	100	Activated sludge consortium enriched by metal spiking	84	1

2.5.5 Effect of staging

Staging provides enhanced capability to manage shock loads providing the biomass as a catalytic activity with sufficient substrate and improving removal rate and process stability. At high effluent treatment value and higher organic loading, the staging was recommended in the RBC system (Radwan and Ramanujam 1997; Banerjee 1997a). The mixing decrease

gradually along the reactor, and the system behaves as the plug flow system to avoid this situation in RBC and staging use. Tawfik et al. (2006) suggested that using staging in the RBC system, the concentration of COD and the *Escherichia coli* was lower in the final effluent of a two-stage than the single-stage. Moreover, in a two-stage system, the nitrification efficiency was shown higher compared to the one-stage system. Andreadakis (1987) assumed each stage of his RBC system was well mixed. The study showed that the system's efficiency was insignificant beyond four stages due to the decrease of the total area for constant influent substrate concentration (BOD5) and effluent substrate concentration (BOD5) as the number of stages increases. Enayathali and Kumar (2012) studied two stages of RBC for treating grey wastewater. The experiment was conducted at various influent loading of COD and rotational speed from 4.5 to 6, and the maximum treatment efficiency was 95.04% and 94.96%, respectively. Based on COD and other effluent concentrations, staging calculations can be done using literature with the appropriate adaptations.

2.5.6 Effect of disc submergence

The percentage of RBC medium submergence influences the microorganisms' oxygen availability and microorganisms' contact time to the substrate. Cortez et al. (2008) Studied that increased submergence of the RBC unit decreased the degradation rate. Moreover, 40% submergence used for municipal wastewater was insufficient for nutrient removal, and submergence had to increase to 60%. Reports are providing additional air drive if submergence increased above 70%. Nahid et al. (2001) found the biofilm growth over the RBC's disc surface; the internal biofilm was growing anaerobically while the external biofilm was growing aerobically. These reduced the overall degradation rate, which could be overcome by providing a large surface area that increased RBC degradation (Patwardhan 2003).

2.5.7 Effect of dissolved oxygen concentration

In most aerobic RBC systems, the dissolved oxygen is necessary to grow biofilms on the discs. Discs with the biofilm are partially submerged in wastewater and partially exposed

to the air. Oxygen is absorbed in the liquid film and over the biofilm surface during disc rotation (Grady 1982). In the biofilm growth stage, the oxygen concentration reaches a minimum level and, as increased along with the reactor substrate concentration, was low. As the rotational speed increased at a particular submergence level, the RBC's oxygen transfer capacity increased (Rodgers and Zhan 2003). As submergence increased at a constant rotational speed, the oxygen transfer rate decreased (Mathure and Patwardhan 2005).

In the late 1960s, concentrations of oxygen above 100% air saturation were documented to cause metabolism inhibition and microorganisms' respiration (Antonino 2004). Numerous literature reports have demonstrated that the oxygen transfer rate often limits the overall reaction rate; it controls the enzyme activity growths, which depend on the proteins and lipids present called reactive oxygen species. Welch (1968) presented data showing a considerable decline of treatment efficiency when operational DO concentration dropped below 1.5 mg/L for his operating conditions of 500 mg/L COD and 30 minutes retention time. Weng and Molof (1974) investigated the six-stage laboratory reactor and found that nitrification took place only in the stages where DO was greater than about 2 mg/L

2.6 Selection of microorganism

2.6.1 Microorganisms degrading azo dyes

Several studies reported that for partial and complete degradation of an azo dye, a wide range of microorganisms is found to reduce these compounds, such as bacteria, yeast, algae, and fungi. Different bacteria groups degrade azo dyes under conventional anaerobic and aerobic conditions. The reductive cleavage of azo bonds (–N = N–) degraded using the microbial mechanism with the help of azoreductase enzymes under anaerobic conditions that contained hazardous-aromatic amines (Chang et al., 2000; Van der Zee and Villaverde, 2005; Saratale et al., 2011). Removal of azo dyes by bacterial strain requires energy, and therefore extra organic source is provided for degradation (Pandey et al. 2007). Only a few bacteria can grow on azo dyes as the source of carbon (Erkurt, 2010). Extensive studies was carried out to determine the effective degradation of azo dyes through the various groups of bacteria (Pandey et al., 2007; Erkurt, 2010; Saratale et al., 2011). Several studies

also demonstrated a trial or wide-range of degradation of reactive azo dyes by single and mixed bacterial strain summarized in Table 2.3.

Literature shows the very few yeast species like *Issatchenkia occidentalis, Candida zeylanoides, Debaryomyces polymorphus, Candida albicans, Candida oleophila, Saccharomyces cerevisiae, and Candida tropicalis* perform putative enzymatic biodegradation and consequent decolorization of different azo dyes (Lucas et al. 2006; Martins et al. 1999; Ramalho et al. 2002, 2004, 2005; Vitor and Corso 2008; Yang et al. 2003). Yeast species like *Kluveromyces marxianus* removed the remazol black B, *Saccharomyces cerevisiae* (MTCC-463) remove Malachite Green, and Methyl Red, *Galactomyces geotrichum* (MTCC 1360) decolorize triphenylmethane, *Trichosporon beigelii* (NCIM-3326) decolorized Navy Blue HER with the enzymatic action and produce toxic byproducts as reported (Jadhav et al. 2007; Jadhav and Govindwar 2006; Meehan et al. 2000; Saratale et al. 2009). *Candida kefyr and Candida catenulata* degrade more than 90% of amaranth by biosorption (Camargo and Corso 2002).

Table 2.3.: Bacterial strain used for azo dye degradation

Bacterial strain	**Dyes**	**Degradation**	**References**
Acinetobacter calcoaceticus NCIM 2890	Direct brown MR		(Ghodake et al. 2009)
Bacillus cereus DC11	Acid Blue 25, Malachite Green, Basic Blue	95-98%	(Deng et al. 2008)
Bacillus fusiformis	Acid Orange 10, Disperse Blue 79	100%	(Kolekar et al. 2008)
Bacillus sp.	Congo red	90-100%	(Gopinath et al. 2009)
Bacillus subtilis HM	Fast Red	99%	(Mabrouk and Yusef 2008)
Bacillus thurengiensis	Acid Red 119	50-60%	(Dave and Dave 2009)
Bacillus velezensis AB	Direct Red 28	-	(Bafana et al. 2008a)

Bacterial strain	Dyes	Degradation	References
Enterococcus gallinarum	Direct Black 38	71-85%	(Bafana et al. 2008b)
Eschericia coli YB	Acid Red 27	75%	(Liu et al. 2009)
Halomonas sp.	Reactive Brilliant Red K, Remazol Black N, Remazol Black, Reactive Brilliant Red X, Acid Black 10B, Acid Scarlet GR, Acid Red B, Sulfonyl Scarlet BNLE, Acid Red G,	70-95%	(Asad et al. 2007; Guo et al. 2008c, b; a)
Pseudomonas luteola, Eschericia coli	Reactive Red 22	-	(Chen et al. 2006)
Pseudomonas luteola	Direct azo dyes, Reactive azo dyes, and leather dyes	59-99%	(Hu 2001)
P. putida, Pseudomonas aeruginosa, P. oleovarons	Methyl Orange, B19, B54, R91, Y87, R90, B69, B15, B36, Y15, R34, B31, Y79, and B86		(Klees and silverstein 1992)
Pseudomonas desmolyticum	Green HE4B , Direct Blue 6, Red HE7B	100%	(Kalme et al. 2009)
Rhodopseudomonas palustris	Reactive Black 5	90%	(Xingzu et al. 2008)

Bacterial strain	Dyes	Degradation	References
Sphingomonas herbicidovorans	Anthraquinone dyes	98%	(Fan et al. 2009)
Shewanella, Aeromonas, Bacillus, Pseudomonas, and Massillia spp.	Acid Red 88, Disperse Orange 3, Direct Red 81, Reactive Black 5		(Khalid et al. 2008a; b)
Klebsiella oxytoca, Citrobacter freundii, Acinotobacter sp.	Disperse Orange 3, Reactive Black 5, Direct Red 81, Acid Red 88		(Khalid et al. 2009)

A review of the literature recommends that algae are able to degrade azo dyes due to its different procedures of assimilative utilization of chromatophores for the production of biomass, CO_2, and H_2O as an end product (Vijayaraghavan and Yun 2007). Several algae species, such as Chlorella and Oscillatoria, can degrade azo dyes and their aromatic amines into simpler organic compounds or CO_2 (Acuner and Dilek 2004). It has been reported that the *Chlorella pyrenoidosa, Chlorella vulgaris,* and *Oscillateria tenuis* decomposed more than 30 azo dye toward simpler aromatic amines (Yan and Pan 2004). Moreover, algae's biosorption process could be implemented as an effective method for dye degradation, and gives the alternative to more costly materials (Banat et al. 1996; Daneshvar et al. 2007). Fungi culture appears to be most appropriate, fast, and efficient in the degradation of various azo dyes and another metallic effluent. The multiple fungi cultures and their lignin modifying enzymes (LME) that are lignin peroxidase (LiP), manganese peroxidase (MnP), and laccase are responsible for the wide range of organic compound degradation (Christian et al., 2005). Literature studies that the azo dye degradation have aimed on fungal culture from white-rot fungi, which was used to develop bioprocesses for the biodegradation of azo dyes (Machado et al., 2006). In white rot fungi most widely studied fungi for azo dye degradation is *Phanerochaete chrysosporium*. Still, others have also received significant consideration, such as, *Aspergillus ochraceus, Trametes (Coriolus) versicolor, species of Pleurotus, Phlebia*, *Bjerkandera adusta,* and a diversity of other fungi (Heinfling et al.,

1998; Pointing and Vrijmoed, 2000; Saratale et al., 2006; Humnabadkar et al., 2008) are shown in Table 2.4.

2.6.1.1 Lignin modifying enzymes (LMEs)

White rot fungi are capable to degrade lignin by evolving a non-specific mechanism. The fungi secrete Ligninolytic enzymes during stress conditions (carbon, nitrogen, or SuLphur nutrient limitation), and these enzymes then degrade the lignin. LMEs being extracellular and non-specific, have been adapted to degrade several pollutants. The extracellular nature of these enzymes enables the fungi to tolerate higher levels of pollutants and further eliminates the requirement of an adaptation period (Barr and Aust 1994). *P. chrysosporium* and *T. versicolor* are well-studied white-rot fungi, and their application in the degradation of environmental pollutants is quite wide.

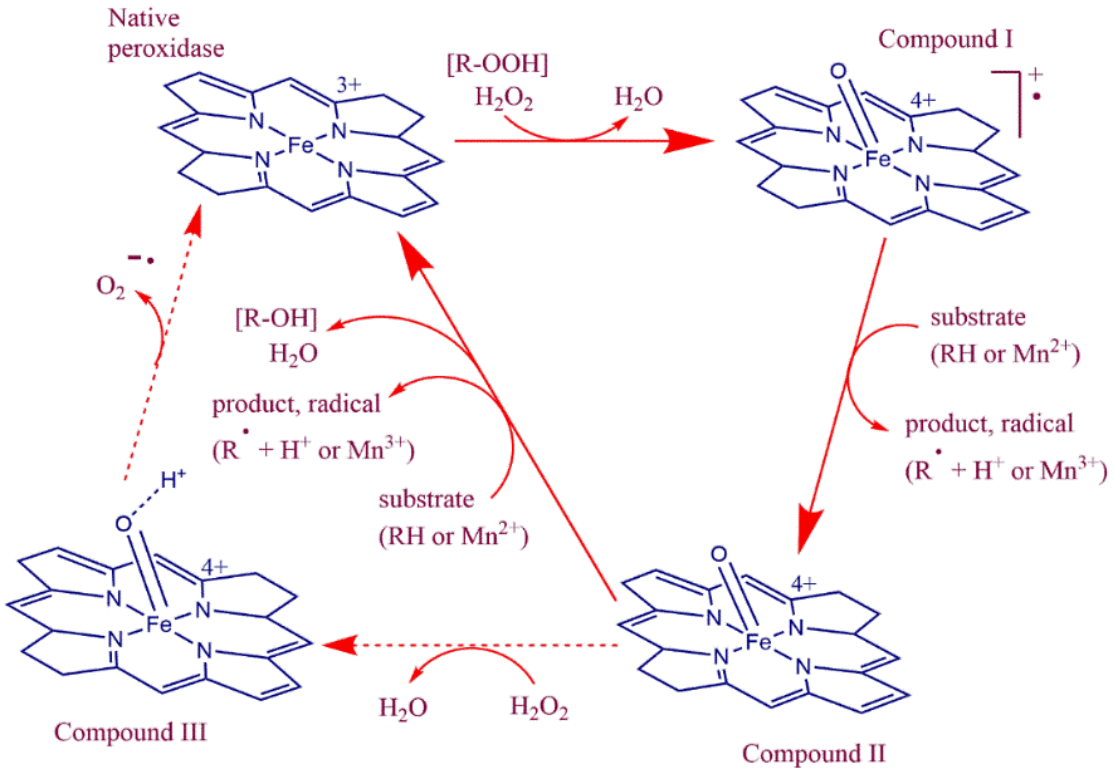

Figure 2.2. The catalytic cycle of peroxidases (Erkurt 2010)

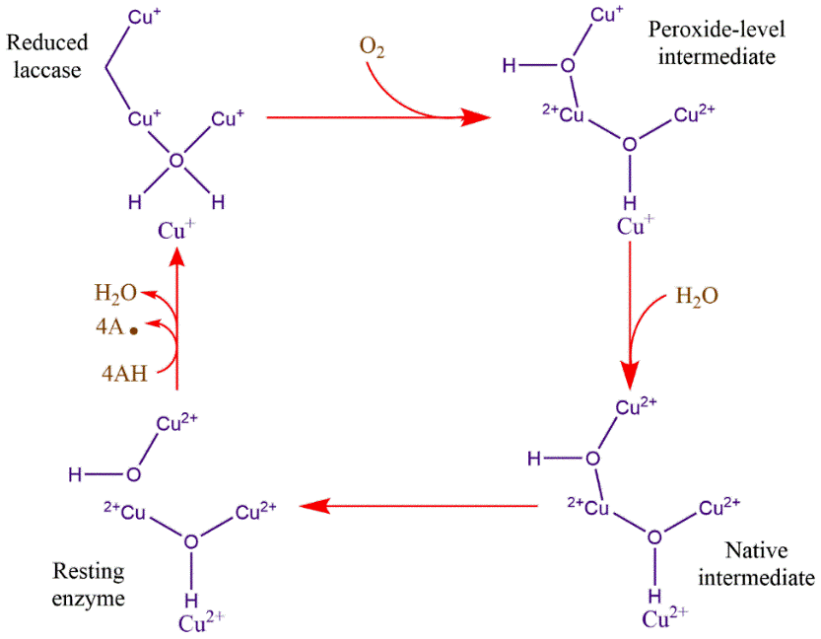

Figure 2.3. The catalytic cycle of Laccase (Erkurt 2010).

Both of these fungi produce oxidoreductases, that is, LiP, and MnP, and Laccase (Erkurt 2010; Wesenberg et al. 2003). These LME catalytic cycles of peroxidase and laccase are given in Figures 2.2 and 2.3, respectively.

2.6.2 Immobilization of microorganisms

In the last two decades, several designs and techniques have been reported to suppress azo dyes by fungi cells used. Immobilization application seems to be more encouraging than those free cells attached within a defined area support material. There are varieties of immobilization methods available (Karel et al. 1985) as "the physical incarceration of intact cells to a certain area of space with preservation of some desired catalytic activity." Mostly two types of cell immobilization are used, such as entrapment and attachment. In the entrapment technique, natural or synthetic polymers have used for cell immobilization (Datta et al. 2013; Markvicheva et al. 1991; Martins et al. 2013).

Table 2.4.: White rot fungus strain used for azo dye degradation

White rot fungus	Enzyme	Dye	Degradation	References
Phanerochaete chrysosporium	LiP LiP and MnP MiP	Amido black 10B Reactive Black 5 Direct Blue 15 Diazo dyes Reactive Brilliant Red K-2BP Amaranth, new coccine, and Orange G	90.3% 95-100% 95-100% 85-89%	(Senthilkumar et al. 2014) (Enayatizamir et al. 2011) (Pazarlioglu et al. 2005) (Pazarlioglu et al. 2005) (Paszczynski et al. 1991) (Martins et al. 2001) (Yu et al. 2006)
Trametes (Coriolus) versicolor	Laccase	Remazol Black B, Congo red, Orange 2, and Acid Orange 6 Reactive Red 198, Reactive Blue 19 Reactive Black 5, Reactive Red 2 Remazol Black B Drimarene Blue	80-100% 77-92.5% 41.2-64.3% 91-99% 70%	(Binupriya et al. 2008) (Aksu et al. 2007) (Legerská et al. 2018) (Borchert and Libra 2001) (Nilsson et al. 2006)

White rot fungus	Enzyme	Dye	Degradation	References
Bjerkandera adusta	LiP, MnP	Reactive Black 5, Reactive Orange 96, Reactive Violet 5, Reactive Blue 15, Reactive Blue 38, Remazol Brilliant Blue R, Reactive Black 5, Reactive Blue 38	40-90% 87%	(Heinfling et al. 1997) (Novotný et al. 2001) (Ammjmatbmsu Heinfling et al., 1998; Annette Heinfling et al., 1998)
Funalia trogii	Laccase	Astrazone Blue Drimarene Blue	75% 75-95%	(Yesilada et al. 2003) (Erkurt et al. 2007)
Phanerochaete sordida	MnP	Reactive Red 120	90.6%	(Harazono et al. 2003)
Pleurotus sajorcaju	Laccase	Amaranth, new coccine, and Orange G Reactive Black 5	96.8-98.5% 62-92%	(Chagas and Durrant 2001), (Murugesan et al. 2007)
Irpex lacteus		Congo Red, Reactive Orange 16, Congo Red, Methyl Red, Reactive Black 5, Black, Chicago Sky Blue, Naphthol Blue	58-100%	(Novotný et al. 2001)

White rot fungus	Enzyme	Dye	Degradation	References
Ganoderma lucidum	Laccase	Reactive Black 5		(Forss and Welander 2009)
Ganoderma sp. WR-1	LiP	Amaranth	100%	(Revankar and Lele 2007)
Ischnoderma resinosum	Laccase	Orange G	94%	(Eichlerová et al. 2005)
Dichomitus squalens	Laccase and MnP	Orange G	95%	(Eichlerová et al. 2005)
Pleurotus calyptratus	Laccase	Orange G	91%	(Eichlerová et al. 2005)
Lentinula edodes	MnP	Amido Black, Trypan Blue, Congo Red	100%	(Boer et al. 2004)
Strain L-25 (newly isolated white-rot fungus)	MnP	Reactive Black 5, Mordant Black 11, Direct-Orange 26, Direct Red 31, Reactive Orange 16, Direct Blue 71, Acid Red 6, Mordant Yellow 3, Acid Orange 56, Mordant Blue 13	84.9-99.6%	(Kariminiaae-Hamedaani et al. 2007)

Some studies reported that the microorganism is entrapped in the agar, alginate, and other polymeric matrixes like gelatin, collagen, and polyvinyl alcohol. (Chang et al. 2000; Daâssi et al. 2013; Enayatizamir et al. 2011; Katzbauer et al. 1995; Norton and D'Amore 1994; Park and Chang 2000). After that, synthetic foams such as nylon polyurethane foam (PuF) or stainless steel sponge have been used for attachment processes (Couto et al. 2004; Flint et al. 1997; Haapala and Linko 1993; Nakamura et al. 1997; Parkar et al. 2001). Other than this, natural supports materials such as wheat straw, jute, hemp, woodchips, and luffa cylindrical sponge have been used to immobilized fungi cells (Erkurt et al. 2007; Rodriguez Couto 2009; Shin et al. 2002; Yum and Peirce 1998). These materials provide then add nutrients and increase their enzymatic activity.

Table 2.5.: Summarizes the azo dye decolorization by fungi immobilized on different supports

Fungus	Azo dye	Support materials	Degradation	References
P. chrysosporium	Diazo dye Red 533	Polyurethane foam (PuF)	>95%	(Yang and Yu 1996)
	Orange II	Alginate beads	90%	(Mielgo et al. 2001)
	Reactive Black 5	Alginate beads	90%	(Urra et al. 2006)
	Acid Orange	Ca-ALG beads	95-100%	(Radha et al. 2005)
	Acid Red 114	ZrOCl2-activated pumice	90%	(Pazarlioglu et al. 2005)
	Congo Red	PuF	93.5%	(Urra et al. 2006)
	Direct Yellow 12	PuF, stainless steel net, polyamide fiber, fiber glass net		(Gao et al. 2008)
	Acid Black 1			
	Reactive Orange 16			
	Basic Blue 41			
	Reactive dye K-2BP			

Fungus	Azo dye	Support materials	Degradation	References
T. versicolor	Acid Violet 7 Amaranth	Activated carbon powder, Maple woodchips Wheat straw, Jute, hemp, Nylon, Polyethylene teraphthalate fibers.	95-100% 95.4-98.5%	(Zhang and Yu 2000) (Shin et al. 2002)
F. trogii	Astrazon Red dye Drimarene Blue Reactive Black 5 Acid Black 52	Activated carbon. L. cylindrica sponge. L. cylindrica sponge. Na-ALG beads.	66-98% 75-95% 99% 90%	(Cing and Yesilada 2004) (Erkurt et al. 2007) (Mazmanci and Ünyayar 2005) (Park et al. 2006)
Irpex lacteus	RBBR Reactive Orange 16 Reactive Orange 16	PuF, Pine wood (PW),PuF straw (source of nutrients) and Al-Schwimmbett® plastic particles	95-100% 80% 50-90% >92%	(Kasinath et al. 2003) (Svobodová et al. 2007) (Sima et al. 2016) (Šíma et al. 2012b)

Fungus	Azo dye	Support materials	Degradation	References
Bjerkandera sp.	Reactive Red 2	Birch wood	80-94%	(Axelsson et al. 2006)
T. pubescens	Reactive Red 243	PuF	95-100%	(Casieri et al. 2008)
P. ostreatus	Reactive Red 243	PuF	96-98%	(Casieri et al. 2008)
Trametes hirsuta	azo, and Anthraquinonic dyes	Alumina pellets	80%	(Abadulla et al. 2000)

2.6.2.1 Dye decolorization by immobilized fungi

Immobilized cultures of *Trametes versicolor* with activated carbon power were investigated for decolorization of acid violet 7 (Zhang and Yu 2000). It showed the maximum dye removal within 6 h. The maximum decolorization rate (Vmax; mg/L h) and half velocity concentration (Ks; mg/L) were calculated at 130.5 and 345.0 in the batch system, respectively. The decolorization of orange II by immobilization of *Phanerochaete chrysosporium* in a continuous packed bed reactor was investigated (Mielgo et al. 2001). In this study, PuF material used as a matrix material, and complete decolorization obtained when working at optimal conditions [temperature 37^{o}C, HRT of 24 h, and organic loading rate 0.2 g/L/d]. A linear correlation was found between MnP activity and decolorization, absence of Laccase, and LiP enzyme activity. Decolorization and degradation of azo dyes through immobilized *Phanerochaete chrysosporium* and *Trametes versicolor* on different supporting materials were investigated and found the highest removal rate, as shown in Table 2.5. The mixture of these two fungi was not investigated to degrade azo dyes by using granular activated carbon as a support material as per our knowledge. Therefore, the degradation of reactive black 5 (RB5) azo dye is investigated in the rotating packed disc bioreactor using mixed culture immobilized on granular activated carbon.

CHAPTER 3

SCOPE AND OBJECTIVES

CHAPTER 3

3 SCOPE AND OBJECTIVES

The literature survey revealed that RBCs demonstrate plug flow behavior. The microorganisms in the first stage would be exposed to the highest pollutant concentration, and the ones present in the last stage would be exposed to the lowest pollutant concentration. Therefore, small variations in the influent quality would affect the biofilm's growth and thence pollutant removal. This requires changing the flow behavior inside the RBC so that the performance does not reduce by varying influent concentrations. The reports suggest the requirement of more surface area for biofilm growth for efficient degradation of the pollutants under variable organic/hydraulic loading. It also suggests that the recycling stream positively influences pollutant removal, but the underlying reason is not reported. Reports suggest that white-rot fungus is the best microorganism for dye degradation as compared to municipal activated sludge. *Phanerochaete chrysosporium* and *Trametes. vesicolar* efficiently degrades dyes, although dye degradation efficiency and COD removal efficiency vary for both the fungi. *P. chrysosporium* degrades color but does not reduce COD as much as *T. vesicolar* culture. In contrast, the latter culture reduces COD but is susceptible to inhibition by high concentrations of dyes. A mixed culture of the two fungi may provide a solution to dye as well as COD removal. Immobilized culture proved to be more efficient in color removal than the suspended cultures. GAC can provide a good immobilization platform for white-rot fungi.

3.2 Based on the literature review, this research work focuses on the following objectives,

1. Design and Development of novel horizontal trough rotating packed disc bioreactor (RPDB)
2. Characterization of the developed bioreactor in terms of hydrodynamics and mass transfer
3. Investigating the suitability of proposed contactor design for biodegradation of azo dyes.

SCOPE AND OBJECTIVES

CHAPTER - 4

RESEARCH METHODOLOGY

CHAPTER 4

4. MATERIALS AND METHODS

4.1 Materials

The Reactive Black-5 dye was purchased from Sigma–Aldrich (Miluwaukee, USA), while yeast extract and malt extract were bought from Himedia (Mumbai, India). The other chemicals were obtained from LOBA CHEMIE Pvt. Ltd. (Mumbai, India). Granular activated carbon (GAC) obtained from "*GCARBON*" Gowrishankar Chemicals Pvt. Ltd. K B Cross, Kibbanahalli, Tumkur, Karnataka, India. This GAC is made up of coconut shells with different techniques, which gives it strength and durability. Initially, granular activated carbon was sieved for the desired size; particles passing through 4 mm screen and retaining on 3.2 mm screen (average size =3.6 mm) were taken for the study. The GAC was washed repeatedly using water to remove all dust, colour, and loose particles. Then, it was dried in an oven for 24 h at 110° C. This dried GAC was then used for immobilization purposes. It is some properties that were determined and used in this study shown in the appendix Table A1.

This chapter deals with details of chemicals used, analytical techniques employed in the present investigation, a different instrument used for analysis, and a description of the experimental setup—the detailed specification of the contactor and operating conditions used in the contactor were also represnted.

4.2 Contractor specifications

This research work involves the use of a modified design of rotary biological contractor for the removal of dye degradation and reduction of COD of synthetic wastewaters. A Rotating Packed Disc Bioreactor (RPDB) has been designing and fabricated. The specification of contactor are given in Table 4.1.

4.2.1 Description of the experimental setup

The experimental line diagram as shown in figure 4.1(a), (b), and (c). The synthetic effluent having the required concentration was prepared, and the feed Tank, having a capacity of

100 L, was filled. Two peristaltic pumps, one for pumping main feed and another for pumping recycle feed, are used. Calibrated rotameters were provided for measuring the flow rates of main and recycled feeds. An RPDB was designed, with emphasis to provide a well-mixed environment.

Table 4.1.: The contactor Specifications

Trough	Hollow Disc	Vanes on disc
✓ Geometry: Rectangular cross-section with a circular bottom ✓ Length: 150 cm ✓ Width:30 cm ✓ Depth: 18.5 cm ✓ Working volume 32.5/65 L	✓ Geometry: Circular ✓ Diameter: 25 cm ✓ Width :3 cm ✓ Perforations: 3mm ✓ Volume: 1.437 L ✓ Number of discs:2/3 /4/6/8 ✓ Spacing between discs 25.5-19-12.5 for 2-3-4 or4-6-8 respectively.	✓ Geometry: Rectangular ✓ Length: 12.5 cm ✓ Width: 3 cm ✓ Thickness: 0.2 cm ✓ Total number: 8 ✓ Orientation: Radial and staggered on both sides.

The novelty lies in the hollow disc's design, which contains radial wanes on the outside of the disc. The contactor made of SS 316 consists of a horizontal trough with a semi-circular bottom with liquid flow through the trough, as shown in Figure 4.1(b). The contactor has three sections; sections 1 and 2 would serve as reactors with overflow from section 2 entering section 3 and draining as final discharge. The contactor could be operated with two different working volumes, 32.5 L and 65 L. Hollow circular discs were shown in Figure 4.1(a) mounted on a shaft and were housed in the trough so that they were partially submerged in the flowing liquid. Flat radial vanes with a 45° staggering on both flat sides of each disc were provided to enhance radial mixing. Holes of 3 mm were provided on both flat sides of each disc. The hollow discs were packed with polymer (LDPE) beads (shape: oval, size: length = 5 mm, width = 2.5 mm, density =0.898 g/ml) for conducting RTD

experiments. The packing material inside the disc provided four times more surface area than the standard disc used in an RBC.

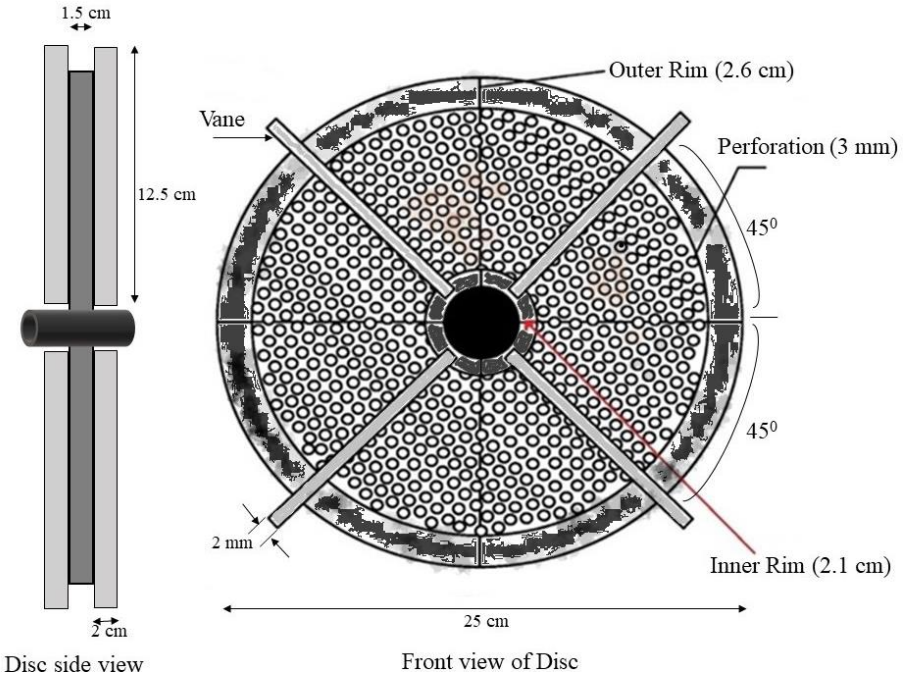

4.1 (a)

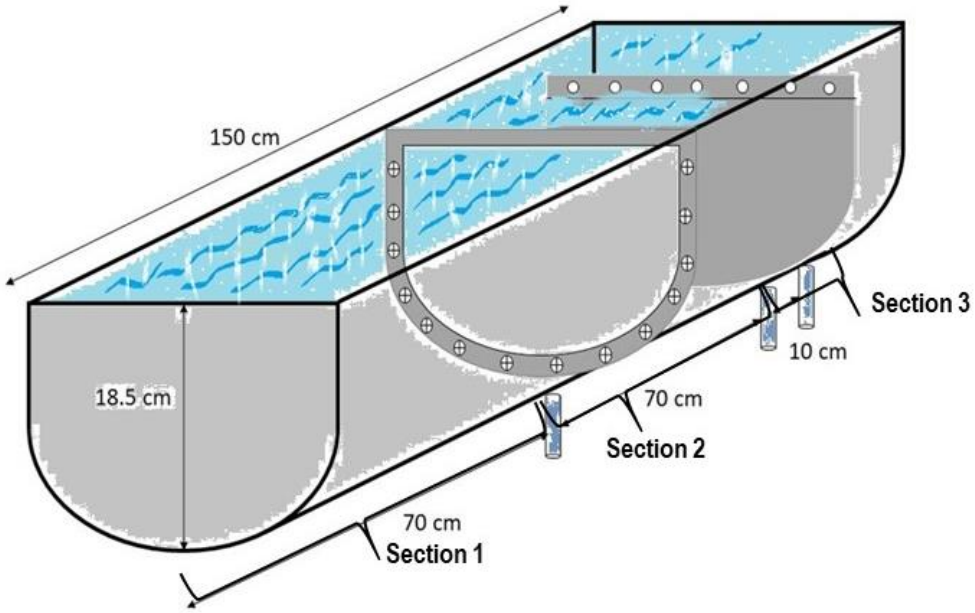

4.1 (b)

The aerobic processes for municipal wastewater treatment typically employ 40-50% submergence of discs (Cortez et al. 2008b; Gupta and Gupta, 2001; Ni, 1994). A 45% submergence was used in this work. A 3 HP variable speed drive rotated the shaft at the required speed.

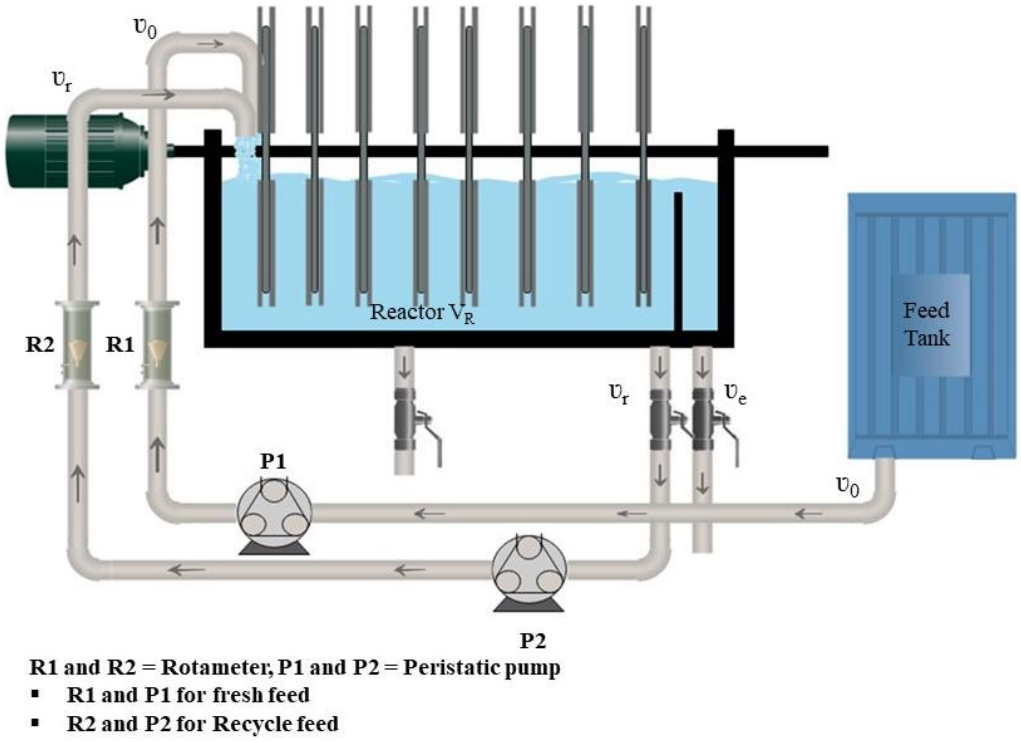

4.1 (c)

Figure 4.1. Schematic diagram (a) hollow circular disc, (b) horizontal trough with a semi-circular bottom (c) Schematic line diagram of rotating packed disc bioreactor experiment setup.

When the contractor would be operated as a bioreactor, appropriate solids containing microorganisms would be used. The liquid would enter the discs through holes under submergence during rotation and reach the microorganisms. The liquid would contain dissolved oxygen as well as nutrients needed for the growth of microorganisms. Besides, when the discs would be exposed to ambient air during rotation, air would enter the discs

through holes, and microbes would receive oxygen. Figure 4.1(c) show the schematic line diagram of the experimental setup. Tap water was used for conducting experiments. Two peristaltic pumps, one for fresh feed (P_1) and the other for the recycle feed (P_2), were used. Calibrated rotameter were used to evaluate the flow rates of fresh (R_1) and recycle feeds (R_2). The tracer used was 2 N potassium dichromate solutions. The required number of discs for a given experiment was fixed onto the shaft with appropriate spacer tubes, lock, and key arrangement. The required flow rates of fresh and recycle streams as well as shaft speed were set and ensured that the contactor was operating under steady-state conditions. 10 mL of tracer was quickly injected as a pulse at the location where the fresh and recycle streams were entering the trough. A pen-type calibrated conductivity meter (Hanna Instruments, Model HI98129) was used to measure liquid conductivity at the exit for different time intervals. The conductivity data were converted into concentration vs. time data using the calibration plot *(C =1.10·t +1.30)* shown in appendix Figure A1. The following equations were used for calculations related to exit age distribution,

$$w = \upsilon_0 \int_0^\infty C(t).\,dt \qquad (4.1)$$

$$E(t) = \frac{C}{\int_0^\infty C.dt} \qquad (4.2)$$

$$\bar{t} = \frac{\int_0^\infty t.C.dt}{\int_0^\infty C.dt} \qquad (4.3)$$

$$\theta = t/\bar{t} \qquad (4.4)$$

$$E(\theta) = \bar{t}.\,E(t) \qquad (4.5)$$

$$\sigma^2 = \int_0^\infty (t-\bar{t})^2.\,E(t).\,dt \qquad (4.6)$$

The tracer balance check was done using equation. 4.1 for each run, and if the error between the quantity of tracer used and obtained from equation. 4.1 was more than ±5%, the experiment was repeated. The exit age distributions were generated, and the corresponding parameters were found using equations 4.2 - 4.6. The area under each $E(\theta)$ curve (in the dimensionless form) was checked and found to be unity. The influence of time taken for

injecting the pulse of tracer on exit age distributions was neglected because it was far less (< 5 s) than the mean residence times observed in the contactor.

Table 4.2.: Experimental conditions used in this work

Sr no	Conditions	Working volume (32.5 L)	Working volume (65 L)
1	Rotational speed, ω	10, 15 & 20 rpm	4, 6, 8, 10, 12, 15 & 20 rpm
2	Number of discs, N	2, 3 & 4	4, 6 & 8
3	Recycle Ratio, R	3.05, 3.78, 5.32 & 9.75	0.102, 1, 1.858 & 9.75

Experiments were conducted with working volumes of 32.5 and 65 L, using packed discs. Both of these working volumes were conducted in a single system using the partition provided at the middle of the bioreactor as shown in figure 4.1(b). The experiments were carried out in triplicates, and the standard error was measured. Since the RTD studies contained a large number of data points and the error obtained for the mean residence time was less than ± 6%, the error bars are not shown in the plots. The operating conditions used in this study are given in Table 4.2.

4.3 Mathematical model

The model developed by Kim et al. (1982) was adopted here for analysis. Figure 4.2 shows the model diagram. The following points were considered for deriving the model equations used in this work.

- There were no stagnant regions in the contactor.
- A recycle would be used when this contactor would be operated as a bioreactor later, and hence a recycle stream was included in the model equations.
- As mentioned in Figure 4.2, the total volume of liquid (V_l) in the contactor for given submergence of discs was divided into three sections as follows.

$$V_l = V_0 + n \cdot V + V_e \qquad (4.7)$$

Where 'n' was the number of equal-sized stages and V was the volume of each stage in a cascade; V_0 and V_e were the volumes of mixing and splitting compartments at the inlet and outlet of the cascade, respectively.

- The fresh and recycle feeds were mixed in $V_{0,}$ and the resulting mixed stream was fed to the first stage of the cascade.
- The exit stream from the last stage of the cascade entered V_e, where it was split into the final exit and recycle streams.
- The volume of each stage consists of upper and lower liquid regions with a cross-flow between these regions.
- The upper liquid region was considered to be well mixed, having a volume of $\alpha \cdot V$, where α is the volume fraction of the upper liquid region. The lower liquid region, having the volume of $(1 - \alpha)$ V, was also considered to be well mixed.
- The cross-flow between the two mixed flow regions was $\beta \cdot \upsilon_m$, where υ_m was the total through flow in the axial direction and β was the volume fraction of cross-flow between two mixed flow regions.
- The contactor operated under steady-state isothermal conditions.
- Since the fluid used was liquid, it would be a constant density system.

For tracer analysis with recycle stream, the recycle ratio, R was defined as

$$\upsilon_m = \upsilon_0 + \upsilon_r = \upsilon_0 + R \cdot \upsilon_0 = (1 + R) \cdot \upsilon_0 \qquad (4.8)$$

Where, $R = \frac{\upsilon_r}{\upsilon_e} = \frac{\upsilon_r}{\upsilon_0}$

In order to obtain an expression to find the inlet concentration of tracer to the first stage of the cascade as a function of time, the following was considered as shown in Figure 4.2 (dotted section only). A pulse of the tracer of mass (w) was quickly injected into the mixing compartment, which was considered to be instantaneously mixed in the entire volume $V_{0,}$ such that at zero time, the concentration would be,

Tracer concentration, $C_0 = w/V_{0.}$

From the transient mass balance of tracer across the volume V_0 (Figure 4.2, the dotted section only), the following relation can be obtained,

$$C = C_0 * e^{\frac{-t}{\tau_0}} \qquad (4.9)$$

Where *C* represent the concentration of the tracer in volume *V,* and $\tau_0 = V_0 / \upsilon_0$. The tracer and the recycle stream having concentration C_e would get mixed to obtain the mixed feed entering the cascade.

A mass balance of tracer in the mixed region (M) (Figure 4.2, the dotted section only) would give the relation,

$$C_m = \frac{C}{(R+1)} + \left(\frac{R}{R+1}\right) * C_e \qquad (4.10)$$

Substitution of equation (4.9) in equation (4.10) would give

$$C_m = \left(\frac{C_0}{R+1}\right) * e^{\frac{-t}{\tau_0}} + \left(\frac{R}{R+1}\right) * C_e \qquad (4.11)$$

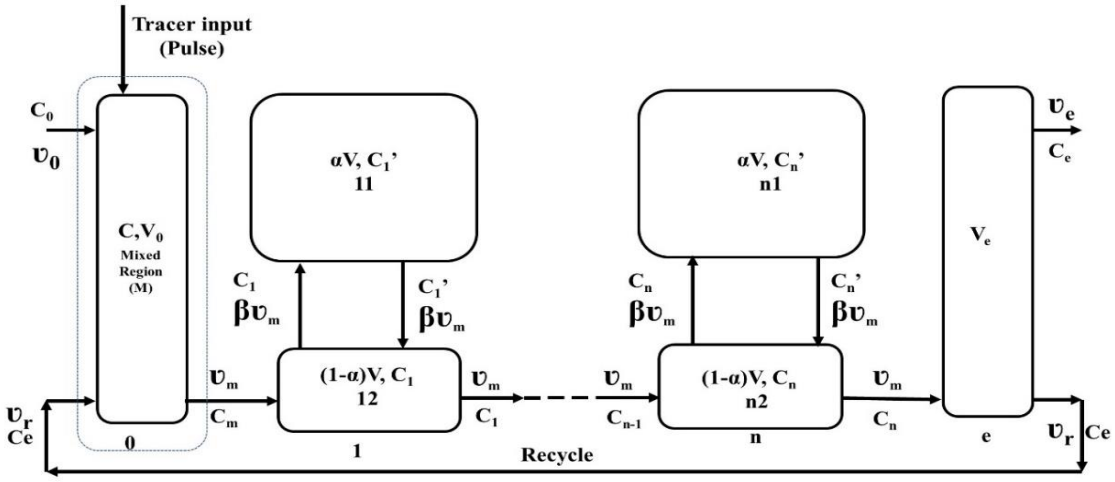

Figure 4.2: Shows the diagram of the RTD model system for each stage in the contactor.

The transient mass balances of tracer across the two mixed flow regions in each stage Figure 4.2 (Stage 1 - n) would be as follows.

Stage 1, Region 11

$$\beta.\upsilon_{m.}C_1 = \beta.\upsilon_{m.}C_1' + \alpha.V.\frac{dC_1'}{dt} \qquad (4.12)$$

$$C_1 = C_1' + \frac{\alpha.\tau}{\beta.(R+1)}.\frac{dC_1'}{dt} \qquad (4.13)$$

Stage 1, Region 12

$$\upsilon_{m.}C_m + \beta.\upsilon_{m.}C_1' = \upsilon_{m.}C_1 + \beta.\upsilon_m C_1 + (1-\alpha).V.\frac{dC_1}{dt} \qquad (4.14)$$

Since, $\upsilon_m = \upsilon_0 \cdot (R+1)$ and $\tau = \frac{V}{\upsilon_0}$, dividing equation 4.14 with v_m and rearranging would yield,

$$C_m + \beta . C_1' = (1+\beta).C_1 + (1-\alpha).\frac{\tau}{R+1}.\frac{dC_1}{dt} \quad (4.15)$$

The following dimensionless constants were defined,

$P_1 = \frac{\alpha}{(R+1)\beta}$ $P_2 = \frac{\alpha.(1-\alpha)}{\beta.(R+1)^2}.$ $P_3 = \frac{\alpha+\beta}{(R+1)\beta}.$ $P_4 = \frac{R}{R+1}.$

In addition, let $\Phi = C_0/(R+1)$

Substitution of dimensionless parameters in equation 4.13 would yield,

Stage 1, Region 11

$$C_1 = C_1' + P_1.\tau.\frac{dC_1'}{dt} \quad (4.16)$$

Similarly, substituting equation.4.11 and equation.4.13 in equation 4.15 and rearranging would give the following equation,

Stage 1, Region 12

$$P_2.\tau^2.\frac{d^2C_1'}{dt^2} + (P_3.\tau.).\frac{dC_1'}{dt} + C_1' = \phi.\exp\left(\frac{-t}{\tau_0}\right) + P_4.C_e \quad (4.17)$$

Similarly, Stage 2, Region 21

$$C_2 = C_2' + P_1.\tau.\frac{dC_2'}{dt} \quad (4.18)$$

Stage 2, Region 22

$$P_2.\tau^2.\frac{d^2C_2'}{dt^2} + (P_3.\tau.).\frac{dC_2'}{dt} + C_2' = C_1 \quad (4.19)$$

Similarly, Stage n, Region n1

$$C_n = C_n' + P_1\tau.\frac{dC_n'}{dt} \quad (4.20)$$

Stage n, region n2

$$P_2.\tau^2.\frac{d^2C_n'}{dt^2} + (P_3.\tau.).\frac{dC_n'}{dt} + C_n' = C_{n-1} \quad (4.21)$$

In the above model, the three parameters, α, β, and n provide information on flow behavior in the RBC. Usually, an increasing number of stages suggest the plug flow behavior in any given contactor. The parameter α provides the volume fraction of the upper region of the two mixed flow regions. A higher value of α suggests a well-mixed region, whereas a lower value of α suggests a plug flow region. The parameter β provides information on the cross-

flow between the two well-mixed regions. Usually, as α increases, the β value would decrease because a higher α value suggests that two different stages would merge to make one stage. Overall, a mixed flow behavior will be observed for high α, low β, and low n value, whereas a plug flow behavior will reduce α and increase β and n.

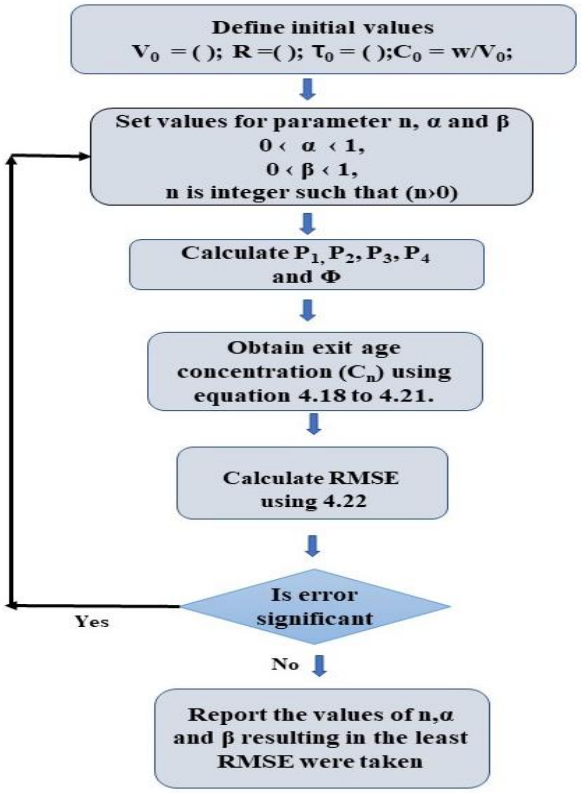

Figure 4.3: The model for estimating the model parameters followed step by step iterative procedure

4.3.1 Estimation of model parameters

All model parameters mentioned above, namely, α, β, and n, were estimated by the nonlinear least square method of parameter estimation. Experimental data were used, and the root mean squared error (RMSE) was minimized using MATLAB (2015a), as given by the following equation,

Minimize,

$$\text{RMSE} = \sqrt{\frac{\sum_{i=1}^{n}(C_{Exp.} - C_{sim})^2}{n}} \qquad (4.22)$$

Where C_{sim}= simulated value of exit age concentration and C_{Expt} = experimental value of exit age concentration. The following (Figure 4.3) step by iterative step procedure was followed for estimating the model parameters using experimental RTD data of each experimental run. MATLAB (2015a) was used to solve the model equations.

4.4 Oxygen mass transfer studies

The oxygen volumetric mass transfer coefficient (k_La) was measured in RPDB using a static gassing-out method (Linek et al. 1987; Van't Riet 1979). Figure 4.4 represents the oxygen transfer concentration outline for the static gassing out method.

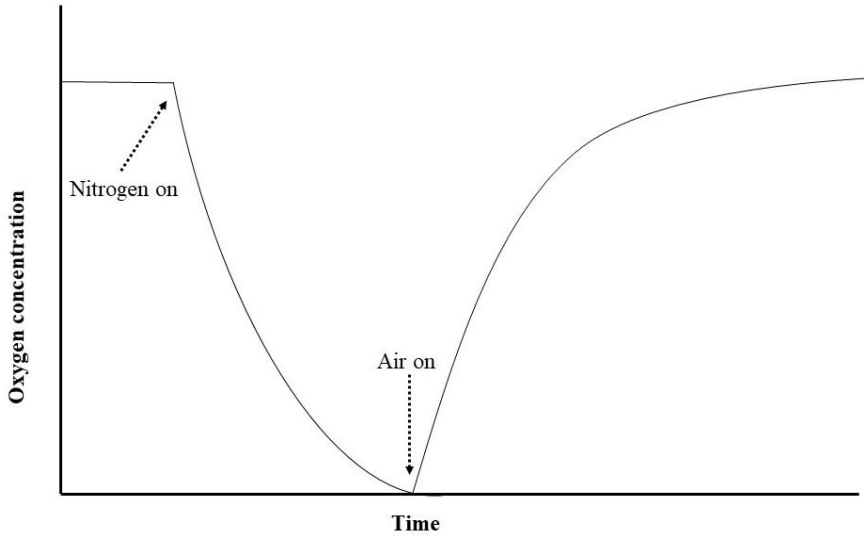

Figure 4.4: Schematic representation of the oxygen concentration for the static gassing out a method to determine the k_La value

The trough was filled with tap water, and nitrogen gas was bubbled from the bottom of the trough to lower the dissolved oxygen (DO) in the water. The DO was measured using a calibrated DO meter (L_{utron} PDO-520, polarographic type). The probe response time was very short in comparison with the time interval of measurement.

The probe was placed 11 cm from the water surface. At the time of nitrogen gas bubbling, the reactor was fully covered with the steel sheet hood to reduce oxygen transfer from surroundings into water. The flow of nitrogen gas was stopped when the DO level dropped

below 0.5 mg-O_2/L. Then the reactor was operated at the given rotation, and the recycle stream was maintained. Instantaneously DO values were measured until it reaches a saturation state. Since all the experiments were conducted at room temperature, *C** value for each experiment was different. During the repeat experiments, the DO value was measured by placing the DO probe at the tank's starting point and at the center. The readings were almost the same and gave uniform mass transfer along the length of the tank. For repeat experiments, the error was <5%. The mass balance of oxygen in water can be described as

$$\frac{dC}{dt} = k_{\mathrm{L}}a \cdot (C^* - C) \qquad (4.23)$$

Integration of equation (4.7) would yield

$$\ln\left[\frac{(C^*-C_0)}{(C^*-C)}\right] = k_{\mathrm{L}}a \cdot (t_{\mathrm{o}} - t) \qquad (4.24)$$

where C^* is the DO concentration at saturation and C is the DO concentration at time t. $k_{\mathrm{L}}a$ was calculated from the slope of the straight line given in equation (4.24) by plotting $\ln\left[\frac{(C^*-C_0)}{(C^*-C)}\right]$ versus time $(t_o\text{-}t)$. k_La was measured for two working volumes of 32.5 and 65 L. The effects of the number of discs from 2 to 8, rotational speed from 5 to 60 RPM, and recycle stream on kLa were investigated in batch mode.

4.5 Microorganisms, medium and subculturing

A pure culture of the white-rot fungus *P. chrysosporium* (MTCC NO: 787) and *T. versicolor* (MTCC NO: 138) strains were obtained from IMTECH Chandigarh, India. Both the strains were periodically transferred to subcultured with an interval of 30 days on growth media. Standard (90 mm diameter × 15 mm) Petri plates (Sterilized and disposable plates, Hemedia laboratories PVT.LTD., Mumbai-400086) were used in this study to cultivate *P. chrysosporium* (MTCC NO:787) and *T. versicolor* (MTCC NO:138) on respective solid media as given in Table 4.3. Which used to maintain the stock culture and subculturing. As suggested by IMTECH Chandigarh India. But, later on, the glucose concentration was reduced to 1% for *P. chrysosporium* culture. All media was autoclaved

at 121°C for 15 min. Cultures were maintained in incubators at a constant temp of 25°C and 30°C, as per the requirement of the experiment.

4.5.1 Growth and degradation on agar plates

The fungi were cultured (*P. chrysosporium* and *T. versicolor*) in a medium containing 20 10 g/L glucose, 20 g/L malt extract, 20g/l nutarian agar, and 1 g/L peptone in solid media having pH 5 were autoclaved at 121°C for 15 min. After that, RB5 dye added inside the laminar air flow chamber containing concentrations of 30, 60, and 100 mg/L were studied for degradation. Growth inhibition and dye degradation were measured on the agar plates simultaneously.

Table 4.3.: Media composition for fungus culture

Components (g/L)	***P. chrysosporium* MTCC NO-787**	***T. versicolor* MTCC NO-138**
Malt extract	20.0 g	N.A.
Yeast extract	N.A.	5.0 g
Glucose	20.0 g	10.0 g
Peptone	1.0 g	N.A.
Agar	20.0 g	15.0 g
Distilled water	1.0 L	1.0 L

Mixed cultures are inoculated at the agar plate's edge and are grown for 7d at 30^0C under an incubator shaker. Growth and dye degradation were expressed according to the width of the inhibition zone, which was visible.

4.5.2 Acclimatization of fungal culture

The white-rot fungus *P. chrysosporium* (MTCC NO:787) and *T. versicolor* (MTCC NO:138) were cultivated in the malt and yeast agar medium containing 100 mL on Petri dishes (90 mm). Cultures were incubated at 30°C in the dark. The fungi were acclimatized with dye concentration at 30 mg/L. Spores from each plate were subcultures onto the fresh

medium with/without the dye, and the process was repeated for five generations. Selected and transferred to a new medium with or without dye concentration for the subsequent generation. This process was repeated five times. The sub-strains obtained from the last cultures were called acclimatization of fungi".

4.6 Shake flask studies

A standard shake flask (250 mL) was used during this study. Liquid media composition was prepared in the shake flask having the dye concentration with fungal strains. The shake flasks were incubated in a rotary-shaken incubator, with adjustable temperature settings, shaking velocity, and throw diameter. Samples were taken manually using a pipette with sterile tips.

4.6.1 Dye Degradation Studies

The strains using in this study were *P. chrysosporium and T. versicolor*. The microbial cultivation was carried out in malt extract medium, and yeast extract medium with specific glucose concentration as a carbon source as shown in Table 4.3. Based on the commercial utility as colouring agent reactive black 5 azo dye chosen in this study. The molecular structure of this compound is shown in figure 5.12. The medium will be added in different concentrations of reactive black 5 (30, 60, and 100 mg/L). The flow chart of the process, as shown in Figure 4.5. The inoculum was a 0.7 mm diameter disc obtained from the 7-day old culture of respective solid media cultures of respective fungi. The discs were made sure to be taken from the outer periphery of the growing fungal mat. Liquid cultures were inoculated with 4 of these discs each. In the case of inoculation by flocs, the flocs were obtained from 7-day old liquid cultures of respective fungi. The flasks containing individual fungal strain and mixed fungal strain with 2-2 discs of each fungi strain were inoculated in a 50 mL culture medium containing specific dye concentration. Three different fungal strain sets were prepared and were incubated under constant agitation/shaking at 200 rpm (Yorko Scientific Orbital Shaker) at 30^0C. All three cultures were incubated for 10 days, and all assays were performed in triplicate. Samples are taken at an interval of 24 hours and centrifuged at 1000 rpm for 10 min. The biomass's dry weight

will be determined by filtering the washed culture through filter paper, drying to a constant weight at 70^0C, and measuring the biomass's dry weight.

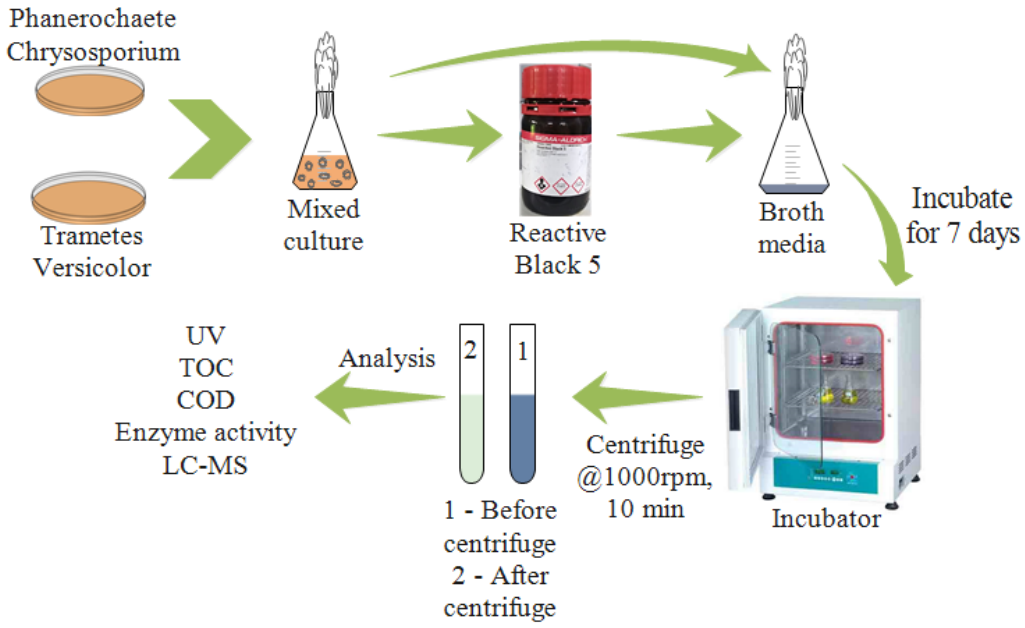

Figure 4.5. Flow chart of dye degradation studies

Degradation of dye was determined by monitoring the absorption spectrum changes at 597 nm using a spectrophotometer. The present sample concentration of the reactive black 5 was calibrated from the standard graph shown in appendix Figure A2

4.6.2 Acclimatization of fungal culture for bioreactor studies

The synthetic dye wastewater used for isolation of dye-decolorizing fungi have been acclimatized for 1-2 weeks, then transfer into a 250 mL conical flask containing 100 ml synthetic dye wastewater. After incubation of the conical flasks, the culture showed quick and stable decolorization activity; then, it was transferred into newly prepared synthetic dye wastewater. After successive transfers, it was plated on synthetic dye wastewater agar containing a different concentration and incubated at 30°C for seven days. The four days of fungal inoculum transfer to the rotating packed disc bioreactor as the startup steps bioreactor.

4.7 Rotating Packed Disc Bioreactor (RPDB) studies

The laboratory scale Rotating Packed Disc Bioreactor (RPDB) was first filled with synthetic textile wastewater of the chosen concentration. And the medium containing 1 g/L of glucose, 1 g/L malt extract, 0.05 g/L peptone, and other supplementary nutrients (0.5 g/L $MgSO_4$, 0.05 g/L $MnSO_4$, 0.1 g/L NaCl, 0.01 g/L $FeSO_4\,7H_2O$, 0.01 g/L $ZnSO_4\,7H_2O$, 0.01g/L $CuSO_4$, 0.01g/L $CoCl_2$,0.1 g/L NaCl, 0.1 g/L $CaCl_2$, 1 mg/L H_3BO_3 and 1 mg/L $Na_2MoO_4\,2H_2O$) was added into the synthetic wastewater.Then, GAC was carefully loaded up to 70% of the volume of the hollow disc to provide space for fungal growth.

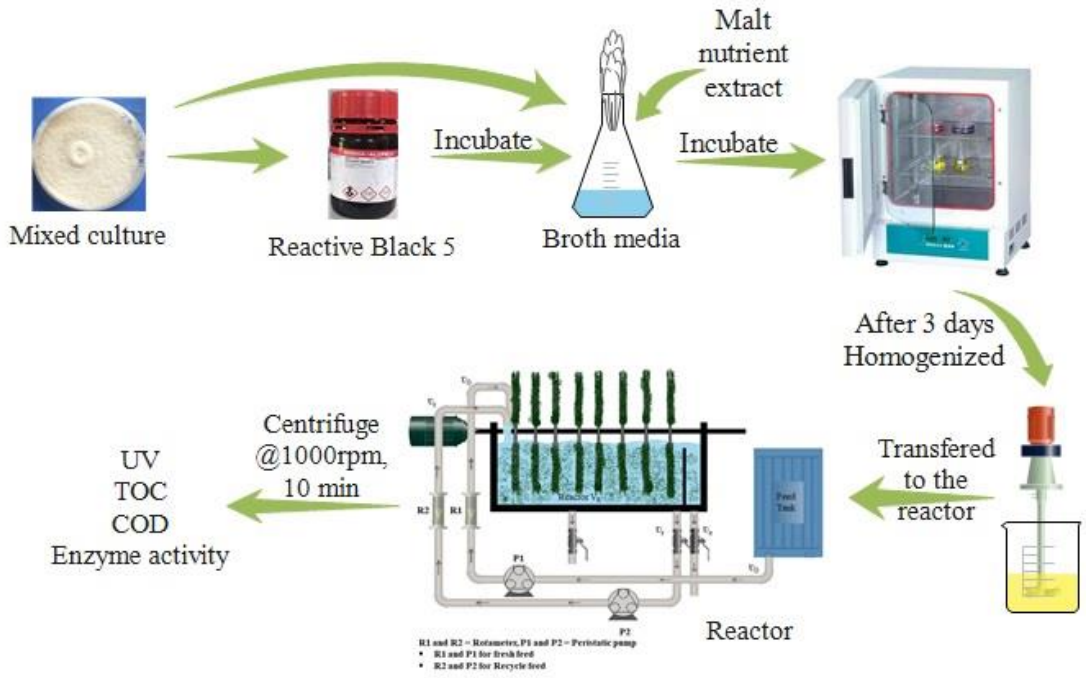

Figure 4.6. Flow chart of the bioreactor studies

In this bioreactor, eight hollow circular discs were mounted on the shaft inside the trough and rotated. The mixed fungal culture was inoculated onto the GAC, and the RPDB was operated in the batch mode to immobilized fungal biomass on the disc. The fresh feed was started in the RPDB on the 7th day onwards at a flow rate of 6 L/h (Hydraulic retention time of 10.83 h) for continuous operation. The 30 mg/L RB5 concentration was used for

batch and continuous studies at 10,20, and 30 rpm and having recycle ratio 1 and 9.75.for two different working volume of 32.5 and 65 L. The total reactor volume is 73 L. The bioreactor's effluent samples were collected at an appropriate time interval and analyzed as per the procedures explained in section 4.8. When the dye concentration in the effluent sample reached a constant value for a long time, it was considered the bioreactor attained steady state and then stopped. All experiments were performed in triplicates, and the average of triplicate experiments are reported with standard error bars. The flow chart of the process, as shown in Figure 4.6.

4.8. Qualitative and quantitative analysis

4.8.1. Spectrophotometric Analysis

The concentration of Reactive Black 5 dye present in a sample was determined by using absorbance measurements. A standard curve was created for Reactive Black 5 dye. A sample containing known concentrations of RB-5 was analyzed at 597 nm using respective media without dye as blank. The absorbance values were converted to concentration values using a standard graph and linear equation λmax = 0.0465.* dye concentration and λmax = 0.0466 * dye concentration for *P. chrysosporium and T. versicolor* respective fungi as shown in appendix Figure A2.

The degradation percentage was calculated as $=(I-F/I) \times 100$.

Where in:

I = Initial Dye Concentration.

F= Final Dye Concentration.

The variations in λmax prior and post degradation were analyzed, taking the respective media without dye as the reference baseline sample.

4.8.2. Chemical oxygen demand estimation

The influence and effluent waste of the system will be measured according to the standard method for waste and wastewater examination (Metcalf & Eddy). The chemical oxygen demand (COD) is one of the most important criteria for characterizing wastewater effluents (Horwitz, W., 1975). The COD determines the amount of dissolved oxygen required for

chemical oxidation of sample solution using a strong chemical oxidant, such as potassium dichromate, under reflux conditions. The traditional method for determining COD with the use of potassium dichromate by the American public health association (APHA) used in this study. For testing the given wastewater sample, first the standard reagents were prepared. Standard potassium dichromate (0.25 N) solution prepared by adding 12.259 g of dry $K_2Cr_2O_7$ in distilled water and diluted to 1000ml. Standard sulfuric acid reagent - Weigh accurately 5.5 g of silver sulphate crystal to a dry clean 1000 ml beaker. To this carefully add about 500 ml of concentrated H_2SO_4 and allowed to stand for 24 h. Std. ferrous ammonium sulphate (0.1 N) was prepared by dissolving 32.2 g $Fe(NH_4)_2(SO_4)$ $6H_2O$ in about 400 ml distilled water. Add 20 ml of concentrated H_2SO_4 and diluted to1000 ml. The reaction mixture prepared in conical flask containing 10 ml Std. potassium dichromate (0.25 N), 0.4 g $HgSO_4$, 30 ml H_2SO_4, and 20 ml of wastewater sample. This reaction mixture kept in digestor for 2 h at 150 °C. Further the reaction mixture was cooled and then the amount of dichromate was calculated by direct titration using Ferrous Ammonium sulfate (FAS) as the titrant and ferroin as an indicator till the color changed from blue green to red/ brown. In the titration process, the titrant (Fe^{2+}) reacts immediately with hexavalent chromium (Cr^{6+}) to form trivalent chromium (Cr^{3+}) and ferric ion (Fe^{3+}). The final hexavalent chromium level is then subtracted from the initial level to find out the amount of hexavalent chromium decreased during digestion. The equation 4.25 used to calculate the COD with the added glucose.

$$\text{Chemical oxygen demand}(\mathbf{COD}) = \frac{(\boldsymbol{A-B})*\boldsymbol{\eta}*\mathbf{8000}}{\textbf{Volume of sample taken}} \qquad (4.25)$$

Where *A*= Volume of ferrous ammonium suLphate for blank in mL

B= Volume of ferrous ammonium suLphate for sample in ml

η= normality of ferrous ammonium suLphate

4.8.3. Total organic carbon estimation

TOC was measured in terms of Non-Purgeable Organic Carbon (NPOC) present in water. TOC analyser was applicable for small concentrations of organic matters. The test was

performed by injecting the known sample amount into a high temperature (temperature rises to 720 ºC) furnace. Organic carbon was oxidized into carbon dioxide in the furnace with a catalyst. Produced carbon dioxide was cooled and dehumidified, then quantitatively measured using an infrared gas analyser (NDIR). Acidification and aeration of the sample before analysis estimate the error due to inorganic carbon. The readings were standardized using known concentrations of Hydrogen Phthalate. The test was becoming more popular due to its fast-analysing techniques.

4.8.4. Adsorbed dye estimation

The amount of dye adsorbed onto the fungal biomass post degradation was estimated using methanol extraction, as suggested in (Ramsay and Goode 2004). 2ml of methanol was added to biomass post centrifugal separation. The sample was vortexed and then centrifuged. The absorbance of methanol was taken, and its concentration of adsorbed dye was estimated using the standard graph shown in appendix Figure A3.

4.8.5. Biomass (dry weight) Estimation

The dry weight of all cultures was primarily taken by centrifuging the flask contents (Ramsay and Goode 2004), and the wet biomass obtained was dried at 70°C until constant weight (1 day). The samples were dried in the centrifuge tubes themselves to facilitate the estimation of adsorbed dye.

4.8.6. Determination of order of degradation kinetics

The degradation amount and color removal rate were determined with 30, 60, and 100 mg/L of the RB-5. Degradation was initiated by adding fungal culture to the dye-containing medium. At fixed time intervals, samples were collected and analyzed to determine the remaining color. Following zero, first, and second-order kinetic equations (Eq. 4.26, 4.27, and 4.28, respectively) were used to determine the order of the degradation kinetics.

$$C_t = C_0 - k_0 \cdot t \quad (4.26)$$

$$ln\,(C_t) = -k_1 t + ln\,(C_0) \quad (4.27)$$

$$(1/C_t) = (1/C_0) + k_2 \cdot t \quad (4.28)$$

Dye concentration (C_t) versus time, $ln\ (C_t)$ versus time, and ($1/C_t$) versus time graphs were plotted respectively for equations (4.26), (4.27), and (4.28) for the RB-5 dye degradation. The equation with the highest regression coefficient (R^2) at all dye concentrations was chosen as the degradation kinetics.

4.8.7. Enzyme Assay

4.8.7.1. Manganese Peroxidase

The assay was conducted as per (Orth et al. 1991); the reaction mixture contained 50 mM Sodium succinate (pH 4.5), 50 mM Sodium lactate (pH 4.5), 0.1 mM Manganese sulphate (MnSO4), 50 µM Hydrogen peroxide, 0.1 mM Phenol red (Ɛ = 4,460 / M/ cm) and 3mg of Gelatin per ml.

The reaction was initiated by Hydrogen peroxide at a temperature of 30 °C for 4 min. MnP activity was assayed in the presence of its substrate phenol red to obtain the product, which was the oxidized form of phenol red that was detected at 610 nm spectrophotometrically. Hydrogen peroxide is also a substrate of MnP, which was used to initiate the oxidation of phenol red by the enzyme in the reaction mixture. From the total volume of 5ml, 1ml reaction mixture at one min intervals and added 15 µl of enzyme sample. To stop the reaction 40 µl of 5N NaOH added. The samples' absorbance was noted and calculated to obtain the enzyme activity. 1 unit of enzyme activity was equivalent to 1 µM of product formed per minute.

4.8.7.2 Lignin Peroxidase

Azure B was used to conduct the Lignin Peroxidase assay. The buffer constituted of 1ml of 125 mM Sodium tartrate buffer (pH 3), 500 µL of 0.16 mM Azure B, 500 µL of culture filtrate, and 500µL 2mM Hydrogen peroxide.

The reaction was started by adding Hydrogen peroxide; 1 unit of enzyme activity was expressed as an O.D. decrease of 0.1 units/ min/ mL of culture filtrate at 651 nm (Archibald 1992). From the total volume of 2.5 mL, 1 mL of sample was drawn at the one-minute interval. The O.D decrease was due to the substrate's disappearance with time and it was caused by the hyperchromic shift of the substrate’s major visible absorbance peak.

4.8.7.3 Laccase

Laccase enzyme oxidizes Guaiacol and forms a reddish-brown product, which was assayed spectrophotometrically at 450 nm. As mentioned in (Sandhu and Arora 1985), the procedure was followed. 5 mL of the reaction mixture for Laccase assay contained 3.9 mL of 0.01 M Acetate buffer (pH 5), 1 mL of 0.00176 M Guaiacol, and 0.1 mL enzyme extract was incubated at 25 °C for 2 h. After that, 1 mL of the sample drawn and noted absorbance values at 450 nm. Enzyme activity was expressed in relative terms as colorimetric units per mL.

4.9. Statistical analysis

Each experiment was performed at least three times. Means of three replicates and the Standard deviations (SD) were calculated with Microsoft office excel 2010 spreadsheet, and values were represented as mean ± standard deviation. All figures were derived from origin 9.0. the error bar in the figures represent standard deviation (±0.05).

RESEARCH METHODOLOGY

CHAPTER - 5

RESULT AND DISCUSSION

CHAPTER 5

5. RESULTS AND DISCUSSION

5.1 Introduction

This research showcases mixing behavior in a modified rotating packed disc biological (RPDB) through rotational speed, number of stages, and recycle ratio, contributing to the variations observed in the RTD behavior. In order to account for these other elements, RTD experiments were carried out in two different working volumes. The solids used in these studies were polymer beds having a size of 3.2 mm and a bulk density of 0.898 g/ml. A few runs were done in open trough without using any discs, and further empty discs were used in the absence of solids in 65 L to understand the influence of disc, over the presence of solids in RTD. The hydrodynamics within the reactor was modeled by developing the three-parameter mathematical model as explained in section 4.3. The model parameters were estimated using MATLAB software.

Figure 5.1 shows the experimental and model-predicted RTD at different operating conditions. Results revealed that the model fitted well with experimental data at different operating conditions, thus validating the model used in the study. The width of exit age distribution would increase as the flow and mixing behavior of a given contactor tended towards a well-mixed flow system. As shown in Figure 5.1 (a) and (b), the flow behavior in 32.5 L as well as in 65 L working volume was mixed flow. Although there was an indication of plug flow behavior in 65 L working volume at low recycle and rotational speed (Figure 5.1 c), the behavior changed to mixed flow at high recycle ratio and rotational speed (Figure 5.1 d). The mixing behavior of a cascade with well-mixed flow (MF) stages in series would become more like a plug flow (PF) system as the number of stages increased. Also, a PF system with recycling would exhibit the MF system's mixing behavior as the recycle ratio increased Levenspiel (Levenspiel 1999).

Moreover, the presence of vanes on discs provided good mixing of liquid present between the discs. In addition, since these vanes were extended beyond the rim of the disc, there would be good mixing beyond the disc because of the vanes' radial flow, hence minimizing

dead water regions in the trough. The model parameters at different experimental conditions are given in Table 5.1 for 32.5 and 65L working volume.

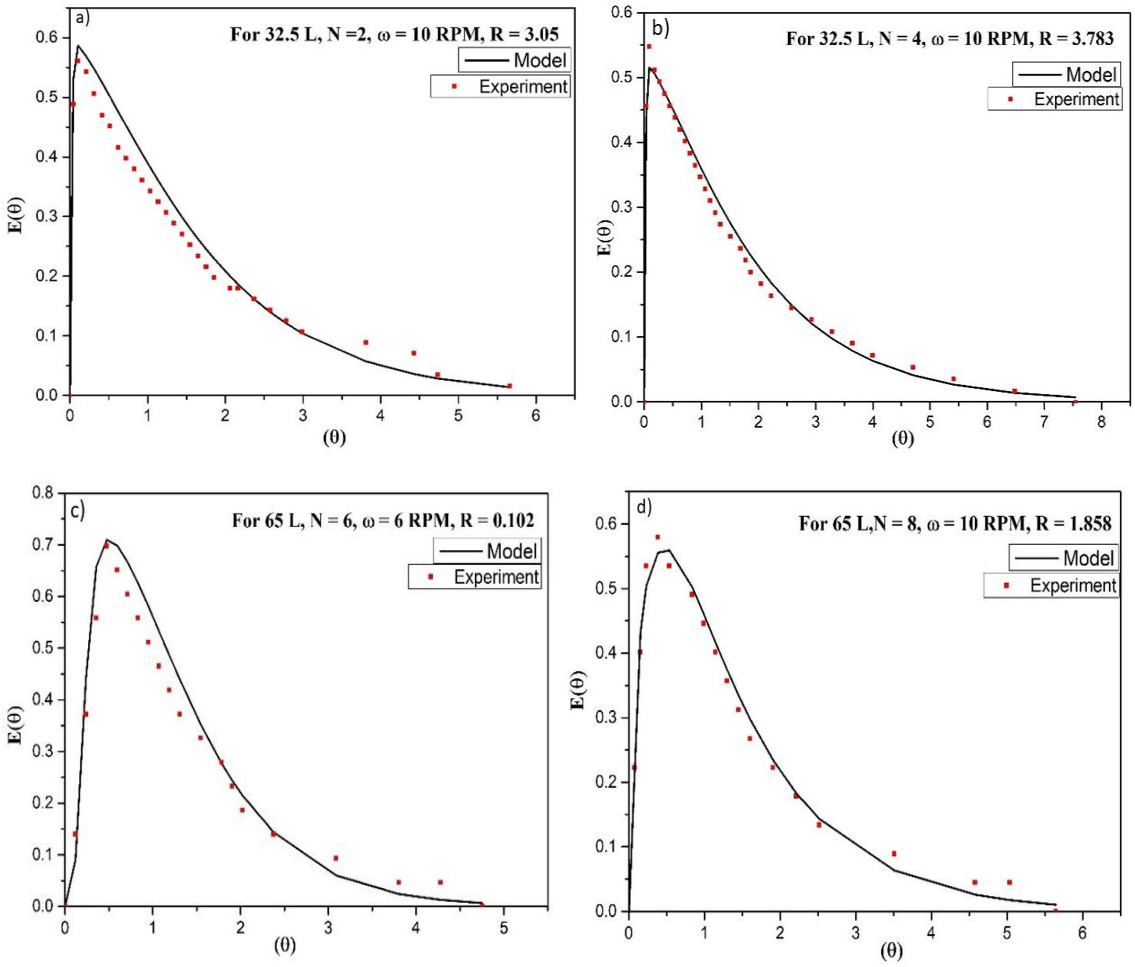

Figure 5.1: Comparison between model and experimental exit age distributions at varied conditions: a, b) for 32.5L; c, d) for 65L.

The results indicate that the new disc design provided mixed-flow behavior, which is in stark contrast with standard RBCs, in which plug flow behavior is observed. The disc wanes improved radial mixing. Thus, the biofilm formed on the packing material would be exposed to the same pollutant concentration throughout the bioreactor. Hence it would be less susceptible to variations in the influent organic loading. Since aerobic biodegradation

is depending on the dissolved oxygen concentration and the oxygen transfer rate from the atmosphere into the liquid, the bioreactor was also characterized in terms of oxygen transfer rate.

Table 5.1. Experimental parameter for RTD analysis for contactor 32.5 L and 65 L

For 32.5 L Reactor

Sr no	*N (n)*	*ω, rpm*	v_o, *(Lph)*	v_r, *(Lph)*	v_m,	*R*	*α*	*β*
1	2(1)	10	6	58.5	64.5	9.75	**0.98**	**0.14**
2	2(1)	10	19.16	58.5	77.66	3.05	**0.94**	**0.32**
3	2(1)	20	6	58.5	64.5	9.75	**0.98**	**0.14**
4	2(1)	20	19.16	58.5	77.66	3.05	**0.99**	**0.35**
5	3(2)	10	6	58.5	64.5	9.75	**0.98**	**0.11**
6	3(2)	10	19.16	58.5	77.66	3.05	**0.91**	**0.23**
7	3(2)	15	6	58.5	64.5	9.75	**0.98**	**0.10**
8	3(2)	15	19.16	58.5	77.66	3.05	**0.96**	**0.24**
9	3(1)	20	6	58.5	64.5	9.75	**0.97**	**0.13**
10	3(3)	20	19.16	58.5	77.66	3.05	**0.94**	**0.31**
11	4(2)	10	6	58.5	64.5	9.75	**0.96**	**0.10**
12	4(2)	10	19.16	58.5	77.66	3.05	**0.91**	**0.26**
13	4(2)	15	6	58.5	64.5	9.75	**0.97**	**0.11**
14	4(2)	15	19.16	58.5	77.66	3.05	**0.90**	**0.26**
15	4(2)	20	6	58.5	64.5	9.75	**0.98**	**0.11**
16	4(2)	20	10.98	58.5	69.48	5.32	**0.96**	**0.16**
17	4(2)	20	15.46	58.5	73.96	3.78	**0.95**	**0.22**
18	4(2)	20	19.16	58.5	77.66	3.05	**0.90**	**0.25**

For 65 L Reactor:

Sr no	*N (n)*	*ω RPM*	v_o *(Lph)*	v_r *(Lph)*	v_m *Lph*	*R*	*α*	*β*
1	4(3)	6	6	58.5	64.5	9.75	**0.89**	**0.09**
2	4(2)	10	6	58.5	64.5	9.75	**0.96**	**0.08**
3	4(2)	12	6	58.5	64.5	9.75	**0.95**	**0.08**
4	4(2)	20	6	58.5	64.5	9.75	**0.97**	**0.10**
5	6(5)	4	6	58.5	64.5	9.75	**0.83**	**0.08**
6	6(5)	6	6	58.5	64.5	9.75	**0.86**	**0.08**
7	6(5)	8	6	58.5	64.5	9.75	**0.90**	**0.09**

8	6(5)	10	6	58.5	64.5	9.75	**0.91**	**0.08**
9	6(5)	12	6	58.5	64.5	9.75	**0.89**	**0.08**
10	6(5)	20	6	58.5	64.5	9.75	**0.95**	**0.09**
11	6(5)	10	31.47	58.5	89.97	1.858	**0.77**	**0.30**
12	6(5)	6	58.5	6	64.5	0.102	**0.65**	**0.38**
13	6(5)	6	31.47	31.47	62.94	1	**0.77**	**0.39**
14	8(5)	6	6	58.5	64.5	9.75	**0.80**	**0.08**
15	8(5)	10	6	58.5	64.5	9.75	**0.88**	**0.08**
16	8(5)	15	6	58.5	64.5	9.75	**0.90**	**0.09**
17	8(5)	20	6	58.5	64.5	9.75	**0.91**	**0.09**
18	8(5)	10	31.47	58.5	89.97	1.858	**0.77**	**0.30**

5.1.1. Influence of the number of discs

Figure 5.2 (a) and (b) show the effect of the number of discs on the flow behavior in 32.5 L and 65 L working volume, respectively. Interestingly, observed mixed flow behavior using the novel disc design. The number of discs had a marginal influence on the change of the flow behavior inside the reactor at a recycle ratio of 9.75. The flow was mostly mixed flow type for the different number of discs. This is also evident from the model predicted values of α and β. As the number of the discs increased, the fraction of upper mixing volume in each stage (α) and a fraction of cross-flow between upper and lower mixing volumes in each stage (β) decreased marginally for 32.5 L working volume, the values of α and β were 0.96 ±0.02 and 0.13 ±0.02, respectively for different numbers of discs. Similarly, for 65 L working volume, the values of α and β were 0.9 ±0.09 and 0.09 ± 0.01, respectively. These values indicate that there was practically only one zone of mixing (α >0.9) at given operating conditions. An upper mixing volume (α) account for mixing occurring by suction and pumping flow between the discs. Lower mixing volume accounts for mixing occurring due to turbulence near the edges of discs and bulk flow in an axial direction (Kim et al. 1984; Nguyen et al. 2016). The flow phenomena explained here, i.e., between the discs and at the edges of discs, would not be profoundly influenced by the distance between discs.

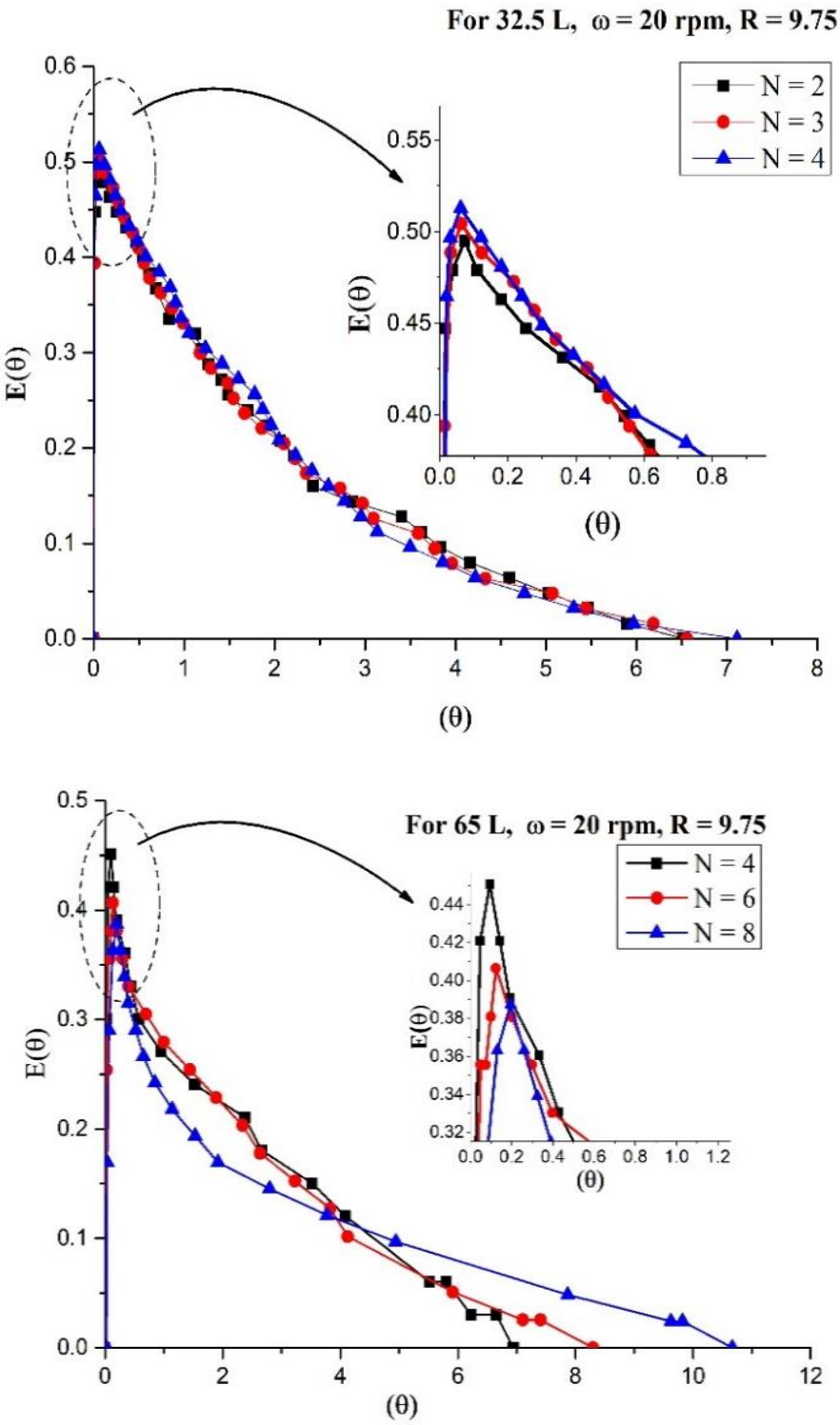

Figure 5.2: Influence of a number of discs on exit age distribution:

(a) for 32.5 L; (b) for 65 L.

So, the influence of N on the $E(\theta)$ was not significant to change the MF behavior to plug flow. Moreover, radial wanes aided in MF behavior. Researchers investigated the effect of the number of discs on the flow behavior inside a rotating biological contactor. They found an increase in the number of discs reduced back mixing and changed the flow behavior from mixed-flow towards plug flow (Ando et al. 1981; Leon et al. 2014). However, their RBC did not contain vanes on the disc. Vanes acted like a radial flow impeller, which enhanced MF behavior (H.F.Haug 1971) for the RPDC under study.

5.1.2. Influence of rotational speed of discs

Figure 5.3 (a) and (b) show the influence of rotational speed on the contactor's flow behavior. The rotational speed employed in the study were in the range of 4 to 20 rpm. For 32.5 L working volume operating at different rotational speeds, the α and β were 0.96 ±0.03 and 0.14 ±0.02, respectively. Similarly, for 65 L working volume, the α and β were 0.90 ±0.09 and 0.08 ±0.02, respectively. Since α was more than 90% of the volume of one cascade and β was less than 10% of the axial flow through the trough, it can be considered as a well MF behavior, which is evident from the experimental results (Dhanasekaran and Karunanithi, 2010). As the disc's rotational speed increased, the rate of back mixing increased (Ando et al., 1981; Basha and Morsi, 2018; Dhanasekaran and Karunanithi, 2010; H.F.Haug, 1971). As the disc's rotation speed increased, the vortices formation rate increased, which occupied the gap between two discs and formed MF (mixed flow) pattern (Basha and Morsi, 2018; Kumaresan and Joshi, 2006; Sirivat, 1991).

5.1.3. Influence of recycle ratio

Figure 5.4 (a) and (b) show the effect of the recycle ratio on the RTD of tracer in 32.5 L and 65 L working volumes. It is evident from experimental results that the recycling played a major role in the width of distribution. Hence, the reactor's flow behavior operated at different operating conditions, especially for 65 L working volume. As the recycle ratio increased, the width of distribution increased (Figure 5.4 (a) and (b)); this was because the recycle stream would contribute to back mixing, making the system well mixed.

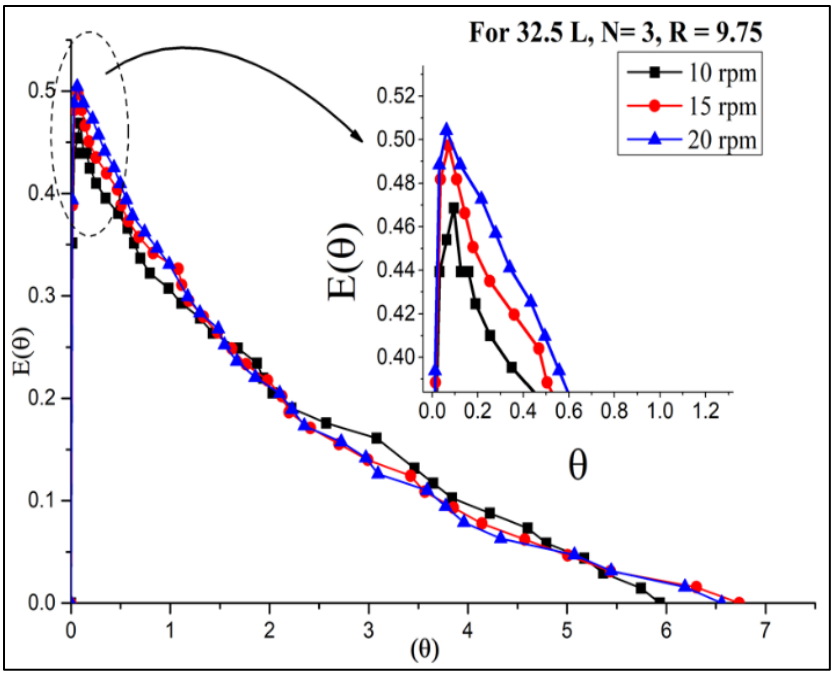

(a)

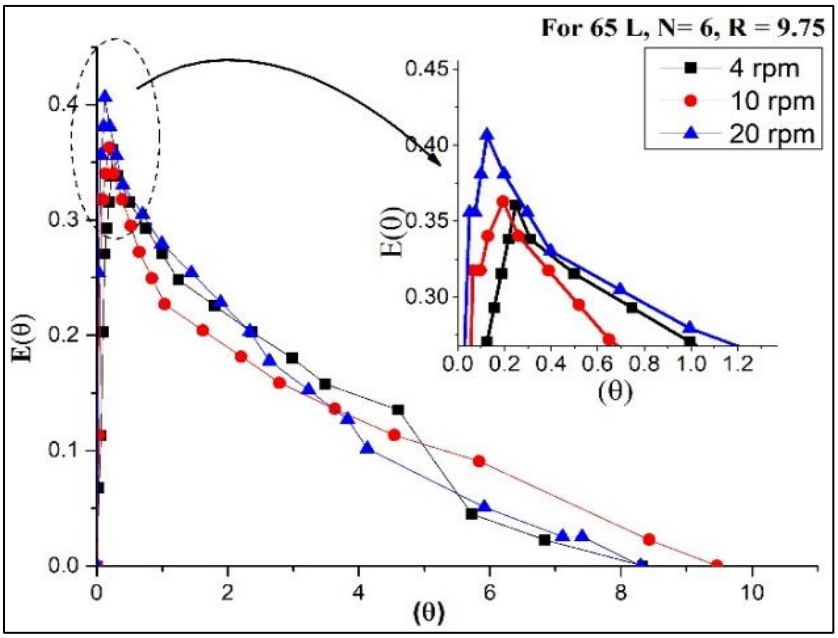

(b)

Figure 5.3: Influence of rotational speed of discs on exit age distribution: (a) for 32.5 L; (b) for 65 L.

This is also evident from the increased α and decreased β values with an increased recycle ratio as given in table 5.1. For the 32.5 L reactor, the α increased from 0.9 to 0.98, with an increase in the recycle ratio from 3.05 to 9.75, whereas β decreased from 0.25 to 0.1. This change in parameters was more pronounced in the 65 L reactor. The α value increased from 0.65 to 0.95 as the recycle ratio increased from 0.1 to 9.75, whereas β values decreased from 0.38 to 0.09. The axial bulk flow of liquid would be through the holes in the discs and the space available between the disc edge and trough wall for a given opening; as the flow rate decreased, the axial velocity and turbulence at the disc edge would decrease. The suction and pumping flow between discs along with lower axial velocities and lesser turbulence could result in an increase in upper mixing volume and a decrease in lower mixing volume. A significant reduction in cross-flow could occur because of lower axial velocities and lower turbulence. This was also evident from the number of theoretical stages (n). At a high recycle ratio, the number of stages decreased.

In the RBC system, recirculation of effluent, up to 100 to 150% of the influent flow improved the bioreactor's performance and minimized the negative effects of the high concentrations in the bioreactor (Brazil 2006; Poon et al. 1979). Moreover, recirculation avoided the excessive biofilm growth in the first stage of the RBC system and doubled the active biofilm life (Patwardhan 2003). The results of this work indicated that recirculation and vanes on the disc enhanced MF behavior in the bioreactor under study. Moreover, there was a good agreement between the model and experimental exit age distributions, indicating that the model proposed by Kim et al. (1984) could be adapted well to understand liquid mixing behavior in the proposed contactor. . However, the following factors were not considered in the model. In the proposed design, there was liquid in each disc; the mixing state could be different from that of the liquid present outside the disc; this volume would be considered the number of discs. Also, there would be axial flow into and out of discs through the perforations provided on the discs, in addition to the bulk flow between the disc edge and trough wall. The percentage of disc submergence in the liquid and disc diameter would also influence the model parameters n, α, and β, which was not considered in this work.

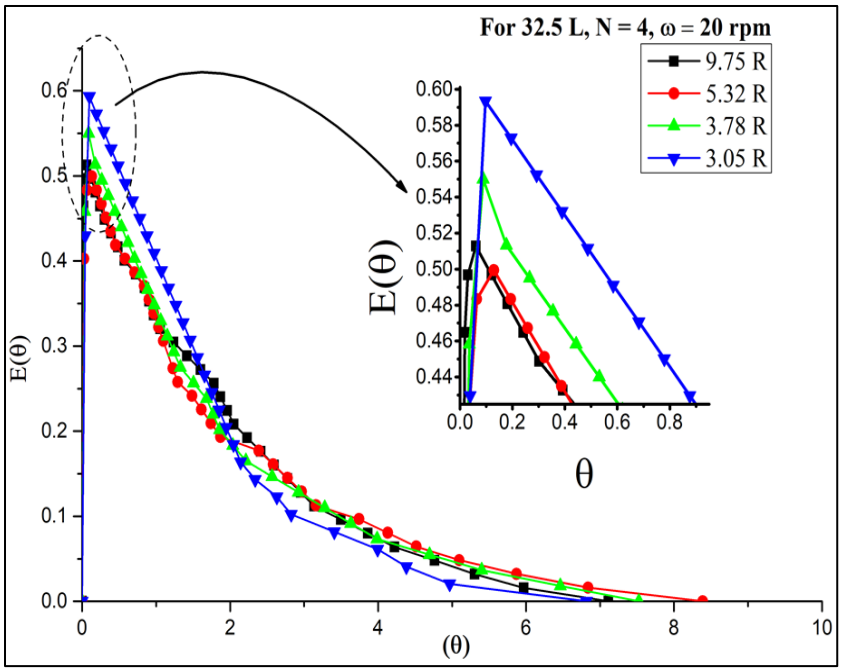

(a)

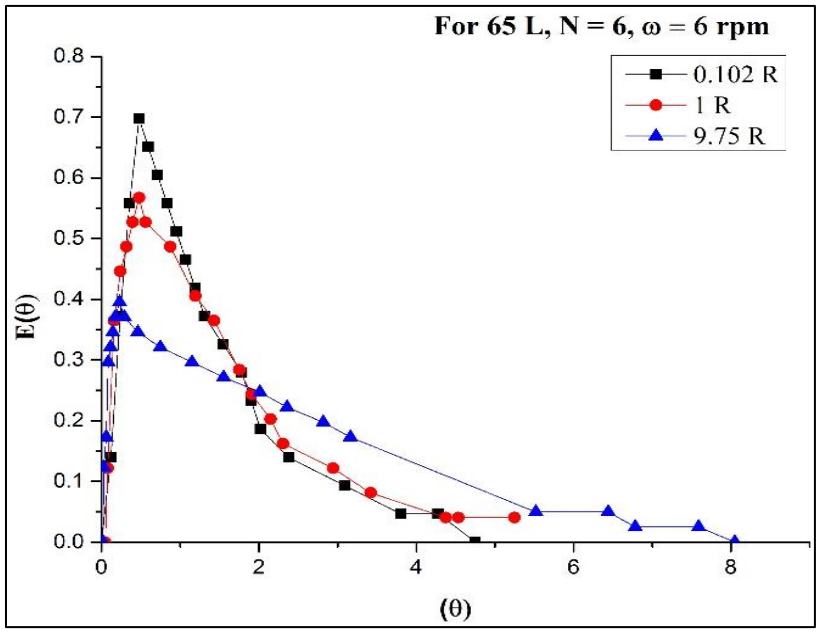

(b)

Figure 5.4: Influence of recycle ratio (R) on exit age distribution: a) for 32.5 L; b) for 65 L.

5.2. Oxygen transfer rate studies

5.2.1. Effect of rotational speed on k_La and oxygen transfer rate

Figure 5.5 shows the effect of rotational speed on the volumetric oxygen transfer coefficient (k_La,/min) and oxygen transfer rate (mgO_2/L/h). As expected, the k_La improved as the rotational speed increased from 10 to 60 rpm. The lowest and the highest k_La was 0.01 and 0.35 min^{-1} for 32.5 L working volume as shown in Figure 5.5 (a) and 0.02 and 0.389, /min for 65 L working volume as shown in Figure 5.5 (b), under the submergence level of 45%. Given disc submergence, the increasing rotational speed provided better liquid mixing. It increased the direct transfer of oxygen from the air into the bulk liquid due to turbulence created by the disc's revolution in the trough as described in the literature (Boumansour and Vasel 1998; Chavan and Mukherji 2008; Li et al. 2019). This effect of rotational speed is in covenant with Friedman et al., (1979), who studied the effect of rotational speed (ω) on biological contactor performance. As the rotational speed increases at a particular disc, the oxygen transfer rate improves from 26.01 - 124.25 and 32.53 – 166.69 mgO_2 /L/h for 32.5 and 65 L, respectively. The effect of rotational speed on increasing k_La is more prominent above 30 rpm. Courtens et al., (2014) studied the oxygen transfer rate for 1.8 to 3.6 rpm speed of rotation with changing the submergence level from 40 to 80% are in the range of 2.91 to 9.167 $mgO_2\ L^{-1}h^{-1}$ is comparatively lower value 19.71 - 166.69 mgO_2 /L/h obtained in this study. Moreover, the k_La values have an extensive range of 2.61 to 22.13 /h in this study by changing the rotational speed at a specific number of discs. In a conventional rotating biological contactor, the value of k_La in the range of 0.72 to 2.88 /h (Mathure and Patwardhan, 2005).

5.2.2. Effect of number of discs on k_La

Figure 5.6 explains the impact of a number of discs on the k_La. The disc numbers varied from 2 to 4 for 32.5 L working volume and from 4 to 8 for 65 L working volume shown in Figure 5.6 (a) and (b). At a constant speed and particular submergence, the oxygen transfer rate increased from 67.66 to 124.26 mgO_2 /L/h for 32.5 L and 126.35 to 166.69 mg O_2 /L/h for 65 L.

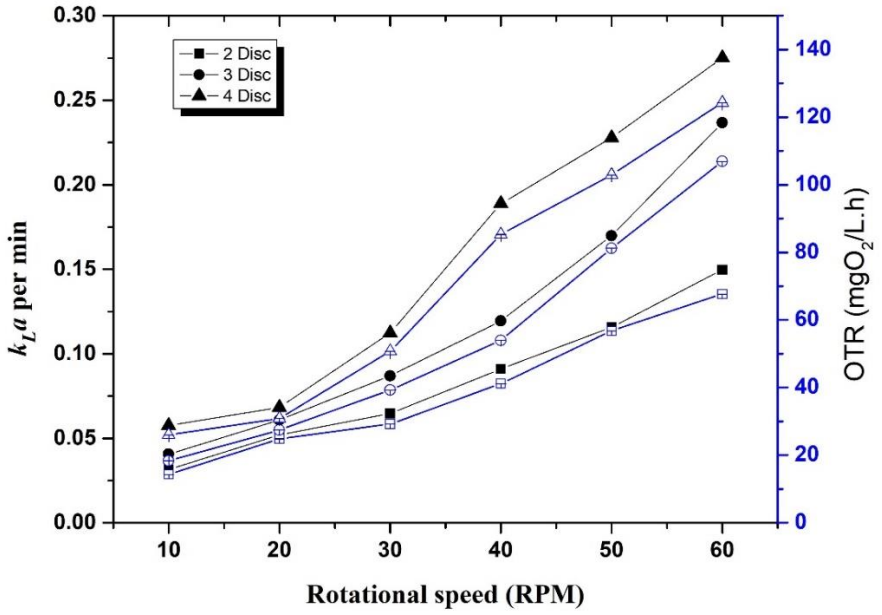

(a)

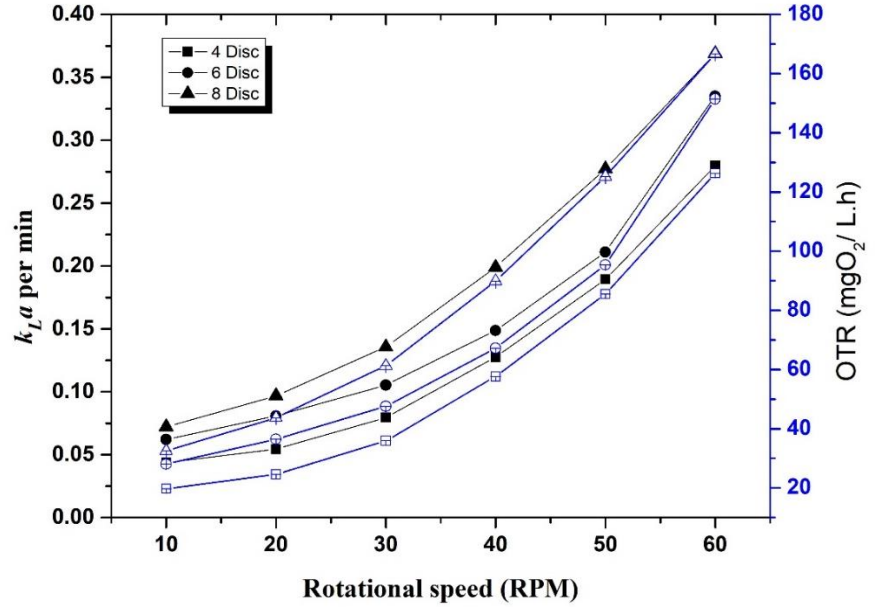

(b)

Figure 5.5: Inffluence of rotational speed and Number of the disc on $k_L a$ and oxygen transfer rate (OTR) value for volume 32.5L (a) and 65L (b).

This is because the gas-liquid contact area, i.e., the exposed liquid film area to the atmospheric oxygen, goes on the increase as the number of disc increases (Mathure and

Patwardhan 2005). Bintaja et al., (1975) and Yamane and Yoshida, (1972) reported that the liquid film thickness over the discs and rotational speed of the discs play a vital role in enhancing the k_La. They reported that the liquid film is established on the disc while the disc moves upwards. This liquid film formed on the disc absorbs atmospheric oxygen and transfers to the bulk liquid in the RBC. Moreover, the discs break the water surface while moving downwards, thus creating turbulence and also suggested to increase the gas-liquid contactors by reducing dead-end volume (Chavan and Mukherji 2008; Mathure and Patwardhan 2005). At a constant speed and particular submergence, the oxygen transfer rate increased in both working volumes. Thus, the more the number of discs, the higher the *kla* of a given RPDB.

5.2.3. Effect of the recycle feed on the k_La

The recycle feed effect was studied at two recycle feed flow rates 6 and 58.5 (L/h), respectively. The results are shown in Figure 5.6. Recycle ratio had a positive influent on the oxygen volumetric mass transfer coefficient at all operating conditions. As the recycle ratio increased, the k_La value also increased. There was about a 10 to 15% increase in k_La due to the recycle ratio. The high liquid flow rate created turbulence on the liquid surface, which lead to increased oxygen transfer from air to liquid. Lewis and Borole (Lewis and Borole 2016) Observed that mass transfer transitions were found at the low liquid flow rate. These were alleviated using high flow rates and a combination of a high flow rate with the recycling condition. This achieved high COD removal up to 74.2 % and improved hydrogen production rate from a switchgrass-derived stream in the biorefinery. In another study, the recycle feed was more effective in the oxygen and nutrient transfer in the biofilm, and as a result, substrate removal efficiency improved (Confer and Logan 1998; Klees and Silverstein 1992). Dutta et al. (Dutta et al. 2007), Klees and Silverstein (Klees and Silverstein 1992), and Tawfik et al. (Tawfik et al. 2006) observed that as the recycle feed of nitrified effluent from the 3rd stage to the 1st stage increased ammonia removal in stage 1 from 23 to 43% in the RBC system.

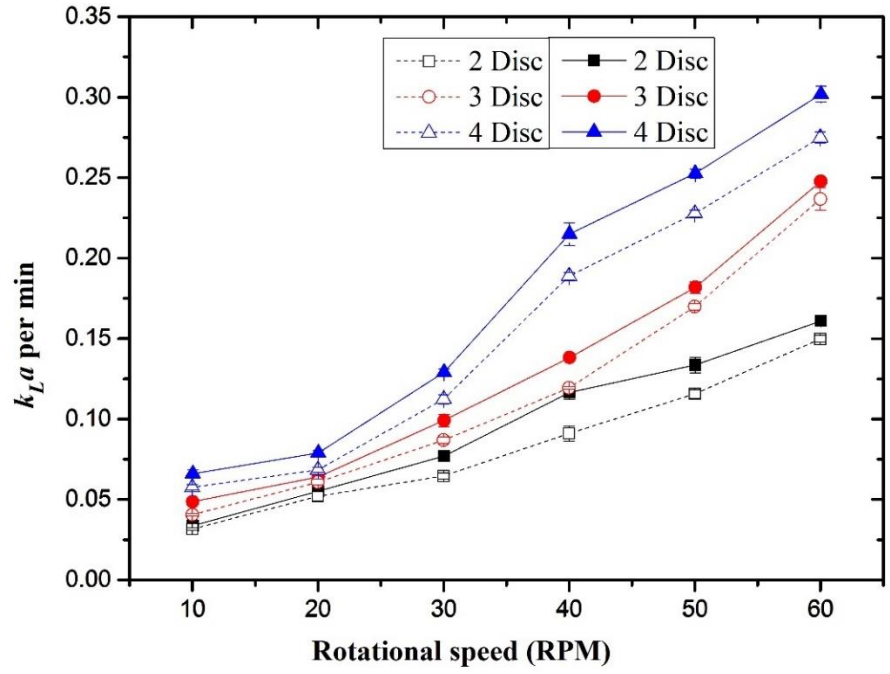

(a)

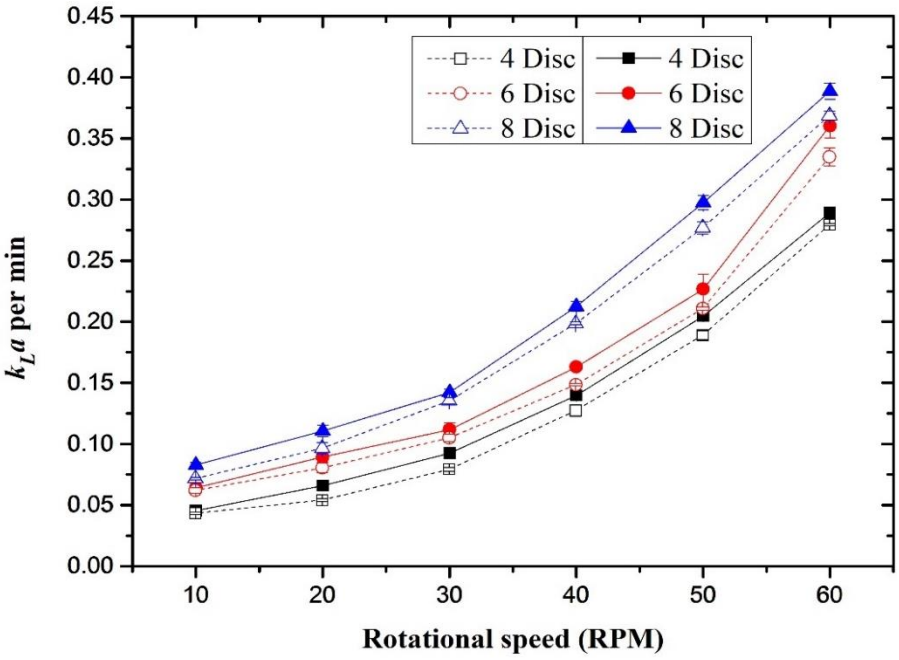

(b)

Figure 5.6: Inffluence of recycle stream on $k_L a$ value for volume 32.5L (a) and 65L (b). Solid symbols indicate RPDB operation with the recycle (58.5 (L/h)), and Open symbols indicate RPDB operation without the recycle.

The findings indicate that the recycle ratio has a positive influence on k_La, due to which the performance of RPDB also improves. Moreover, the recycle feed also increases suspended solids in the liquid, further improving RPDB performance (Neu 1994).

The obtained k_La values from this study are compared with the reported values of k_La in conventional RBCs in Table 4.2. All these studies were done using tap water and clear discs filled with solid materials. The highest k_La of 0.48 min^{-1} was reported at 55 rpm and using 21 discs in an RBC with a working volume of 32 Liters (Mathure and Patwardhan 2005). The highest k_La value of 0.389 min-1 is reported at 60 rpm using only 8 discs in the present work as shown in Figure 5.6(b). This high k_La value is due to the modified disc design as well as the recycle ratio. Each hollow disc was filled with 1.8 kg of spherical low-density polyethylene beads of 4.5 mm diameter and a density of 0.45 g/cm^3.

Table 5.2: Comparison of the k_La values reported by different researchers

Authors	**Working volume (L)**	**RPM**	**Number of discs**	**Highest k_La value(1/min)**	**Lowest k_La value(1/min)**
Boumansour and Vasel (1998)	2.9	35	09	0.24	0.06
Paolini (1986)	7.4	25	11	0.23	0.017
Bintaja et al. (1975).	26	35	10	0.28	0.043
Hewawasam et al. (2017)	110	0.66	32	0.07	0.014
Chavan and Mukherji (2008)	4	60	27	0.27	0.035
Kubsad et al. (2004)	24	60	42	0.25	0.028
Present study	65	60	8	0.39	0.048

The surface area for the transfer of oxygen from the air to the water film formed on the beads was about 1.46 m^2. This was about four times higher than the surface area of a similar size standard disc used in a standard rotating biological contactor. The vanes mounted on the disc also improved radial mixing. Both these effects enhanced the oxygen volumetric

mass transfer coefficient. Since fewer discs are required to achieve comparable k_La, the effective working volume of the RPDB would be more than the conventional RBC system. Several researchers reported empirical and theoretical models for the oxygen volumetric mass transfer coefficient in the RBCs such as (Boumansour and Vasel 1998; Chavan and Mukherji 2008; Kim and Molof 1982; Kubsad et al. 2004; Paolini 1986; Suga and Boongorsrang 1983; Taylor et al. 1985; Yamane and Yoshida 1972). The most recent model was developed by Chavan and Mukherji (2008) as shown in equation 5.1, which has the advantage of being dimensionless and incorporates the effects of essential parameters, as reported in the previous literature.

$$\left(\frac{k_L a\ \rho A_d}{\mu}\right) = \left(\frac{D}{A_d^{0.5}}\right)^{-0.327} \left(\frac{\rho\ A_d \omega}{\mu}\right)^{1.018} \left(\frac{A_d}{A_t}\right)^{0.624} \left(\frac{\delta}{V^{\frac{1}{3}}}\right)^{0.743} \quad (5.1)$$

The most recent model developed for RBC showed that their correlation is also valid for the data from other literature reported. Hence, the correlation was adopted to fit the experimental data of this work to predict oxygen volumetric mass transfer more accurately. Equation 5.2 demonstrates the empirical model for the volumetric oxygen transfer coefficient. In equation 5.2 the first four terms on the right-hand side are used in the Chavan and Mukherji model. Chavan and Mukherji used the exposed surface area of the disc in the model. Since the discs used in this study were filled with packing material, the surface area available because of the packing material is also included in the exposed surface area of the disc. Moreover, the recycle stream was also incorporated into the model. The following equation was derived after incorporating the mentioned changes.

$$\left(\frac{k_L a\ \rho A_d}{\mu}\right) = \left(\frac{D}{A_d^{0.5}}\right)^{-0.202} \left(\frac{\rho\ A_d \omega}{\mu}\right)^{0.705} \left(\frac{A_d}{A_t}\right)^{0.501} \left(\frac{\delta}{V^{\frac{1}{3}}}\right)^{1.01} \left(1 + \frac{R}{V.\omega}\right)^{0.045} \quad (5.2)$$

Where, R = Recycle flow rate (L/min)

The coefficients of model terms (equation. 5.2) are different from those reported by Chavan and Mukherjee. This could be because of the disc's modified design and the different surface area available for oxygen transfer. The recycle stream had a positive influence on

k_La, which is evident from the recycle stream's coefficient value of 0.2. Figure 5.7 shows the experimental data with the model predicted values of k_La. As Figure 5.7 shows, the model fits very well with the experimental data as almost all data points lie within the ±20% range.

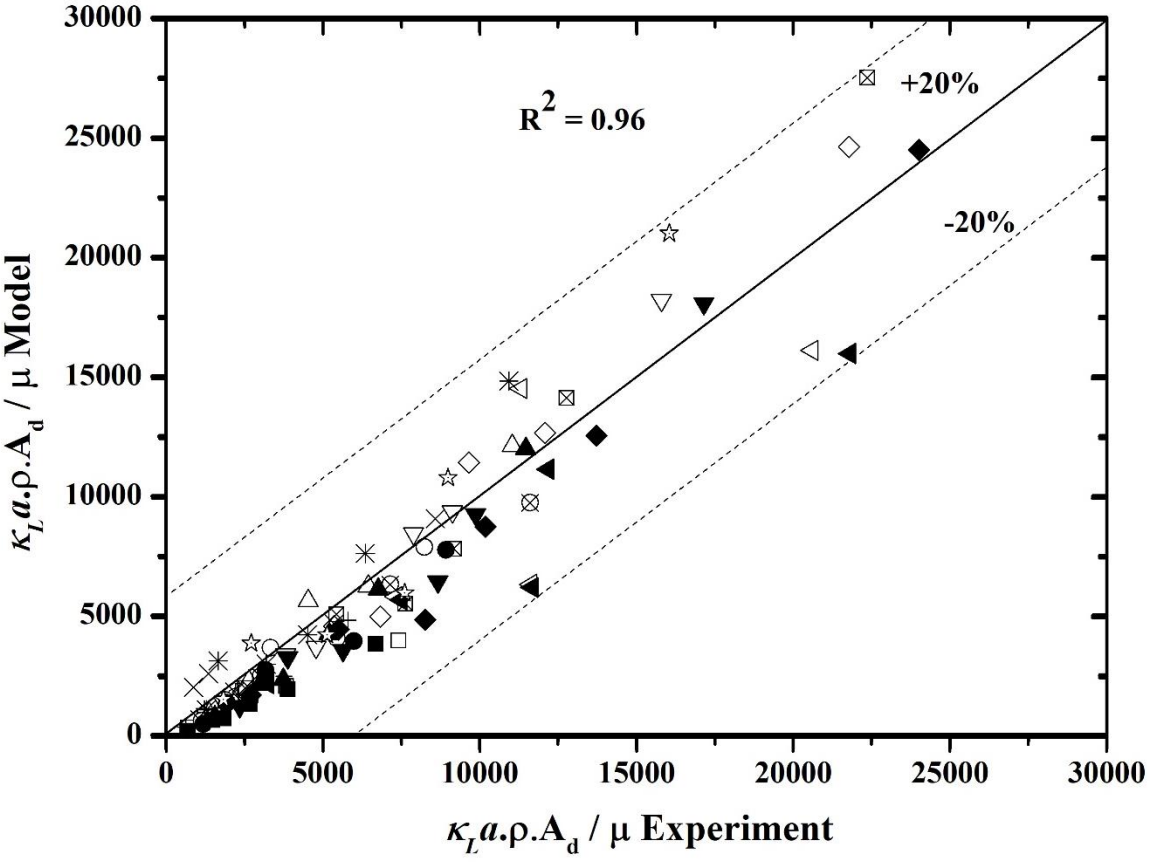

Figure 5.7: Parity part showing experiment and model predicated value of oxygen volumetric mass transfer coefficient (k_La) with two different recycle ratios. Solid symbols indicate, 58.5 (L/h) recycle stream (■ (10rpm),● (20rpm),▲ (30rpm),▼ (40rpm),◆(50 rpm), and ◀ (60 rpm)), Open symbols indicate, 6 (L/h) recycle ratio (□(10 rpm),○(20 rpm),△(30 rpm),▽(40 rpm),◇(50 rpm), and◁(60 rpm)) and symbols for without recycle (+(10 rpm),×(20 rpm),✳(30 rpm),✯(40 rpm),⊠(50 rpm), and ⊗(60 rpm)).

The results reveal that the novel disc design improved the oxygen transfer rate by almost four folds compared to the standard RBC. The required number of discs were only 6 to

achieve the highest oxygen transfer rate in the present scenario, whereas standard RBC requires about 22 discs to achieve the equivalent oxygen transfer rate. Thus, the new disc design also provides more liquid volume to work with because space utilization by the disc is reduced considerably. The number of discs, revolutions per minute, and the recycle ratio positively influenced on the oxygen transfer rate. Since aerobic degradation of any effluent is dissolved oxygen-dependent, and the dissolved oxygen is always the limiting factor for degradation, the present design offers four times more efficient degradation than the conventional rotating biological contactor. The azo dye effluent was treated in the bioreactor to assess the performance of the bioreactor. Although the increased revolutions of the discs provide increased oxygen transfer rate, the study of biological degradation was limited to 40 rpm only because of the effluent's spillage.

5.3. Biodegradation of Reactive Black-5

5.3.1. Growth and Dye Degradation on Solid Media

Both species showed little to no retardation in growth rate when grown on respective media with varying dye concentration. It was difficult to notice any minor decrease in the growth rate of *P. chrysoporium* because it would cover the plate within 2 days after inoculation. However, data of the minor reduction in the growth rate of *T. versicolor* could be obtained. The minor differences observed in the area covered in the presence and absence of dye could be due to dye interference with the nutrient uptake (Barr and Aust 1994). Figure 5.8 shown the visible degradation of various concentrations of dye added to solid media. Both species of fungi were able to degrade dye but at different rates. *P. chrysosporium* was able to degrade the varying dye concentrations much before *T. versicolor*. Although there was variation in the rate of degradation among triplicates, they were minor, and ultimately degradation was achieved in all. Studied dye degradation of concentrations of 30 mg/L (Figure 8), 60 mg/L, and 100 mg/L in solid media. Degradation was achieved for all concentrations though the rate of degradation was different.

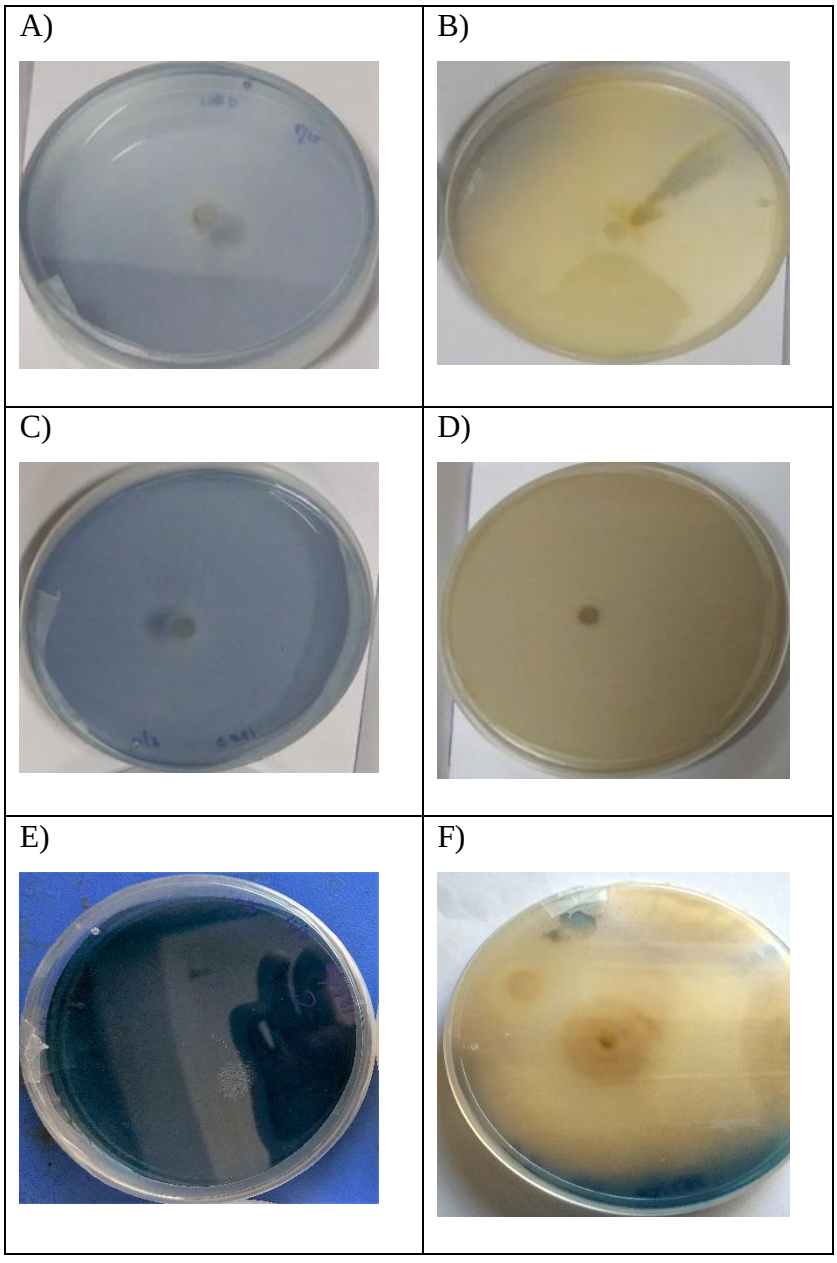

Figure 5.8: Dye (30mg/L) degradation by *T. versicolor*, day 1(A) and day 7 (B); *P.chrysosporium* day 1(C) and day 7(D), Mixed culture day 1(E) and day 7(F).

5.3.2. Growth and dye degradation in liquid media

Ideally, both fungi formed flocs when cultured in respective liquid media. The flocs were of varying size, and varying dye concentrations had no visible effect on floc density. Both

fungi were cultured successfully on media using different types of inoculums such as by spores, flocs, and agar discs with dye concentration ranging from 30mg/L to 100 mg/L

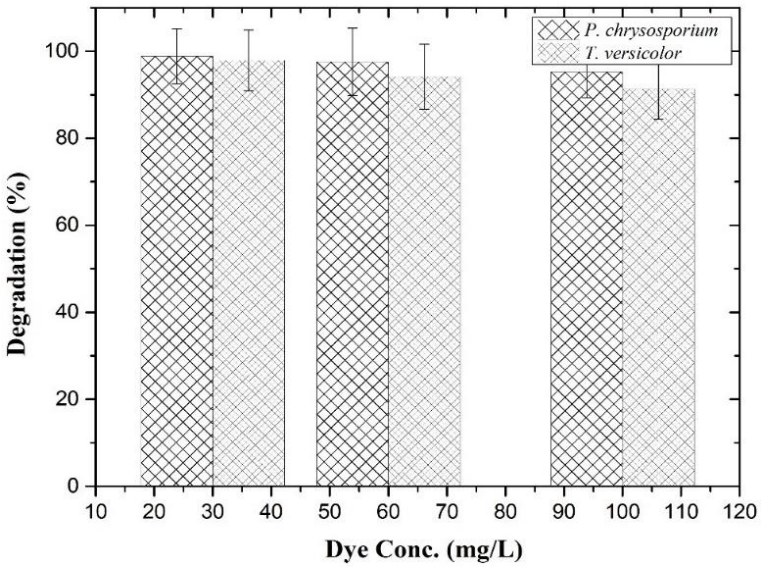

Figure 5.9: Degradation of dye by *P. chrysosporium* and *T. versicolor* (day 7) (inoculation by discs).

Among this inoculation of liquid cultures by agar discs yielded better results than those obtained for inoculation by flocs. Inoculation of all flasks was also uniform since the disc size of each agar disc was the same. Moreover, it was certain that all the inoculum was in the same stage of the life cycle since they were all bored at the external periphery of the same culture. Figure 5.9 shows the highest degradation achieved in this form of inoculation was 99% and 97% by *P. chrysosporium* and *T. versicolor*, respectively, 7 days post-inoculation. At the end of the 7 days growing period with glucose concentration a huge amount of biomass observed having compact pellet form with an average diameter of 3.05 ± 0.5 mm. Which indicate that a high concentration of oxygen tends to lead the formation of compact pellet form of fungi. The total amount of biomass obtained in this study was 3.5 ± 0.5 g/L, all in the form of pellets. Obtained biomass concentration played important role in decolourization of dye. Methanol extraction revealed that there was the bare minimum of dye that was adsorbed on to the fungal biomass after degradation. From the various flasks containing increasing dye concentration (30 mg/L, 60 mg/L and 100 mg/L),

the maximum absorbed dye concentration was up to 2mg/L for *P. chrysosporium* and 1mg/L for *T. versicolor*.

5.3.3. Degradation in the shake flask

Reactive black-5 is a complex organic compound with different aromatic rings and functional groups (-N=N-) that make it quite resilient to the conventional form of biodegradation (Lucas and Peres 2006). It was observed that the fungal cells show great potential for the removal of various azo dyes from textile wastewater effluents. The degradation of Reactive Black 5 was examined by individual fungi and mixed fungi culture (inoculated by agar disc) in the sterile conditions with the optimum malt extract medium at 30, 60, and 100 mg/L dye concentration. Degradation was allowed to proceed for 7 days, but day 5 data shown in Figure 5.10.

5.3.3.1. Comparative study of the decolorization of RB-5 by using individual fungal culture (*P. chrysosporium and T. visicolour*) and mixed fungal culture

Figure 5.10 shows the mixed fungal culture *(P. chrysosporium and T. visicolour)* with a high decolorization efficiency of 100 mg/L RB-5 was obtained in the sterile enrichment cultivation 5 days as compared to individual fungal strain. Figure 5.10 (a) shown that the individual fungal strain decolourizes 90% and 80% for *P. chrysosporium* and *T. visicolour*, respectively, was significantly lower than that observed for mixed fungal culture 5 days. Above 90% decolourization of reactive black 5 azo dye was reached after 5 days in the mixed fungal strain, indicating an improvement in biomass concentration compared with the induvial fungal culture. The total biomass obtained in the mixed fungal culture was 4.02± 0.50 g/L all in the form of pellets.

Improved decolorization efficiency of various azo dyes by using mixed fungal culture has been reported earlier(Huijun and Xuemei 2007; Karunya et al. 2014; Nascimento et al. 2011; Przystaś et al. 2013; Yang et al. 2009a). In this study, we observed that the mixed culture decolorized 100% RB-5 within 5 days with a maximum decolorization rate of 0.04 per h; on the other hand, the *P. chrysosporium* 0.02 per h and *T. visicolour* 0.19 per h required more time (more than 7 days) to achieve overall decolorization. The rate of decolorization higher for mixed culture due to the synergetic action of microbial enzymatic

activity. was observed by Saratale et al., (2009) explain that. Also observed that the microorganisms' biodiversity helps to attack at different positions of the dye molecules and reduced stress between connecting dye molecules (Nascimento et al. 2011; Saratale et al. 2011b; Yang et al. 2009a)

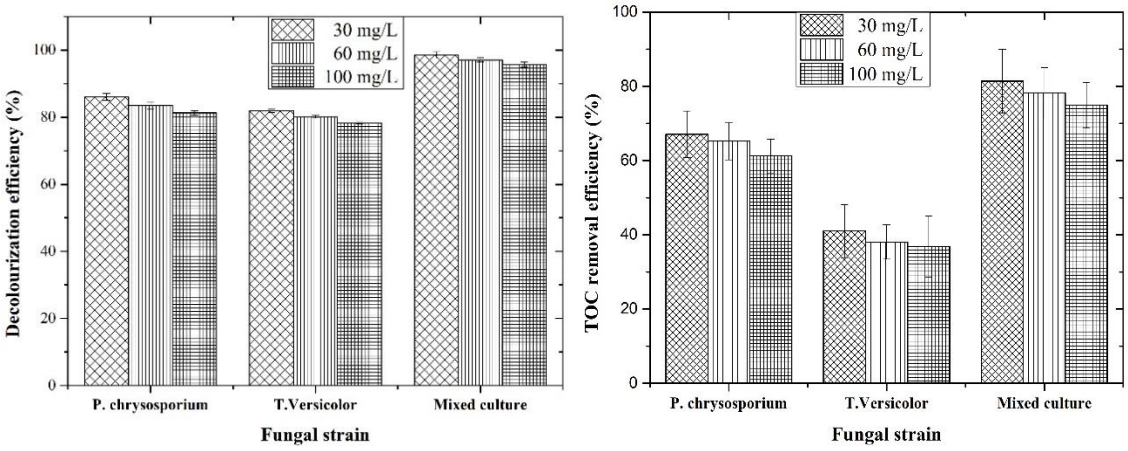

(a) (b)

Figure 5.10: Degradation of RB-5 studies in shake flask: (a) decolorization of RB-5 dye (30,60 and 100mg/L) by using *P. chrysosporium*, *T. versicolor, and mixed culture.* (b) TOC removal efficiency for different dye concentrations (30,60 and 100 mg/L) by using *P. chrysosporium*, *T. versicolor,* and mixed culture.

The result confirmed that the mixed culture was more efficient than using individual fungal strain (Nascimento et al. 2011; Yang et al. 2009a).

5.3.3.2. Effect of initial dye degradation

Figure 5.10 shows the percentage of decolorization of the effluent containing Reactive black-5 dye, with the individual and mixed fungal culture with five days of treatment in Showssterile condition. Figure 5.10 (a) observed that the treated effluent with P. *chrysosporium* and T. *versicolor* fungal strain degrades more than 85% up to 100 mg/L dye concentration solution. However, the mixed culture of *P. chrysosporium* and *T. versicolor* decolorized 100% of dye in 5 days.

The individual and mixed fungal cultures was tested for degradation of azo dye RB-5 by using TOC analyzer. Figure 5.10 (b) indicated that the mixed culture have a higher degradation of 100 mg/L of RB-5 with a significant TOC reduction above 75% within 5 days. The TOC removal of RB-5 by using individual culture was 62% (*P. chrysosporium*) and 35% (*T. versicolor*), respectively, as shown in Figure 5.10(b). However, the effluent TOC value obtained with individual fungi culture was higher than the mixed culture due to its synergistic effects on microorganisms to tolerate the toxic effects (Krishnamoorthy et al. 2018; Saratale et al. 2009; Yang et al. 2009b). There was a notable difference in the biomass obtained for both fungi; because of that, specific degradation of the fungi differed for similar dye concentrations.

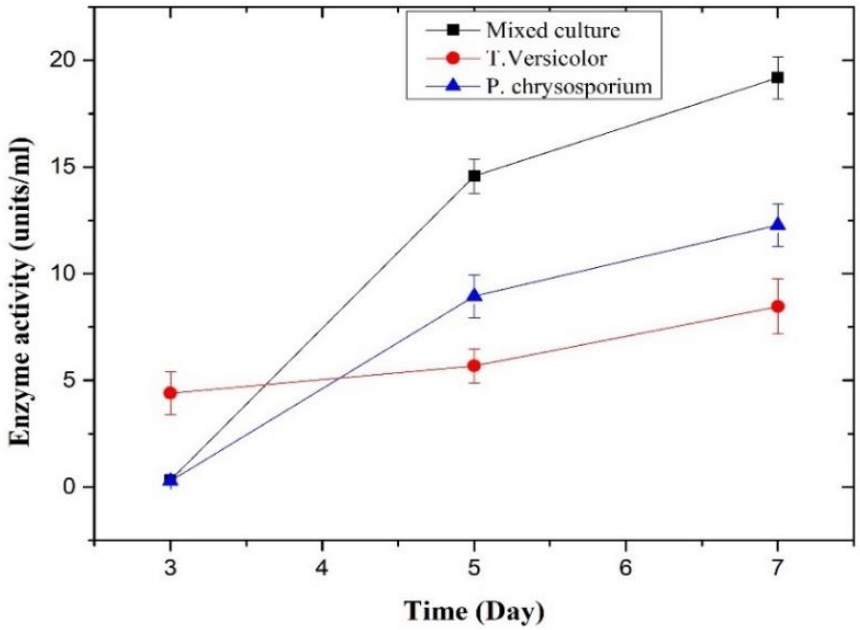

Figure 5.11. LiP enzyme activity in the presence of RB-5 dye at 100 mg/L.

The decolorization of RB-5 over a range of concentration between 30 to 100 mg/L at 28 °C, pH 5.8, was studied with an individual and mixed culture, as shown in Figure 5.11. This suggested Lip activity of mixed culture higher (19.17units /ml) compared to individual fungi due to multiple substrate-binding sites. Also, Lip's are stronger oxidants with higher redox potential as compared to usual peroxidases and have a porphyrin ring with an iron, which are more electron deficient than in usual peroxidases (Datta et al. 2017; González-

Ramírez et al. 2014; Millis et al. 1989; Moldes et al. 2012; Moldes and Sanromán 2006; Singh et al. 2015).

The degradation efficiency of RB-5 in mixed culture was increase with increased the LiP activity, within 5 days as shown in Figure 5.11. Although, for *P. chrysosporium,* LiP was found to be responsible for the degradation of the dyes, in agreement with the result reported previously for *P. chrysosporium* (Cripps et al. 1990; González-Ramírez et al. 2014; Podgornik et al. 1999; Spadaro et al. 1992). Whereas, degradation percentage of RB-5 by *T. versicolor* range was less than 50% as given in Figure 5.10 (b) due to lack of enzyme production, or it is produced and not released from the mycelium, or that it is produced and released, but the medium inhibits its detection (Abdel-Raheem and Shearer 2002; Egger 1986; Pointing 1999). Also, intermediate toxic metabolites formation could be the reason for the less degradation by *T. vesicular* (Daveetal.,2015).

5.3.3.3. Prediction of degradation pathway of RB-5 by using LC-MS/MS

Metabolite analysis of the degradation of RB-5 dye by individual and mixed culture was monitored by LC-MS/MS analysis. Appendix Figure B.1 shows molecular mass spectra of intermediate products obtained from single cultures of *P. chrysosporium* and *T. versicolor* on 5^{th} day. As shown in Figure B.1, the fragmentation analysis revealed peaks of higher m/z ratio, such as 665, 405, 305, 373, and 175. The mass 175 corresponds to 8-amino-naphthalene-1,2-diol, and 305 corresponds to 4-sulfooxyethylsulfonyl-1-phenol.

This proved that *T. versicolor* produced a laccase enzyme, which acts upon azo bond present in the dye but could not completely degrade it. Accumulation of toxic phenolic chemicals might be the reason for partial degradation and reduced TOC removal by *T. versicolor*. As shown in Figure B.2, similar peaks were observed in *P. chrysosporium* cultures, which confirmed enzymatic reaction by laccase. However, there was also a significant peak of mass 209 and 94 units. These peaks suggest that the cultures further oxidized 8-amino-naphthalene-1,2-diol to 2-amino-6-(2-carboxy-ethyl)-benzoic acid and phenylamine. Thus, cultures of *P. chrysosporium* were able to degrade the dye to lower molecular weight compounds but could not completely oxidize the residues.

However, no significant metabolite peaks were detected in the mixed cultures suggesting complete degradation of the RB-5. This degradation mechanism (Figure 5.12) was also observed by Adnan et al. (2014), although they used a different WRF culture. These findings suggest that different WRF cultures may have a similar mechanism for azo dye degradation.

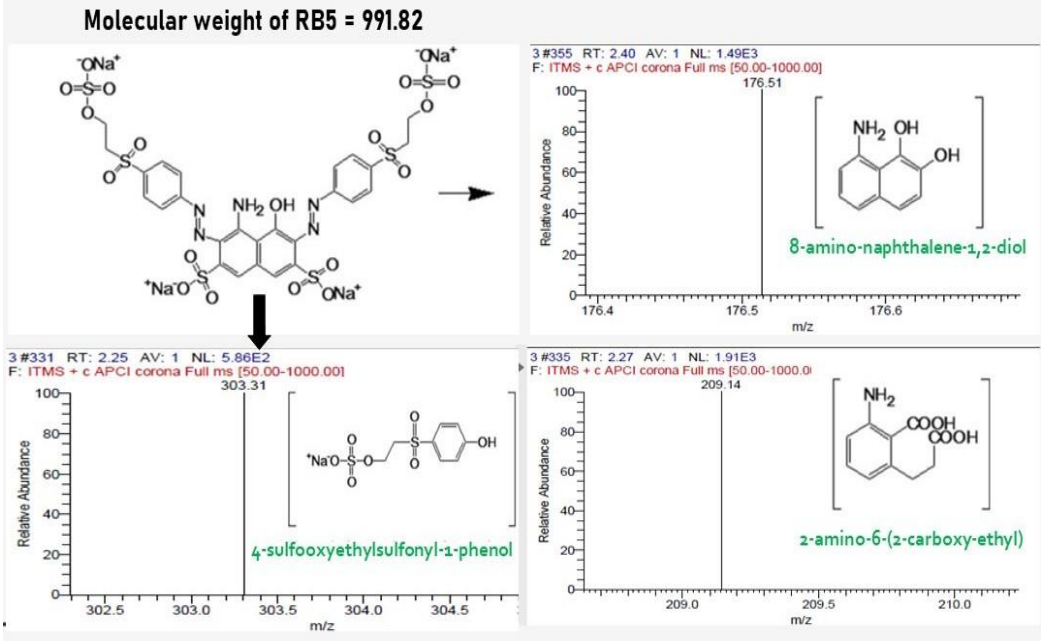

Figure 5.12. Mass/charge ratios detected for a degraded (by Mixed culture) RB5 sample, post-extraction

Efficient and complete degradation of RB5 in the mixed culture was due to the synergistic action of microbial consortia to tolerate the toxic effects (Krishnamoorthy et al. 2018; Saratale et al. 2009; Yang et al. 2009b). Therefore, further studies were performed using a mixed culture system.

5.3.3.4. Determination of reaction order for Reactive Black-5 degradation:

The rate constants *(k)* of decolorization experiments and coefficients of least square method analysis for individual and mixed fungal cultures are tabulated in Table 5.3. The correlation coefficients R^2 lies between 0.93 to 0.97, which suggests that the RB-5 decolorization at various concentration was the first-order reaction kinetics for individual and mixed fungal

culture. The reaction rate of decolorization is inversely proportional to the initial dye concentration. Also, found the first-order kinetics in other literature concerning dye concentration(Weber and Lee Wolfe 1987; Wuhrmann et al. 1980; Yang et al. 2016; Van der Zee et al. 2001).

Table 5.3 Kinetics of decolorization of RB-5 under the various concentration

Fungal culture	**Constants**	**Concentration (mg /L)**		
		30	**60**	**100**
Phanerochaete chrysosporium	k_0 (mg/L/h)	0.91	0.39	0.64
	R^2	0.91	0.91	0.90
	k_1 (1/h)	0.015	0.015	0.015
	R^2	**0.94**	**0.97**	**0.98**
	k_2 (L/mg/h)	0.0022	0.001	0.0005
	R^2	0.59	0.80	0.80
Trametes versicolor	k_0 (mg/L/h)	0.18	0.013	0.61
	R^2	0.96	0.93	0.93
	k_1 (1/h)	0.013	0.014	0.012
	R^2	**0.96**	**0.97**	**0.98**
	k_2 (L/mg/h)	0.0015	0.0008	0.0003
	R^2	0.55	0.77	0.77
Mixed culture	k_0 (mg/L/h)	0.22	0.43	0.72
	R^2	0.86	0.86	0.87
	k_1 (1/h)	0.026	0.026	0.026
	R^2	**0.91**	**0.93**	**0.89**
	k_2 (L/mg/h)	0.0149	0.0072	0.0057
	R^2	0.56	0.53	0.36

5.3.4. Bioreactor studies

This section includes the biodegradation studies carried out in a rotating packed disc bioreactor for reactive black – 5 azo dye using immobilized mixed fungal culture on

activated carbon. The bioreactor's hydrodynamics and mass-transfer characteristics were studied at a different feed flow rate and rotational speed with the influence of the recycle stream. Based on hydrodynamic investigations, the recycle ration provides better mixing by the circulation of the fluid at a high flow rate and generates turbulence in the mixed liquor surface, increasing the surface volume mass transfer(Kalnake et al. 2020). Moreover, the effect of rotation provides better aeration by exposed liquid film into the air by completes its full cycle. Thus, it was decided to use this reactor consisting of hollow discs filled with the fungi immobilized on the granular activated carbon (GAC) to biologically degrade the synthetic azo dyes. The performance of the bioreactor is investigated by a percentage reduction of color and COD. The bioreactor is investigated and compared for batch and continuous operation.

5.3.4.1.Biodegradation studies in batch operation

The initial concentration of 30 mg/L reactive black-5 dye with a mixed fungus culture was grown as a suspension culture in the rotating packed disc bioreactor. Each experiment was continuous operation until the seventh day to maintain continuity. The effluent dye concentration, COD, dissolved oxygen, pH, enzyme activity, reduced sugar, and TOC, was measured. The results obtained from the bioreactor are reported in Appendix-II. The initial concentration was maintained constant (30 mg/L), the dissolved oxygen concentration ranging between 2.5 to 7 mg/L for different recycle feed from 6 to 58.5 L/h.

5.3.4.1.1. Effect of rotational speed

Figure 5.13 shows the degradation of RB-5 by using a mixed culture system in a batch mode of operation at different rotational speeds of 10 to 30 rpm. Higher rotational speed had a positive influence on the removal of color and COD. The results reveal that the COD removal efficiency increased from 64.5% to 90.6% for a rotational speed of 30 rpm, as shown in Figure 5.13 (a). This increase in degradation efficiency was correlated with the dissolved oxygen concentration and enzyme activity profile. The DO values were consistently higher at 30 rpm as compared to 10 and 20 rpm. The DO was 3.9 - 7 mg/L at 30 rpm compared to 2.5 - 6 mg/L at 10 rpm, shown in Figure 5.13 (b). In the presence of

oxygen, the intermediate degradation of the azo bond occurred through the laccase enzyme. During the degradation experiments, the activities of the enzymes involved in dye degradation were determined. LiP activity varied from 5.67 – 8.11 unit/mL at 30 rpm compared to 5.1 – 7.14 unit/mL at 10 rpm are shown in Figure 5.13 (c). Thus, increased DO concentrations improved the azo bond degradation. Moreover, it also improved the diffusion of oxygen into the biomass's inner layers formed on the GAC's surface, which imparted more active biomass. The TOC removal efficiency was around 80%, as shown in Figure 5.13 (d). Tang et al. (2015) reported a 68% increase in chloroacetic acid's removal efficiency by increasing the DO concentration. Israni et al.(2002) (Israni et al. 2002) also found that as dissolved oxygen increased from 2.4 to 4.8 mg/L, an increase in the amount of removal from 30.9 mg/L to 114 mg/L in the RBC.

5.3.4.1.2. Effect of recycle stream

In the batch reactor operation, three recycle ratios; namely, 1, 5.18, and 9.75 were investigated. The objective was to compare the effect of the recycle ratio on the efficiency of the RPDB. The significant COD reduction was observed at a 9.75 recycle ratio, and therefore, only the 9.75 recycle ratio data are compared at the rotational speed of 10, 20, and 30 rpm in Figure 5.14 (a). During seven days of batch operation, COD removal efficiency increased as shown in Figure 5.14 (a). As the recycle ratio increased, the DO also increased. As shown in Figure 5.14 (b). The recycle ratio improved mixing in the trough, which in turn improved DO concentration, which helped in dye degradation. The improved mixing provided better diffusion of dye, oxygen, and media components into the active biomass's inner layers, which resulted in an overall increase in dye degradation by about 10 to 12% compared to that without recycling.

The overall production of LiP and MnP enzyme activity in the recycling was relatively high compared to that without recycle stream that helped mineralize the dye components. Researchers also reported improved ligninolytic enzyme activities in the presence of the recycle stream. (Asses et al. 2018; Kabbout and Taha 2014; Sarkar et al. 2017). LiP activity was high under the carbon limiting conditions, which proved that the fungus produces more

LiP activity under nutrient (carbon and nitrogen) limiting conditions (Pakshirajan and Kheria 2012).

Figure 5.14 (c) reveals that at 9.75 recycle ratio and 30 rpm, LiP activity was maximum. Also, in Figure 5.14 (d), the TOC removal efficiency was 71.3%, 78.3%, and, 86.4%, with a high recycling ratio at 10, 20, and 30 rpm, respectively RPDB.

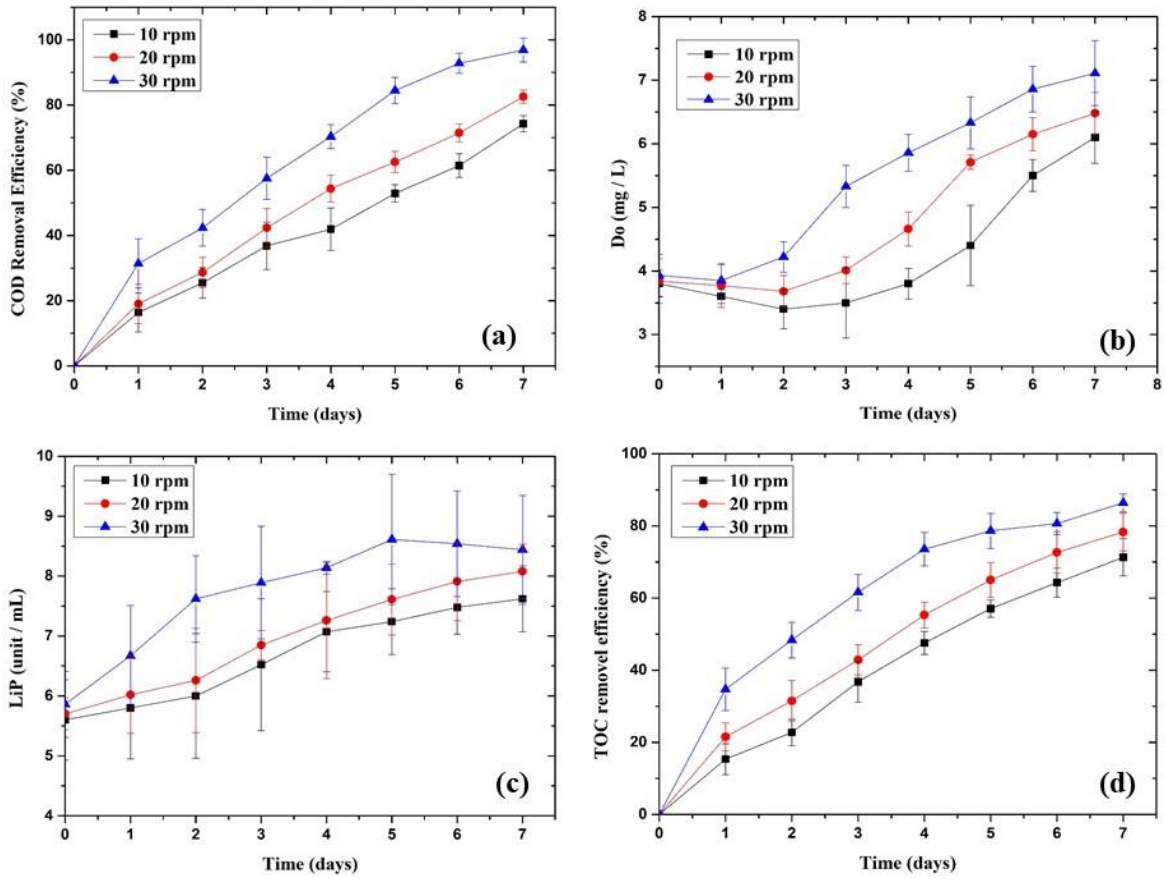

Figure 5.13. Effect of rotational speed on the COD removal (a), DO(b), LiP activity (c), and TOC removal efficiency (d) by using immobilized mixed culture in a batch operation.

Significant variation in TOC was observed between the recycle ratio of 1, 5.18, and 9.75. Results indicate a higher reduction of TOC (86.4%) at 9.75 recycle ratio and 30 rpm, which correlated with the higher dissolved oxygen.

Figure 5.15 is an SEM image of mixed culture immobilized on GAC particles. The fungal cell's growth can be observed on GAC's surface (Samples have been collected after 7 days from a 65-litre vessel that contains a feed concentration of 30 mg/L RB-5 dye).

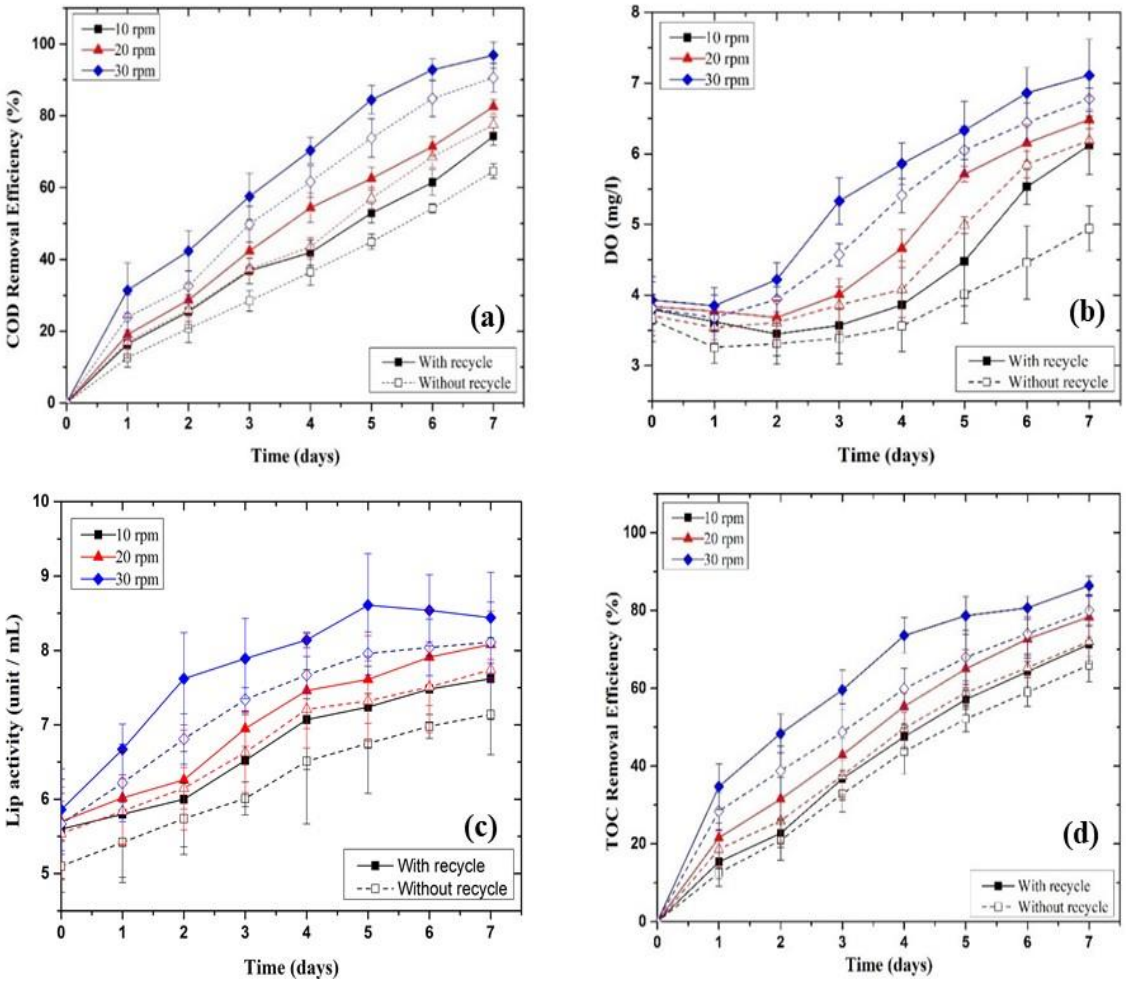

Figure 5.14. Effect of recycle feed and compared without the recycle on the COD removal (a), DO (b), LiP activity (c), and TOC removal efficiency(d) by using immobilized mixed culture in a batch operation.

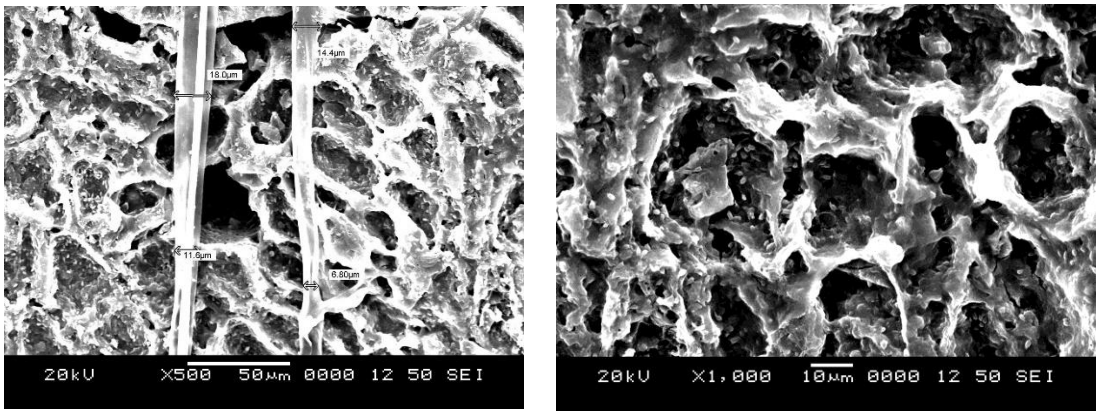

Figure 5.15 SEM of immobilized cells on granular activated carbon, the sample from 65 liters, after being fed with 30 mg/L RB-5 dye over a period of 7 days.

5.3.4.2.Continuous treatment of synthetic wastewater in RPDB

Figure 5.16 shows degradation in COD removal efficiency, DO, Enzyme activity (LiP), and TOC removal efficiency in a continuous RPDB at 30 rpm. The RPDB operation was started as a batch mode, and the enzyme activity was the highest on the seventh day of the culture. The RPDB was operated in batch mode until the seventh day, and then fresh feed was introduced with the residence time of 10.83 h. The enzyme activity and degradation reduced for a short time as expected due to washing out of the active enzymes and stabilized.

Researchers reported a positive effect of glucose concentrations up to 1 g/L on dye degradation using WRF as glucose acted as a reducing agent. Therefore, the glucose concentration in the continuous RPDB was maintained between 0.7 to 1 g/L throughout the experiment. As continuous operation started after day 7, a decrease in COD removal rate coincided with glucose depletion by day 10. As the glucose was added on day 10, the COD removal rate increased as shown in figure 5.16. To maintain a high rate of COD removal for a longer period, the fed culture of glucose adapted. In this fed-culture, a known amount of glucose was added within 3 days of the interval as shown in the vertical dotted line in figure 5.16 to prevent glucose depletion. The COD removal of more than 65% was achieved for 25 days of continuous operation. Figure 5.16 showed the effect of the recycle stream on the COD removal. The COD removal rate at 30 rpm with a 9.75 recycle ratio

experiment was 737.9 mg/L/which was the highest degradation rate of azo dye effluent reported so far in the literature under the given operating conditions.

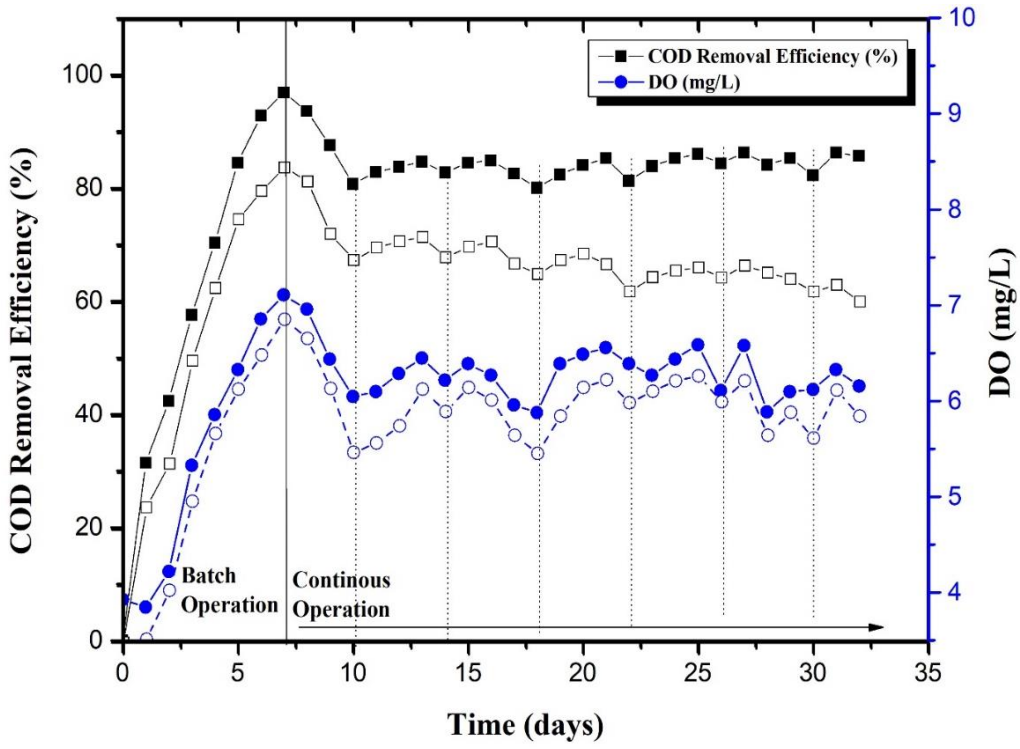

Figure 5.16. Degradation of RB-5 dye: COD removal efficiency and dissolved oxygen concentration for “with recycle” and “without recycle” stream in the continuous operation using immobilized mixed culture in the RPDB.

The recycle stream improved the COD removal efficiency by more than 80% due to improved mixing and oxygen transfer rate (Zhong 2010). The recycle stream improved steady-state DO concentrations from 4 to 6.5 mg/L, which improved dye degradation (Figure 5.16).

Researchers reported a positive influence of the recycle stream on the degradation of dyes in continuous RBC (Ayoub and Saikaly 2004; Klees and Silverstein 1992; Neu 1994). Surampalli and Baumann (1997) (Surampalli and Baumann 1997) reported that the recycle stream improved aeration, which increased the DO level in the medium due to which higher COD removal rate was achieved in the continuous RBC. Ayoub and Saikaly (2004)(Ayoub

and Saikaly 2004) reported that the recycle stream improves the NH_3–H removal efficiency from 64.3% to 90.6% and improves the effluent DO concentration in the RBC system.

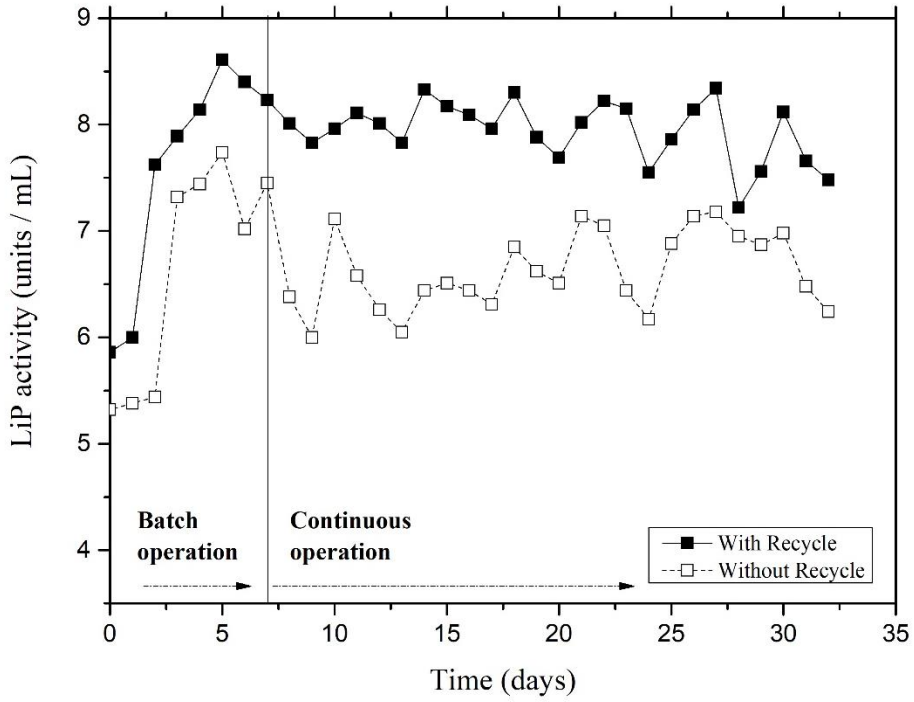

Figure 5.17. Enzymatic activity during continuous experiments in the RPDB with and without the recycle stream.

As expected, the high enzymatic activity was observed in the RPDB with the recycle stream as compared to the RPDB without the recycle stream, as shown in Figure 5.17. The results reveal that achieved 10 to 15% higher degradation using the recycle stream within 25 days of operation, which counts for 3665 L treated effluent. Higher recycle ratio ($^{v_e}/_{v_f} = 9.75$) provided more back mixing of liquid resulting and higher oxygen transfer, which improved the removal efficiency. Thus, it appears that through the recycle stream, the performance of the bioreactor improved in terms of COD removal and to maintain the amount of glucose for the fungus to perform better in higher dye concentration loading.

CHAPTER - 6
CONCLUSIONS AND FUTURE SCOPE

CHAPTER 6

6. CONCLUSIONS AND FUTURE SCOPE

Residence time distribution revealed that the liquid mixing behavior of the RPDC was towards a well-mixed system for working volumes of 32.5 and 55 Liters. The recycle ratio helped to improve the well-mixed system by increasing the back mixing. A three-parameter mathematical model simulation predicted the mixing behavior, which was similar to experimental results.

The gas-liquid mass transfer in the partially filled horizontal packed disc reactor mainly occurred through the disc surface. The result revealed that the modified disc design improved the oxygen transfer rate by eight folds compared to the standard RBC. The highest k_La of 0.39 min^{-1} with only 8 discs was obtained at 60 rpm due to the discs' modified design and enhanced surface area for mass transfer. Recycle ratio further improved k_La value by about 10 to 15%. The experimental results fitted the empirical model with a regression coefficient of 0.96.

The mixed white-rot fungal cultures degrade the effluent within 5 days with a high degradation rate compared to individual fungal strain, due to high LiP activity present in the mixed culture. The COD reduction was achieved above 100% in the shake flask studies using mixed culture. The bioreactor studies revealed that the maximum COD reduction of more than 90% was achieved in batch mode on the 7^{th} day. In contrast, more than 80% COD removal was consistently achieved for 25 days with the rate of 737.9 mg/L/h at 30 rpm and 9.75 recycle ratio in the continuous operation, which accounts to 3665 Liters of treated effluent. SEM confirmed the immobilization of the fungus, and microscopic images were studied. It can be concluded that GAC is a suitable support for mixed culture immobilization.

FUTURE SCOPE

In this work, RPDB is described and characterized in terms of a working prototype laboratory-scale bioreactor. The immobilized biomass growth would not be defined due to the compact design of the hollow disc. Thus, it reduced the oxygen mass transfer from gas to the bulk of the liquid also improper mixing within the bioreactor. This is due to the capacity of the packed disc and the design of the vane's angles.

Therefore, any future work based on the designs detailed in this thesis should include an adaptation of the 65L RPDB, increasing the mass transfer capability, mixing and homogeneity in the bioreactor to make it more effective for processes. The operationality of the RPDB could be improved as follows:

- Increasing the volume of the packed disc, may result in a reduction of channeling and easy handling of immobilized biomass growth.
- Changing the vanes' angle may affect the mixing characteristic within the bioreactor.
- Reducing the length of the 'rim' may provide a large surface area for immobilized biomass growth.
- Using a CFD model to the bioreactor may help in investigating the effect of hydrodynamic forces' and optimizing bioreactors performance.
- Multiple fungal species can be used for wastewater treatment using this design.

Incorporating these modifications in the design can be used as a novel method to treat the wastewater effectively. This could enable better oxygen mass transfer rate and mixing performance followed by improvement in the cell growth to achieve the higher potential.

REFERENCES

References:

Abadulla, E., Tzanov, T., Costa, S., Robra, K.-H., Cavaco-Paulo, A., and Gübitz, G. M. (2000). "Decolorization and detoxification of textile dyes with a laccase from Trametes hirsuta." *Appl. Environ. Microbiol.*, 66(8), 3357–3362.

Abdel-Raheem, A., and Shearer, C. (2002). "Extracellular enzyme production byfreshwater ascomycetes." *Fungal Divers.*, 11, 1–19.

Abraham, T. E., Senan, R. C., Shaffiqu, T. S., Roy, J. J., Poulose, T. P., and Thomas, P. P. (2003). "Bioremediation of textile azo dyes by an aerobic bacterial consortium using a rotating biological contactor." *Biotechnol. Prog.*, 19(4), 1372–1376.

Acuner, E., and Dilek, F. B. (2004). "Treatment of tectilon yellow 2G by Chlorella vulgaris." *Process Biochem.*, 39(5), 623–631.

Adnan, L. A., Mohd Yusoff, A. R., Hadibarata, T., and Khudhair, A. B. (2014). "Biodegradation of bis-azo dye reactive black 5 by white-rot fungus Trametes gibbosa sp. WRF 3 and its metabolite characterization." *Water. Air. Soil Pollut.*, 225(10).

Aghdasinia, H., Arehjani, P., Vahid, B., and Khataee, A. (2016). "Optimization of a textile dye degradation in a recirculating fluidized-bed reactor using magnetite/$S_2O_8^{2-}$ process." *Environ. Technol.*, 3330(December), 1–11.

Aksu, Z., Kılıç, N. K., Ertuğrul, S., and Dönmez, G. (2007). "Inhibitory effects of chromium (VI) and Remazol Black B on chromium (VI) and dyestuff removals by Trametes versicolor." *Enzyme Microb. Technol.*, 40(5), 1167–1174.

Alemzadeh, I., and Vossoughi, M. (2001). "Biodegradation of toluene by an attached biofilm in a rotating biological contactor." *Process Biochem.*, 36(8–9), 707–711.

Allegre, C., Moulin, P., Maisseu, M., and Charbit, F. (2006). "Treatment and reuse of reactive dyeing effluents." *J. Memb. Sci.*, 269(1–2), 15–34.

REFERENCES

Ando, K., Shirahige, M., Fukuda, T., and Endoh, K. (1981). "Effects of perforated partition plate on mixing characteristics of horizontal stirred vessel." *AIChE J.*, 27(4), 599–604.

Anliker, R. (1979). "Ecotoxicology of dyestuffs—a joint effort by industry." *Ecotoxicol. Environ. Saf.*, 3(1), 59–74.

Arregui, L., Ayala, M., Gómez-Gil, X., Gutiérrez-Soto, G., Hernández-Luna, C. E., los Santos, M. H. de, Levin, L., Rojo-Domínguez, A., Romero-Martínez, D., and Saparrat, M. C. N. (2019). "Laccases: structure, function, and potential application in water bioremediation." *Microb. Cell Fact.*, 18(1), 200.

Asad, S., Amoozegar, M. A., Pourbabaee, A., Sarbolouki, M. N., and Dastgheib, S. M. M. (2007). "Decolorization of textile azo dyes by newly isolated halophilic and halotolerant bacteria." *Bioresour. Technol.*, 98(11), 2082–2088.

Asses, N., Ayed, L., Hkiri, N., and Hamdi, M. (2018). "Congo Red Decolorization and Detoxification by Aspergillus niger: Removal Mechanisms and Dye Degradation Pathway." *Biomed Res. Int.*, 2018.

Axelsson, J., Nilsson, U., Terrazas, E., Aliaga, T. A., and Welander, U. (2006). "Decolorization of the textile dyes Reactive Red 2 and Reactive Blue 4 using Bjerkandera sp. Strain BOL 13 in a continuous rotating biological contactor reactor." *Enzyme Microb. Technol.*, 39(1), 32–37.

Ayed, L., Mahdhi, A., Cheref, A., and Bakhrouf, A. (2011). "Decolorization and degradation of azo dye Methyl Red by an isolated Sphingomonas paucimobilis: biotoxicity and metabolites characterization." *Desalination*, 274(1–3), 272–277.

Ayoob Torkian, K. Alinejad, S. J. H. (2015). "Posttreatment a Rotating of Anaerobic Upflow Wastewater Industrial Biological Contactor Sludge by." 75(3), 232–237.

Ayoub, G. M., and Saikaly, P. (2004). "The combined effect of step-feed and recycling on RBC performance." *Water Res.*, 38(13), 3009–3016.

REFERENCES

Bafana, A., Chakrabarti, T., and Devi, S. S. (2008a). "Azoreductase and dye detoxification activities of Bacillus velezensis strain AB." *Appl. Microbiol. Biotechnol.*, 77(5), 1139–1144.

Bafana, A., Krishnamurthi, K., Devi, S. S., and Chakrabarti, T. (2008b). "Biological decolourization of CI Direct Black 38 by E. gallinarum." *J. Hazard. Mater.*, 157(1), 187–193.

Balaji, K., and Poongothai, S. (2012). "Evaluation of Fluidized Bed Reactor in treating Dyeing effluent." *Int. J. Eng. Sci. Technol.*, 4(07), 3134–3139.

Banat, I. M., Nigam, P., Singh, D., and Marchant, R. (1996). "Microbial decolorization of textile-dye-containing effluents: A review." *Bioresour. Technol.*, 58(3), 217–227.

Banerjee, G. (1997a). "Treatment of phenolic wastewater in RBC reactor." *Water Res.*, 31(4), 705–714.

Banerjee, G. (1997b). "Hydraulics of bench-scale rotating biological contactor." *Water Res.*, 31(10), 2500–2510.

Basha, O. M., and Morsi, B. I. (2018). "Effects of Sparger and Internals Designs on the Local Hydrodynamics in Slurry Bubble Column Reactors Operating under Typical Fischer-Tropsch Process Conditions-I." *Int. J. Chem. React. Eng.*, 16(3).

Bintaja, H., Vandererve, J., and Boelhouwer, C. (1975). "Oxygen transfer in a rotating disc treatment plant." *Water Res.*, 9(12), 1147–1153.

Binupriya, A. R., Sathishkumar, M., Swaminathan, K., Kuz, C. S., and Yun, S. E. (2008). "Comparative studies on removal of Congo red by native and modified mycelial pellets of Trametes versicolor in various reactor modes." *Bioresour. Technol.*, 99(5), 1080–1088.

Boer, C. G., Obici, L., Souza, C. G. M. de, and Peralta, R. M. (2004). "Decolorization of synthetic dyes by solid state cultures of Lentinula (Lentinus) edodes producing manganese peroxidase as the main ligninolytic enzyme." *Bioresour. Technol.*, 94(2),

107–112.

Borchert, M., and Libra, J. A. (2001). “Decolorization of reactive dyes by the white rot fungus *Trametes versicolor* in sequencing batch reactors.” *Biotechnol. Bioeng.*, 75(3), 313–21.

Boumansour, B.-E., and Vasel, J.-L. (1998). “A new tracer gas method to measure oxygen transfer and enhancement factor on RBC.” *Water Res.*, 32(4), 1049–1058.

Brazil, B. L. (2006). “Performance and operation of a rotating biological contactor in a tilapia recirculating aquaculture system.” *Aquac. Eng.*, 34(3), 261–274.

Brüschweiler, B. J., and Merlot, C. (2017). “Azo dyes in clothing textiles can be cleaved into a series of mutagenic aromatic amines which are not regulated yet.” *Regul. Toxicol. Pharmacol.*, 88, 214–226.

Camargo, A. T. de, and Corso, C. R. (2002). “Remoçao do corante amaranto (CI 16.185) por biomassa de leveduras do género Candida através de biosorçao.”

Casieri, L., Varese, G. C., Anastasi, A., Prigione, V., Svobodova, K., Marchisio, V. F., and Novotný, Č. (2008). “Decolorization and detoxication of reactive industrial dyes by immobilized fungi Trametes pubescens and Pleurotus ostreatus.” *Folia Microbiol. (Praha).*, 53(1), 44.

Chagas, E. P., and Durrant, L. R. (2001). “Decolorization of azo dyes by Phanerochaete chrysosporium and Pleurotus sajorcaju.” *Enzyme Microb. Technol.*, 29(8–9), 473–477.

Chang, J.-S., Kuo, T.-S., Chao, Y.-P., Ho, J.-Y., and Lin, P.-J. (2000). “Azo dye decolorization with a mutant Escherichia coli strain.” *Biotechnol. Lett.*, 22(9), 807–812.

Chavan, A., and Mukherji, S. (2008). “Dimensional analysis for modeling oxygen transfer in rotating biological contactor.” *Bioresour. Technol.*, 99(9), 3721–3728.

Chen, B.-Y., Chen, S.-Y., Lin, M.-Y., and Chang, J.-S. (2006). “Exploring

bioaugmentation strategies for azo-dye decolorization using a mixed consortium of Pseudomonas luteola and Escherichia coli." *Process Biochem.*, 41(7), 1574–1581.

Chern, J.-M., Chou, S.-R., and Shang, C.-S. (2001). "Effects of impurities on oxygen transfer rates in diffused aeration systems." *Water Res.*, 35(13), 3041–3048.

Cing, S., and Yesilada, O. (2004). "Astrazon Red dye decolorization by growing cells and pellets of Funalia trogii." *J. Basic Microbiol. An Int. J. Biochem. Physiol. Genet. Morphol. Ecol. Microorg.*, 44(4), 263–269.

Confer, D. R., and Logan, B. E. (1998). "A conceptual model describing macromolecule degradation by suspended cultures and biofilms." *Water Sci. Technol.*, 231–234.

Cortez, S., Teixeira, P., Oliveira, R., and Mota, M. (2008). "Rotating biological contactors: a review on main factors affecting performance." *Rev. Environ. Sci. Biotechnol.*, 7(2), 155–172.

Courtens, E. N. P., Boon, N., Clippeleir, H. De, Berckmoes, K., Mosquera, M., Seuntjens, D., and Vlaeminck, S. E. (2014). "Control of nitratation in an oxygen-limited autotrophic nitrification/denitrification rotating biological contactor through disc immersion level variation." *Bioresour. Technol.*, 155, 182–188.

Couto, S. R., Sanromán, M. A., Hofer, D., and Gübitz, G. M. (2004). "Stainless steel sponge: a novel carrier for the immobilisation of the white-rot fungus Trametes hirsuta for decolourization of textile dyes." *Bioresour. Technol.*, 95(1), 67–72.

Cripps, C., Bumpus, J. A., and Aust, S. D. (1990). "Biodegradation of azo and heterocyclic dyes by Phanerochaete chrysosporium." *Appl. Environ. Microbiol.*, 56(4), 1114–1118.

Daâssi, D., Mechichi, T., Nasri, M., and Rodriguez-Couto, S. (2013). "Decolorization of the metal textile dye Lanaset Grey G by immobilized white-rot fungi." *J. Environ. Manage.*, 129, 324–332.

Daneshvar, N., Ayazloo, M., Khataee, A. R., and Pourhassan, M. (2007). "Biological

decolorization of dye solution containing Malachite Green by microalgae Cosmarium sp." *Bioresour. Technol.*, 98(6), 1176–1182.

Datta, R., Kelkar, A., Baraniya, D., Molaei, A., Moulick, A., Meena, R. S., and Formanek, P. (2017). "Enzymatic degradation of lignin in soil: A review." *Sustain.*, 9(7), 1–18.

Datta, S., Christena, L. R., and Rajaram, Y. R. S. (2013). "Enzyme immobilization: an overview on techniques and support materials." *3 Biotech*, 3(1), 1–9.

Dave, S. R., and Dave, R. H. (2009). "Isolation and characterization of Bacillus thuringiensis for Acid red 119 dye decolourisation." *Bioresour. Technol.*, 100(1), 249–253.

Dave, S. R., Patel, T. L., and Tipre, D. R. (2015). "Bacterial degradation of azo dye containing wastes." *Microb. Degrad. Synth. Dye. Wastewaters*, Springer, 57–83.

Dawood, S., and Sen, T. K. (2014). "Review on Dye Removal from Its Aqueous Solution into Alternative Cost Ef- fective and Non-Conventional Adsorbents." *J Chem Proc Engg J Chem Proc Eng*, 1(1), 1–11.

Deng, D., Guo, J., Zeng, G., and Sun, G. (2008). "Decolorization of anthraquinone, triphenylmethane and azo dyes by a new isolated Bacillus cereus strain DC11." *Int. Biodeterior. Biodegradation*, 62(3), 263–269.

Dhanasekaran, S., and Karunanithi, T. (2010). "Axial mixing in a novel perforated plate bubble column." *Int. J. Chem. React. Eng.*, 8(1), 1–24.

Dutta, S., Hoffmann, E., and Hahn, H. H. (2007). "Study of rotating biological contactor performance in wastewater treatment using multi-culture biofilm model." *Water Sci. Technol.*, 55(8–9), 345–353.

Egger, K. N. (1986). "Substrate hydrolysis patterns of post-fire ascomycetes (Pezizales)." *Mycologia*, 78(5), 771–780.

Eichlerová, I., Homolka, L., Lisá, L., and Nerud, F. (2005). "Orange G and Remazol

Brilliant Blue R decolorization by white rot fungi Dichomitus squalens, Ischnoderma resinosum and Pleurotus calyptratus." *Chemosphere*, 60(3), 398–404.

Enayatizamir, N., Tabandeh, F., Rodríguez-Couto, S., Yakhchali, B., Alikhani, H. A., and Mohammadi, L. (2011). "Biodegradation pathway and detoxification of the diazo dye Reactive Black 5 by Phanerochaete chrysosporium." *Bioresour. Technol.*, 102(22), 10359–10362.

Erkurt, E. A., Ünyayar, A., and Kumbur, H. (2007). "Decolorization of synthetic dyes by white rot fungi, involving laccase enzyme in the process." *Process Biochem.*, 42(10), 1429–1435.

Erkurt, H. A. (2010). *Biodegradation of azo dyes*. Springer.

Fan, L., Zhu, S., Liu, D., and Ni, J. (2009). "Decolorization of 1-amino-4-bromoanthraquinone-2-sulfonic acid by a newly isolated strain of Sphingomonas herbicidovorans." *Int. Biodeterior. Biodegradation*, 63(1), 88–92.

Flint, S. H., Brooks, J. D., and Bremer, P. J. (1997). "The influence of cell surface properties of thermophilic streptococci on attachment to stainlesssteel." *J. Appl. Microbiol.*, 83(4), 508–517.

Fogler, H. S. (2010). *Essentials of Chemical Reaction Engineering: Essenti Chemica Reactio Engi*. Pearson Education.

Forss, J., and Welander, U. (2009). "Decolourization of reactive azo dyes with microorganisms growing on soft wood chips." *Int. Biodeterior. Biodegradation*, 63(6), 752–758.

Franzini, A. K. L. (1980). "Water Resources Engineering." *McGraw-Hill. New York*, 3, 1980.

Friedman, A. A., Robbins, L. E., and Woods, R. C. (1979). "Effect of Disk Rotational Speed on Biological Contactor Efficiency." *J. (Water Pollut. Control Fed.*, 51(11), 2678–2690.

REFERENCES

Gao, D., Zeng, Y., Wen, X., and Qian, Y. (2008). "Competition strategies for the incubation of white rot fungi under non-sterile conditions." *Process Biochem.*, 43(9), 937–944.

Garcia-Ochoa, F., and Gomez, E. (2009). "Bioreactor scale-up and oxygen transfer rate in microbial processes: An overview." *Biotechnol. Adv.*, 27(2), 153–176.

Ghodake, G., Jadhav, S., Dawkar, V., and Govindwar, S. (2009). "Biodegradation of diazo dye Direct brown MR by Acinetobacter calcoaceticus NCIM 2890." *Int. Biodeterior. Biodegradation*, 63(4), 433–439.

González-Ramírez, D. F., Muro-Urista, C. R., Arana-Cuenca, A., Téllez-Jurado, A., and González-Becerra, A. E. (2014). "Enzyme production by immobilized Phanerochaete chrysosporium using airlift reactor." *Biologia (Bratisl).*, 69(11), 1464–1471.

Gopinath, K. P., Sahib, H. A. M., Muthukumar, K., and Velan, M. (2009). "Improved biodegradation of Congored by using Bacillus sp." *Bioresour. Technol.*, 100(2), 670–675.

Grover, V. I. (2006). *Water: global common and global problems*. Science Publishers.

Guerra, E., Llompart, M., and Garcia-Jares, C. (2018). "Analysis of dyes in cosmetics: challenges and recent developments." *Cosmetics*, 5(3), 47.

Guimaraes, C., Porto, P., Oliveira, R., and Mota, M. (2005). "Continuous decolourization of a sugar refinery wastewater in a modified rotating biological contactor with Phanerochaete chrysosporium immobilized on polyurethane foam disks." *Process Biochem.*, 40(2), 535–540.

Guo, J., Ma, F., Jiang, K., and Cui, D. (2008a). "Bioaugmentation combined with biofilim process in the treatment of petrochemical wastewater at low temperatures." *2008 2nd Int. Conf. Bioinforma. Biomed. Eng.*, IEEE, 3252–3255.

Guo, J., Zhou, J., Wang, D., Tian, C., Wang, P., and Uddin, M. S. (2008b). "A novel

moderately halophilic bacterium for decolorizing azo dye under high salt condition." *Biodegradation,* 19(1), 15–19.

Guo, J., Zhou, J., Wang, D., Yang, J., and Li, Z. (2008c). "The new incorporation bio-treatment technology of bromoamine acid and azo dyes wastewaters under high-salt conditions." *Biodegradation,* 19(1), 93–98.

Gupta, A. B., and Gupta, S. K. (2001). "Simultaneous Carbon and Nitrogen Removal From High Strength Domestic Wastewater in an aerobic RBC biofilm." *Water Res.*, 35(7), 1714–1722.

H.F.Haug. (1971). "Backmixing in Multistage Agitated Contactors-a Correlation." *AIChE J.*, 17(3), 585–589.

Haapala, R., and Linko, S. (1993). "Production of Phanerochaete chrysosporium lignin peroxidase under various culture conditions." *Appl. Microbiol. Biotechnol.*, 40(4), 494–498.

Harazono, K., Watanabe, Y., and Nakamura, K. (2003). "Decolorization of azo dye by the white-rot basidiomycete Phanerochaete sordida and by its manganese peroxidase." *J. Biosci. Bioeng.*, 95(5), 455–459.

Hassard, F., Biddle, J., Cartmell, E., Jefferson, B., Tyrrel, S., and Stephenson, T. (2015). "Rotating biological contactors for wastewater treatment - A review." *Process Saf. Environ. Prot.*, 94(C), 285–306.

Heinfling, A., Bergbauer, M., and Szewzyk, U. (1997). "Biodegradation of azo and phthalocyanine dyes by Trametes versicolor and Bjerkandera adusta." *Appl. Microbiol. Biotechnol.*, 48(2), 261–266.

Heinfling, A., Martinez, M. J., Martinez, A. T., Bergbauer, M., and Szewzyk, U. (1998a). "Transformation of industrial dyes by manganese peroxidases from Bjerkandera adusta and Pleurotus eryngii in a manganese-independent reaction." *Appl. Environ. Microbiol.*, 64(8), 2788–2793.

REFERENCES

Heinfling, A., Ruiz-Dueñas, F. J., Martínez, M. J., Bergbauer, M., Szewzyk, U., and Martínez, A. T. (1998b). "A study on reducing substrates of manganese-oxidizing peroxidases from Pleurotus eryngii and Bjerkandera adusta." *FEBS Lett.*, 428(3), 141–146.

Hewawasam, C., Matsuura, N., Maharjan, N., Hatamoto, M., and Yamaguchi, T. (2017). "Oxygen transfer dynamics and nitrification in a novel rotational sponge reactor." *Biochem. Eng. J.*, 128, 162–167.

Hu, T.-L. (2001). "Kinetics of azoreductase and assessment of toxicity of metabolic products from azo dyes by Pseudomonas luteola." *Water Sci. Technol.*, 43(2), 261–269.

Huijun, Z. H. Y. Q. L., and Xuemei, C. J. L. (2007). "Screening of decolorizing fungi and decolorizing research for active red M-3BE [J]." *Chinese J. Environ. Eng.*, 11.

Israni, S. H., Koli, S. S., Patwardhan, A. W., Melo, J. S., and D'Souza, S. F. (2002). "Phenol degradation in rotating biological contactors." *J. Chem. Technol. Biotechnol.*, 77(9), 1050–1057.

Jadhav, J. P., and Govindwar, S. P. (2006). "Biotransformation of malachite green by Saccharomyces cerevisiae MTCC 463." *Yeast*, 23(4), 315–323.

Jadhav, J. P., Parshetti, G. K., Kalme, S. D., and Govindwar, S. P. (2007). "Decolourization of azo dye methyl red by Saccharomyces cerevisiae MTCC 463." *Chemosphere*, 68(2), 394–400.

Kabbout, R., and Taha, S. (2014). "Biodecolorization of textile dye effluent by biosorption on fungal biomass materials." *Phys. Procedia*, 55, 437–444.

Kalme, S., Jadhav, S., Jadhav, M., and Govindwar, S. (2009). "Textile dye degrading laccase from Pseudomonas desmolyticum NCIM 2112." *Enzyme Microb. Technol.*, 44(2), 65–71.

Kalnake, R. P., Murthy, D. V. R., Achar, A., and Raval, K. (2020). "Residence Time

Distribution Studies in a Modified Rotating Packed Disc Contactor: Mathematical Modeling and Validation." *Int. J. Chem. React. Eng.*, 1(ahead-of-print).

Kapdan, I. K., Kargi, F., Mcmullan, G., and Marchant, R. (2010). "Biological Decolorization of Textile Dyestuff by Coriolus Versicolor in a Packed Column Reactor." *Environ. Technol.*, 21(2), 231–236.

Kapdan, I. K., Kargi, F., McMullan, G., and Marchant, R. (2000). "Biological decolorization of textile dyestuff by Coriolus versicolor in a packed column reactor." *Environ. Technol.*, 21(2), 231–236.

Karel, S. F., Libicki, S. B., and Robertson, C. R. (1985). "The immobilization of whole cells: engineering principles." *Chem. Eng. Sci.*, 40(8), 1321–1354.

Kariminiaae-Hamedaani, H.-R., Sakurai, A., and Sakakibara, M. (2007). "Decolorization of synthetic dyes by a new manganese peroxidase-producing white rot fungus." *Dye. Pigment.*, 72(2), 157–162.

Karunya, A., Nachiyar, C. V., Ananth, P. B., Sunkar, S., and Jabasingh, S. A. (2014). "Development of microbial consortium CN-1 for the degradation of Mordant Black 17." *J. Environ. Chem. Eng.*, 2(2), 832–840.

Kasinath, A., Novotný, Č., Svobodová, K., Patel, K. C., and Šašek, V. (2003). "Decolorization of synthetic dyes by Irpex lacteus in liquid cultures and packed-bed bioreactor." *Enzyme Microb. Technol.*, 32(1), 167–173.

Katzbauer, B., Narodoslawsky, M., and Moser, A. (1995). "Classification system for immobilization techniques." *Bioprocess Eng.*, 12(4), 173–179.

Khalid, A., Arshad, M., and Crowley, D. E. (2008a). "Accelerated decolorization of structurally different azo dyes by newly isolated bacterial strains." *Appl. Microbiol. Biotechnol.*, 78(2), 361–369.

Khalid, A., Arshad, M., and Crowley, D. E. (2008b). "Decolorization of azo dyes by Shewanella sp. under saline conditions." *Appl. Microbiol. Biotechnol.*, 79(6), 1053–

1059.

Khalid, A., Arshad, M., and Crowley, D. E. (2009). “Biodegradation potential of pure and mixed bacterial cultures for removal of 4-nitroaniline from textile dye wastewater.” *Water Res.*, 43(4), 1110–1116.

Kim, B. J., and Molof, A. H. (1982). “The scale-up and limitation of physical oxygen transfer in rotating biological contractors.” *Water Sci. Technol.*, 14(6–7), 569–579.

Kim, M. J., Ghim, Y. S., and Chang, H. N. (1984). “Residence time distribution analysis in controllable flow conditions: case of rotating disk reactor.” *Chem. Eng. Sci.*, 39(5), 813–819.

Klees, R., and Silverstein, J. (1992). “Improved biological nitrification using recirculation in rotating biological contactors.” *Water Sci. Technol.*, 26(3–4), 545–553.

Kolekar, Y. M., Pawar, S. P., Gawai, K. R., Lokhande, P. D., Shouche, Y. S., and Kodam, K. M. (2008). “Decolorization and degradation of Disperse Blue 79 and Acid Orange 10, by Bacillus fusiformis KMK5 isolated from the textile dye contaminated soil.” *Bioresour. Technol.*, 99(18), 8999–9003.

Krishnamoorthy, R., Jose, P. A., Ranjith, M., Anandham, R., Suganya, K., Prabhakaran, J., Thiyageshwari, S., Johnson, J., Gopal, N. O., and Kumutha, K. (2018). “Decolourisation and degradation of azo dyes by mixed fungal culture consisted of Dichotomomyces cejpii MRCH 1-2 and Phoma tropica MRCH 1-3.” *J. Environ. Chem. Eng.*, 6(1), 588–595.

Kubsad, V., Chaudhari, S., and Gupta, S. K. (2004). “Model for oxygen transfer in rotating biological contactor.” *Water Res.*, 38(20), 4297–4304.

Kumaresan, T., and Joshi, J. B. (2006). “Effect of impeller design on the flow pattern and mixing in stirred tanks.” *Chem. Eng. J.*, 115(3), 173–193.

Legerská, B., Chmelová, D., and Ondrejovič, M. (2018). “Decolourization and detoxification of monoazo dyes by laccase from the white-rot fungus Trametes

versicolor.” *J. Biotechnol.*, 285, 84–90.

Leon, M. A., Maas, R. J., Bieberle, A., Schubert, M., Nijhuis, T. A., Schaaf, J. Van Der, Hampel, U., and Schouten, J. C. (2013). “Hydrodynamics and gas – liquid mass transfer in a horizontal rotating foam stirrer reactor.” *Chem. Eng. J.*, 217, 10–21.

Leon, M. A., Nijhuis, T. A., Schaaf, J. Van Der, and Schouten, J. C. (2014). “Residence time distribution and reaction rate in the horizontal rotating foam stirrer reactor.” *Chem. Eng. Sci.*, 117, 8–17.

Levenspiel, O. (1999). “Chemical reaction engineering.” *Ind. Eng. Chem. Res.*, 38(11), 4140–4143.

Lewis, A. J., and Borole, A. P. (2016). “Understanding the impact of flow rate and recycle on the conversion of a complex biorefinery stream using a flow-through microbial electrolysis cell.” *Biochem. Eng. J.*, 116, 95–104.

Li, N., Zeng, W., Yang, Y., Wang, B., Li, Z., and Peng, Y. (2019). “Oxygen mass transfer and post-denitrification in a modified rotating drum biological contactor.” *Biochem. Eng. J.*, 48–56.

Linek, V., Vacek, V., and Beneš, P. (1987). “A critical review and experimental verification of the correct use of the dynamic method for the determination of oxygen transfer in aerated agitated vessels to water, electrolyte solutions and viscous liquids.” *Chem. Eng. J.*, 34(1), 11–34.

Liu, G., Zhou, J., Wang, J., Zhou, M., Lu, H., and Jin, R. (2009). “Acceleration of azo dye decolorization by using quinone reductase activity of azoreductase and quinone redox mediator.” *Bioresour. Technol.*, 100(11), 2791–2795.

Lucas, M. S., Amaral, C., Sampaio, A., Peres, J. A., and Dias, A. A. (2006). “Biodegradation of the diazo dye Reactive Black 5 by a wild isolate of Candida oleophila.” *Enzyme Microb. Technol.*, 39(1), 51–55.

Mabrouk, M. E. M., and Yusef, H. H. (2008). “Decolorization of fast red by Bacillus

subtilis HM." *J Appl Sci Res*, 4(3), 262–269.

Malachova, K., Rybkova, Z., Sezimova, H., Cerven, J., and Novotny, C. (2013). "Biodegradation and detoxification potential of rotating biological contactor (RBC) with Irpex lacteus for remediation of dye-containing wastewater." *Water Res.*, 47(19), 7143–7148.

Manikandan, B., Ramamurthi, V., Karthikeyan, R., and Sundararaman, T. R. (2009). "Biobleaching of Textile Dye Effluent Using Mixed Culture through an Immobilized Packed Bed Bio Reactor (IPBBR)." *Mod. Appl. Sci.*, 3(5), 131–135.

Mansouri, Y., Zinatizadeh, A. A., Mohammadi, P., Irandoust, M., Akhbari, A., and Davoodi, R. (2012). "Hydraulic characteristics analysis of an anaerobic rotatory biological contactor (AnRBC) using tracer experiments and response surface methodology (RSM)." *Korean J. Chem. Eng.*, 29(7), 891–902.

Markvicheva, E. A., Kuz'kina, I. F., Pashkin, I. I., Plechko, T. N., Kirsh, Y. E., and Zubov, V. P. (1991). "A novel technique for entrapment of hybridoma cells in synthetic thermally reversible polymers." *Biotechnol. Tech.*, 5(3), 223–226.

Martins, M. A. M., Cardoso, M. H., Queiroz, M. J., Ramalho, M. T., and Campus, A. M. O. (1999). "Biodegradation of azo dyes by the yeast Candida zeylanoides in batch aerated cultures." *Chemosphere*, 38(11), 2455–2460.

Martins, M. A. M., Ferreira, I. C., Santos, I. M., Queiroz, M. J., and Lima, N. (2001). "Biodegradation of bioaccessible textile azo dyes by Phanerochaete chrysosporium." *J. Biotechnol.*, 89(2–3), 91–98.

Martins, S. C. S., Martins, C. M., Fiúza, L. M. C. G., and Santaella, S. T. (2013). "Immobilization of microbial cells: A promising tool for treatment of toxic pollutants in industrial wastewater." *African J. Biotechnol.*, 12(28).

Mathure, P., and Patwardhan, A. (2005). "Comparison of mass transfer efficiency in horizontal rotating packed beds and rotating biological contactors." *J. Chem.*

Technol. Biotechnol. Int. Res. Process. Environ. Clean Technol., 80(4), 413–419.

Matias, N., Nielsen, A. H., Vollertsen, J., Ferreira, F., and Matos, J. S. (2017). "Liquid-gas mass transfer at drop structures." *Water Sci. Technol.*, 75(10), 2257–2267.

Mazmanci, M. A., and Ünyayar, A. (2005). "Decolourisation of Reactive Black 5 by Funalia trogii immobilised on Luffa cylindrica sponge." *Process Biochem.*, 40(1), 337–342.

Meehan, C., Banat, I. M., McMullan, G., Nigam, P., Smyth, F., and Marchant, R. (2000). "Decolorization of Remazol Black-B using a thermotolerant yeast, Kluyveromyces marxianus IMB3." *Environ. Int.*, 26(1–2), 75–79.

Metcalf, E. (2003). *Wastewater engineering treatment and reuse*. Mc Graw Hill education (india)private limited.

Mielgo, I., Moreira, M., Feijoo, G., and Lema, J. (2001). "A packed bed fungal Bioreactor for continuous decolourisation of azo dyes(Orange II)." *J Biotech*, 89, 99–106.

Millis, C. D., Cai, D., Stankovich, M. T., and Tien, M. (1989). "Oxidation-reduction potentials and ionization states of extracellular peroxidases from the lignin-degrading fungus Phanerochaete chrysosporium." *Biochemistry*, 28(21), 8484–8489.

Moldes, D., Fernández-Fernández, M., and Sanromán, M. (2012). "Role of laccase and low molecular weight metabolites from Trametes versicolor in dye decolorization." *Sci. World J.*, 1–9.

Moldes, D., and Sanromán, M. Á. (2006). "Amelioration of the ability to decolorize dyes by laccase: relationship between redox mediators and laccase isoenzymes in Trametes versicolor." *World J. Microbiol. Biotechnol.*, 22(11), 1197–1204.

Monayerie, D. S. El, Atta, N. N., Din, D. S. El, and Daif, S. (2012). "Modeling of oxygen transfer in self-rotating biological contactors (sRBC)." *Proc. Int. Water Technol. Conf. (IWTC16), Istanbul, Turkey, May*, 1–11.

Murugesan, K., Dhamija, A., Nam, I.-H., Kim, Y.-M., and Chang, Y.-S. (2007). "Decolourization of reactive black 5 by laccase: optimization by response surface methodology." *Dye. Pigment.*, 75(1), 176–184.

Nahid, P., Vossoughi, M., and Alemzadeh, I. (2001). "Treatment of bakers yeast wastewater with a Biopack system." *Process Biochem.*, 37(5), 447–451.

Najafpour, G., Yieng, H. A., Younesi, H., and Zinatizadeh, A. (2005). "Effect of organic loading on performance of rotating biological contactors using Palm Oil Mill effluents." *Process Biochem.*, 40(8), 2879–2884.

Nakamura, Y., Sawada, T., Sungusia, M. G., Kobayashi, F., Kuwahara, M., and Ito, H. (1997). "Lignin peroxidase production by Phanerochaete chrysosporium immobilized on polyurethane foam." *J. Chem. Eng. Japan*, 30(1), 1–6.

Nascimento, C., Magalhães, D. de P., Brandão, M., Santos, A. B., Chame, M., Baptista, D., Nishikawa, M., and Silva, M. da. (2011). "Degradation and detoxification of three textile azo dyes by mixed fungal cultures from semi-arid region of Brazilian Northeast." *Brazilian Arch. Biol. Technol.*, 54(3), 621–628.

Neu, K. E. (1994). "Upgrading of rotating biological contactor (RBC) systems to achieve higher effluent quality, including biological nutrient enrichment and reduction techniques." *Water Sci. Technol.*, 29(12), 197.

Nguyen, L. N., Hai, F. I., Dosseto, A., Richardson, C., Price, W. E., and Nghiem, L. D. (2016). "Continuous adsorption and biotransformation of micropollutants by granular activated carbon-bound laccase in a packed-bed enzyme reactor." *Bioresour. Technol.*, 210, 108–116.

Ni, X. (1994). "Residence time distribution measurements in a pulsed baffled tube bundle." *J. Chem. Technol. Biotechnol. Int. Res. Process. Environ. Clean Technol.*, 59(3), 213–221.

Nilsson, I., Möller, A., Mattiasson, B., Rubindamayugi, M. S. T., and Welander, U.

(2006). “Decolorization of synthetic and real textile wastewater by the use of white-rot fungi.” *Enzyme Microb. Technol.*, 38(1–2), 94–100.

Norton, S., and D’Amore, T. (1994). “Physiological effects of yeast cell immobilization: applications for brewing.” *Enzyme Microb. Technol.*, 16(5), 365–375.

Novotný, Č., Rawal, B., Bhatt, M., Patel, M., Šašek, V., and Molitoris, H. P. (2001). “Capacity of Irpex lacteus and Pleurotus ostreatus for decolorization of chemically different dyes.” *J. Biotechnol.*, 89(2–3), 113–122.

Novotny, C., Trost, N., Susla, M., Svobodova, K., Mikeskova, H., Valkova, H., Malachov, K., and Pavko, A. (2012). “The use of the fungus Dichomitus squalens for degradation in rotating biological contactor conditions.” *Bioresour. Technol.*, 114, 241–246.

Pakshirajan, K., and Kheria, S. (2012). “Continuous treatment of coloured industry wastewater using immobilized Phanerochaete chrysosporium in a rotating biological contactor reactor.” *J. Environ. Manage.*, 101, 118–123.

Pakshirajan, K., Sivasankar, A., and Sahoo, N. K. (2011). “Decolourization of synthetic wastewater containing azo dyes by immobilized Phanerochaete chrysosporium in a continuously operated RBC reactor.” *Appl. Microbiol. Biotechnol.*, 89(4), 1223–1232.

Palma, L. Di, and Verdone, N. (2009). “The effect of disk rotational speed on oxygen transfer in rotating biological contactors.” *Bioresour. Technol.*, 100(3), 1467–1470.

Pandey, A., Singh, P., and Iyengar, L. (2007). “Bacterial decolorization and degradation of azo dyes.” *Int. Biodeterior. Biodegradation*, 59(2), 73–84.

Paolini, A. E. (1986). “Effect of Biomass on Oxygen Transfer in RBC Systems.” *J. Water Pollut. Control Fed.*, 58(4), 306–311.

Park, C., Lee, B., Han, E.-J., Lee, J., and Kim, S. (2006). “Decolorization of acid black 52 by fungal immobilization.” *Enzyme Microb. Technol.*, 39(3), 371–374.

Park, J. K., and Chang, H. N. (2000). "Microencapsulation of microbial cells." *Biotechnol. Adv.,* 18(4), 303–319.

Park, Y. S., Yun, J. W., Kim, D. S., and Song, S. K. (1998). "Wastewater treatment in a packed-bed reactor with immobilized cells onto a new ceramic carrier." *Biotechnol. Tech.,* 12(6), 459–462.

Parkar, S. G., Flint, S. H., Palmer, J. S., and Brooks, J. D. (2001). "Factors influencing attachment of thermophilic bacilli to stainless steel." *J. Appl. Microbiol.,* 90(6), 901–908.

Paszczynski, A., Pasti, M. B., Goszczynski, S., Crawford, D. L., and Crawford, R. L. (1991). "New approach to improve degradation of recalcitrant azo dyes by Streptomyces spp. and Phanerochaete chrysosporium." *Enzyme Microb. Technol.,* 13(5), 378–384.

Patwardhan, A. W. (2003). "Rotating biological contactors: a review." *Ind. Eng. Chem. Res.,* 42(10), 2035–2051.

Patwardhan, A. W. (2008). "Rotating Biological Contactors: A Review." *EnvironSci Biotechno,* 155–172.

Pazarlioglu, N. K., Urek, R. O., and Ergun, F. (2005). "Biodecolourization of Direct Blue 15 by immobilized Phanerochaete chrysosporium." *Process Biochem.,* 40(5), 1923–1929.

Pei, L., and Schmidt, M. (2018). "Fast-growing engineered microbes: new concerns for gain-of-function research?" *Front. Genet.,* 9, 207.

Podgornik, H., Grgić, I., and Perdih, A. (1999). "Decolorization rate of dyes using lignin peroxidases of Phanerochaete chrysosporium." *Chemosphere,* 38(6), 1353–1359.

Pointing, S. B. (1999). "Qualitative methods for the determination of lignocellulolytic enzyme production by tropical fungi." *Fungal Divers.,* 2, 17–33.

Poon, C. P. C., Chao, Y.-L., and Mikucki, W. J. (1979). "Factors controlling rotating

biological contactor performance." *J. (Water Pollut. Control Fed.,* 51(3), 601–611.

Priya Ak, Nagan, S., Rajeswari, M., Nithya, M., Priyanka, P. M., and Vanitha, R. (2001). "Rotating biological contactor for the treatment of textile industry wastewater." *Int J Adv Engg Tech,* VII(I), 209–213.

Przystaś, W., Zabłocka-Godlewska, E., and Grabińska-Sota, E. (2013). "Effectiveness of dyes removal by mixed fungal cultures and toxicity of their metabolites." *Water, Air, Soil Pollut.,* 224(5), 1534.

Qiu, M., Shou, J., and Lu, Y. (2014). "Degradation of organic compounds by fluidized bed fenton process." *J. Chem. Pharm. Res.,* 6(7), 2033–2038.

Radha, K. V, Regupathi, I., Arunagiri, A., and Murugesan, T. (2005). "Decolorization studies of synthetic dyes using Phanerochaete chrysosporium and their kinetics." *Process Biochem.,* 40(10), 3337–3345.

Raghuraman, J., and Varma, Y. B. G. (1974). "A stochastic model for residence time and contact time distributions of the gas in multistage fluidised beds." *Chem. Eng. Sci.,* 29(3), 697–703.

Ramalho, P. A., Cardoso, M. H., Cavaco-Paulo, A., and Ramalho, M. T. (2004). "Characterization of azo reduction activity in a novel ascomycete yeast strain." *Appl. Environ. Microbiol.,* 70(4), 2279–2288.

Ramalho, P. A., Paiva, S., Cavaco-Paulo, A., Casal, M., Cardoso, M. H., and Ramalho, M. T. (2005). "Azo reductase activity of intact Saccharomyces cerevisiae cells is dependent on the Fre1p component of plasma membrane ferric reductase." *Appl. Environ. Microbiol.,* 71(7), 3882–3888.

Ramalho, P. A., Scholze, H., Cardoso, M. H., Ramalho, M. T., and Oliveira-Campos, A. M. (2002). "Improved conditions for the aerobic reductive decolourisation of azo dyes by Candida zeylanoides." *Enzyme Microb. Technol.,* 31(6), 848–854.

Revankar, M. S., and Lele, S. S. (2007). "Synthetic dye decolorization by white rot

fungus, Ganoderma sp. WR-1." *Bioresour. Technol.*, 98(4), 775–780.

Rodriguez Couto, S. (2009). "Dye removal by immobilised fungi." *Biotechnol. Adv.*, 27(3), 227–235.

Sant'Anna, G. L. (1980). "Contribution à l'étude de l'hydrodynamique des réacteurs biologiques utilisés en traitement des eaux usées. INSA, Touslouse, France (model form cited from Kubsad et al., 2004)."

Saratale, R. G., Saratale, G. D., Chang, J. S., and Govindwar, S. P. (2011a). "Bacterial decolorization and degradation of azo dyes: A review." *J. Taiwan Inst. Chem. Eng.*, 42(1), 138–157.

Saratale, R. G., Saratale, G. D., Chang, J. S., and Govindwar, S. P. (2011b). "Decolorization and Degradation of Reactive Azo Dyes by Fixed Bed Bioreactors Containing Immobilized Cells of Proteus vulgaris NCIM-2027." *Biotechnol. Bioprocess Eng.*, 16(4), 830–842.

Saratale, R. G., Saratale, G. D., Kalyani, D. C., Chang, J. S., and Govindwar, S. P. (2009). "Enhanced decolorization and biodegradation of textile azo dye Scarlet R by using developed microbial consortium-GR." *Bioresour. Technol.*, 100(9), 2493–2500.

Sarkar, S., Banerjee, A., Halder, U., Biswas, R., and Bandopadhyay, R. (2017). "Degradation of synthetic azo dyes of textile industry: a sustainable approach using microbial enzymes." *Water Conserv. Sci. Eng.*, 2(4), 121–131.

Sassi, G., Ruggeri, B., Bosco, F., and Specchia, V. (1996). "Relaxation time analysis of a rotating biological contactor." *Chem. Eng. Sci.*, 51(11), 2853–2858.

Selvakumar, D., and Kumar, V. N. (2007). "Effect of rotatinal speed of disc for treating sugar and dairy effluent streams in rotating biological contactorsS." 23(2), 247–249.

Senan, R. C., Shaffiqu, T. S., Roy, J. J., and Abraham, T. E. (2003). "Aerobic degradation of a mixture of azo dyes in a packed bed reactor having bacteria-coated

laterite pebbles." *Biotechnol. Prog.*, 19(2), 647–651.

Senthilkumar, S., Perumalsamy, M., and Prabhu, H. J. (2014). "Decolourization potential of white-rot fungus Phanerochaete chrysosporium on synthetic dye bath effluent containing Amido black 10B." *J. Saudi Chem. Soc.*, 18(6), 845–853.

Shin, M., Nguyen, T., and Ramsay, J. (2002). "Evaluation of support materials for the surface immobilization and decoloration of amaranth by Trametes versicolor." *Appl. Microbiol. Biotechnol.*, 60(1–2), 218–223.

Sima, J., Pocedi, J., and Hasal, P. (2012). "Hydrodynamics of a Laboratory Scale Rotating Biological Contactor and its Application for Decolorization of Textile Dyes by White Rot Fungus Irpex lacteus." 27.

Šíma, J., Pocedi, J., and Hasal, P. (2012a). "Hydrodynamics of a Laboratory Scale Rotating Biological Contactor and its Application for Decolorization of Textile Dyes by White Rot Fungus Irpex lacteus." 27.

Sima, J., Pocedič, J., and Hasal, P. (2016). "Decolorization of Reactive Orange 16 in Rotating Drum Biological Contactor." *J. Environ. Chem. Eng.*, 4(4), 4540–4548.

Šíma, J., Pocedič, J., Roubíčková, T., and Hasal, P. (2012b). "Rotating drum biological contactor and its application for textile dyes decolorization." *Procedia Eng.*, 42, 1579–1586.

Singh, S. N. (2014). *Microbial degradation of synthetic dyes in wastewaters*. Springer.

Singh, S. N., Mishra, S., and Jauhari, N. (2015). "Degradation of anthroquinone dyes stimulated by fungi." *Microb. Degrad. Synth. Dye. Wastewaters*, Springer, 333–356.

Sirianuntapiboon, S. (2006). "Treatment of wastewater containing Cl2 residue by packed cage rotating biological contactor (RBC) system." *Bioresour. Technol.*, 97(14), 1735–1744.

Sirivat, A. (1991). "Stability experiment of flow between a stationary and a rotating disk." *Phys. Fluids A Fluid Dyn.*, 3(11), 2664–2671.

REFERENCES

Soares, G. M. B., Miranda, T., Campos, A. M. F. O., Hrdina, R., Ferreira, M. C., and Amorim, M. T. P. de. (2004). "Current situation and future perspectives for textile effluent decolourisation." *Enzyme*, 1–8.

Spadaro, J. T., Gold, M. H., and Renganathan, V. (1992). "Degradation of azo dyes by the lignin-degrading fungus Phanerochaete chrysosporium." *Appl. Environ. Microbiol.*, 58(8), 2397–2401.

Srikattanaprom, S. S. and P. (2000). "Effects of SDS on Efficiency of Packed Cage." *Thammasat Int. J. Sc. Tech*, 5(3), 16–27.

Suga, K., and Boongorsrang, A. (1983). "A new model of mass transfer in a rotating disc contactor." *Chem. Eng. Sci.*, 39(4), 767–773.

Šuleková, M., Smrčová, M., Hudák, A., Heželová, M., and Fedorová, M. (2017). "Organic colouring agents in the pharmaceutical industry." *Folia Vet.*, 61(3), 32–46.

Surampalli, R. Y., and Baumann, E. R. (1997). "Role of supplemental aeration in improving overloaded first-stage RBC performance." *Water. Air. Soil Pollut.*, 98(1–2), 1–15.

Svobodová, K., Senholdt, M., Novotný, Č., and Rehorek, A. (2007). "Mechanism of Reactive Orange 16 degradation with the white rot fungus Irpex lacteus." *Process Biochem.*, 42(9), 1279–1284.

Tawfik, A., Temmink, H., Zeeman, G., and Klapwijk, B. (2006). "Sewage treatment in a rotating biological contactor (RBC) system." *Water. Air. Soil Pollut.*, 175(1–4), 275–289.

Taylor, P., Vaidya, R. N., and Pangarkar, V. G. (1985). "Hydrodynamics and mass transfer in a rotating biological contactor." *Chem. Eng. Commun.*, 39, 37–41.

Teixeira, P., Alves, M., and Oliveira, R. (2001). "Hydraulic characteristics of an anoxic rotating biological contactor: influence of biofilm." *Environ. Technol.*, 22(10), 1169–75.

REFERENCES

Teixeira, S. C. Æ. P., and Mota, Æ. R. O. Æ. M. (2008). "Rotating biological contactors : a review on main factors affecting performance." 155–172.

Tisa, F., Ramam, A. A. A., and Daud, W. M. A. W. (2014). "Basic Design of a Fluidized Bed Reactor for Wastewater Treatment Using Fenton Oxidation." *Int. J. Innov. Manag. Technol.*, 5(2), 93–98.

Urra, J., Sepúlveda, L., Contreras, E., and Palma, C. (2006). "Screening of static culture and comparison of batch and continuous culture for the textile dye biological decolorization by Phanerochaete chrysosporium." *Brazilian J. Chem. Eng.*, 23(3), 281–290.

Van't Riet, K. (1979). "Review of measuring methods and results in nonviscous gas-liquid mass transfer in stirred vessels." *Ind. Eng. Chem. Process Des. Dev.*, 18(3), 357–364.

Vijayaraghavan, K., and Yun, Y.-S. (2007). "Utilization of fermentation waste (Corynebacterium glutamicum) for biosorption of Reactive Black 5 from aqueous solution." *J. Hazard. Mater.*, 141(1), 45–52.

Vitor, V., and Corso, C. R. (2008). "Decolorization of textile dye by Candida albicans isolated from industrial effluents." *J. Ind. Microbiol. Biotechnol.*, 35(11), 1353–1357.

Weber, E. J., and Lee Wolfe, N. (1987). "Kinetic studies of the reduction of aromatic azo compounds in anaerobic sediment/water systems." *Environ. Toxicol. Chem. An Int. J.*, 6(12), 911–919.

Wesenberg, D., Kyriakides, I., and Agathos, S. N. (2003). "White-rot fungi and their enzymes for the treatment of industrial dye effluents." *Biotechnol. Adv.*, 22(1–2), 161–187.

Wuhrmann, K., Mechsner, K. L., and Kappeler, T. H. (1980). "Investigation on rate—Determining factors in the microbial reduction of azo dyes." *Eur. J. Appl. Microbiol.*

Biotechnol., 9(4), 325–338.

Xingzu, W., CHENG, X., Dezhi, S. U. N., and Qi, H. (2008). "Biodecolorization and partial mineralization of Reactive Black 5 by a strain of Rhodopseudomonas palustris." *J. Environ. Sci.*, 20(10), 1218–1225.

Yamane, T., and Yoshida, F. (1972). "Absorption in a rotating-disk gas-liquid contactor." *J. Chem. Eng. Japan*, 5(4), 381–385.

Yamjala, K., Nainar, M. S., and Ramisetti, N. R. (2016). "Methods for the analysis of azo dyes employed in food industry–a review." *Food Chem.*, 192, 813–824.

Yan, H., and Pan, G. (2004). "Increase in biodegradation of dimethyl phthalate by Closterium lunula using inorganic carbon." *Chemosphere*, 55(9), 1281–1285.

Yang, F.-C., and Yu, J.-T. (1996). "Development of a bioreactor system using an immobilized white rot fungus for decolorization." *Bioprocess Eng.*, 15(6), 307–310.

Yang, H.-Y., He, C.-S., Li, L., Zhang, J., Shen, J.-Y., Mu, Y., and Yu, H.-Q. (2016). "Process and kinetics of azo dye decolourization in bioelectrochemical systems: effect of several key factors." *Sci. Rep.*, 6(April), 27243.

Yang, Q., Li, C., Li, H., Li, Y., and Yu, N. (2009a). "Degradation of synthetic reactive azo dyes and treatment of textile wastewater by a fungi consortium reactor." *Biochem. Eng. J.*, 43(3), 225–230.

Yang, Q., Li, C., Li, H., Li, Y., and Yu, N. (2009b). "Degradation of synthetic reactive azo dyes and treatment of textile wastewater by a fungi consortium reactor." *Biochem. Eng. J.*, 43(3), 225–230.

Yang, Q., Yang, M., Pritsch, K., Yediler, A., Hagn, A., Schloter, M., and Kettrup, A. (2003). "Decolorization of synthetic dyes and production of manganese-dependent peroxidase by new fungal isolates." *Biotechnol. Lett.*, 25(9), 709–713.

Yesilada, O., Asma, D., and Cing, S. (2003). "Decolorization of textile dyes by fungal pellets." *Process Biochem.*, 38(6), 933–938.

REFERENCES

Young seek park, Jong won yun, D. seog kim. (1998). “Wastewater treatment n a packed-bed reactor with immobilized cells onto a new ceramic carrier.” Biotechnology techniques.

Yu, G., Wen, X., Li, R., and Qian, Y. (2006). “In vitro degradation of a reactive azo dye by crude ligninolytic enzymes from nonimmersed liquid culture of Phanerochaete chrysosporium.” *Process Biochem.*, 41(9), 1987–1993.

Yum, K.-J., and Peirce, J. J. (1998). “Biodegradation kinetics of chlorophenols in immobilized-cell reactors using a white-rot fungus on wood chips.” *Water Environ. Res.*, 70(2), 205–213.

Zahmatkesh, M., Tabandeh, F., and Ebrahimi, S. (2010). “Biodegradation of Reactive Orange 16 By Phanerochaete Chrysosporium Fungus : Application in a.” *Iran. J. Environ. Heal. Sci. Eng*, 7(5), 385–390.

Zee, F. P. Van der, Lettinga, G., and Field, J. A. (2001). “Azo dye decolourisation by anaerobic granular sludge.” *Chemosphere*, 44(5), 1169–1176.

Zee, F. P. Van der, and Villaverde, S. (2005). “Combined anaerobic–aerobic treatment of azo dyes—a short review of bioreactor studies.” *Water Res.*, 39(8), 1425–1440.

Zeevalkink, J. A., Kelderman, P., and Boelhouwer, C. (1978). “Liquid film thickness in a rotating disc gas-liquid contactor.” *Water Res.*, 12(8), 577–581.

Zeevalkink, J. A., Kelderman, P., Visser, D. C., and Boelhouwer, C. (1979). “Physical mass transfer in a rotating disc gas-liquid contactor.” *Water Res.*, 13(9), 913–919.

Zhan, C., Hagrot, E., Brandt, L., and Chotteau, V. (2019). “Study of hydrodynamics in wave bioreactors by computational fluid dynamics reveals a resonance phenomenon.” *Chem. Eng. Sci.*, 193, 53–65.

Zhang, F., and Yu, J. (2000). “Decolourisation of Acid Violet 7 with complex pellets of white rot fungus and activated carbon.” *Bioprocess Eng.*, 23(3), 295–301.

Zheng, Z., and Obbard, J. P. (2002). “Removal of surfactant solubilized polycyclic

aromatic hydrocarbons by Phanerochaete chrysosporium in a rotating biological contactor reactor." *J. Biotechnol.*, 96(3), 241–249.

Zhong, J. J. (2010). "Recent advances in bioreactor engineering." *Korean J. Chem. Eng.*, 27(4), 1035–1041.

APPENDICES

Appendix: A

Table A1.: Properties of granular activated carbon

Iodine Number	mg/L	1000 min
Ash Content	%	4.0 max
Apparent Density	g/mL	0.45 to 0.55
pH		8 to 10
Over size tolerance	%	5.0 max
Undersize tolerance	%	5.0 max
Moisture as packed	%	5.0 max
Ball Pan Hardness Number		96

Table A2. Potassium dichromate calibration.

Sr. No	**Concentration mg/L**	**Conductivity (µs)**
1	0	0
2	1	3
3	2	4
4	3	5
5	4	6
6	5	7
7	6	8
8	7	9
9	8	10
10	9	11

Figure A1: Plot of Potassium dichromate concentration vs conductivity for Potassium dichromate calibration.

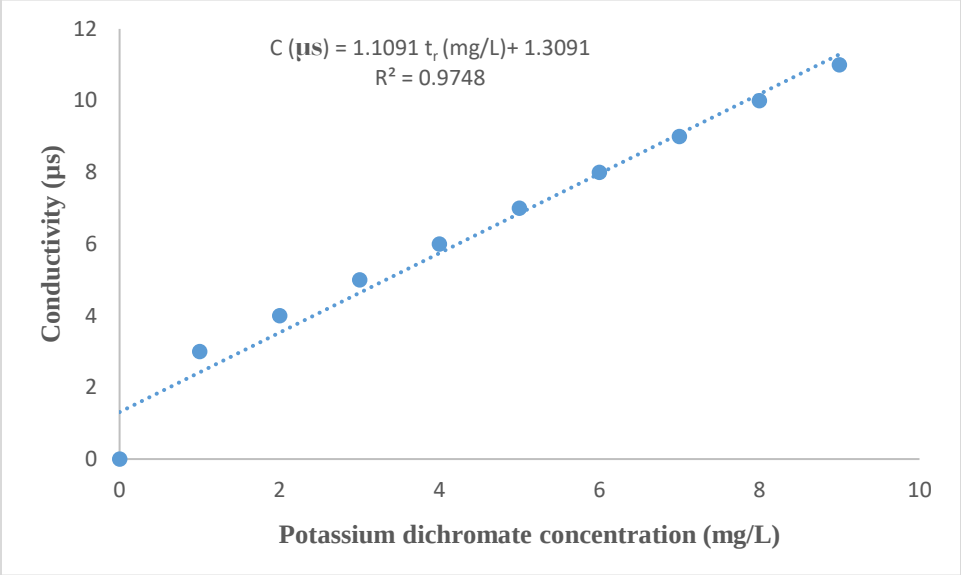

Figure A2. Standard curve for *P. chrysosporium* (a) and *T. Versicolor* (b) with different RB-5 concentration vs absorbance for RB-5 calibration.

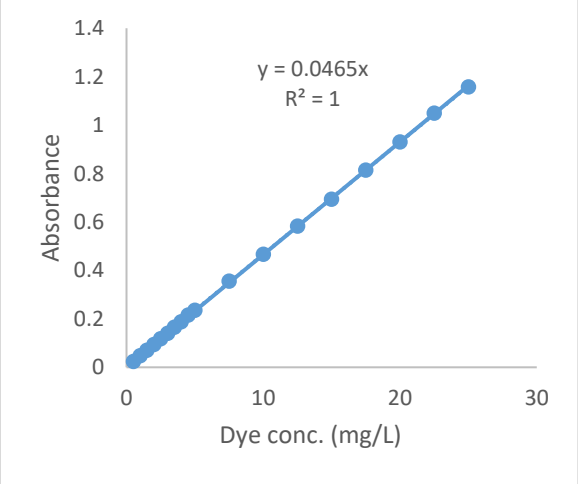

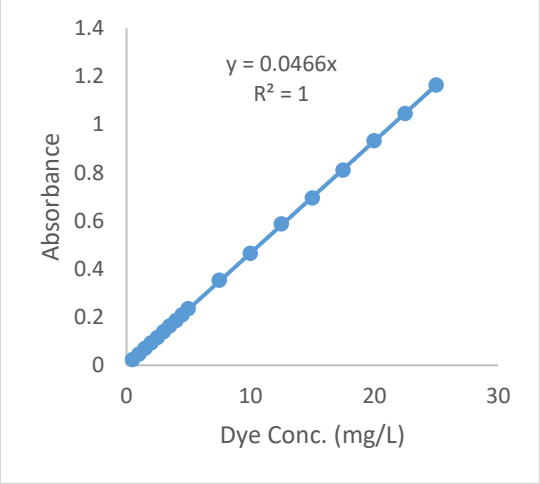

(a) (b)

Figure A3. Standard curve for methanol with different RB-5 concentration vs absorbance for RB-5 calibration.

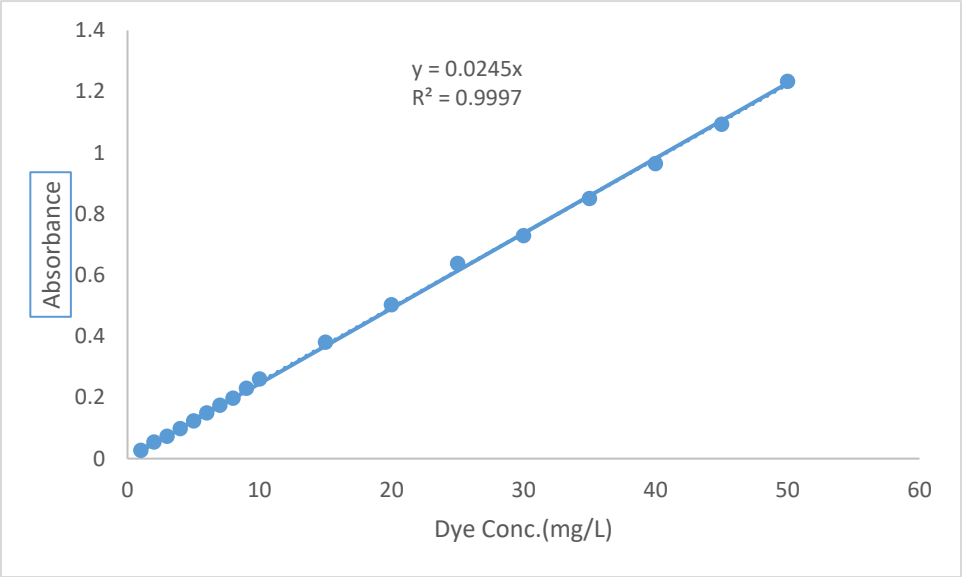

Appendix: B

LC-MS Analysis data:

Figure. B1. Molecular mass spectra of intermediate products obtained from *T. Versicolor* on 5th day.

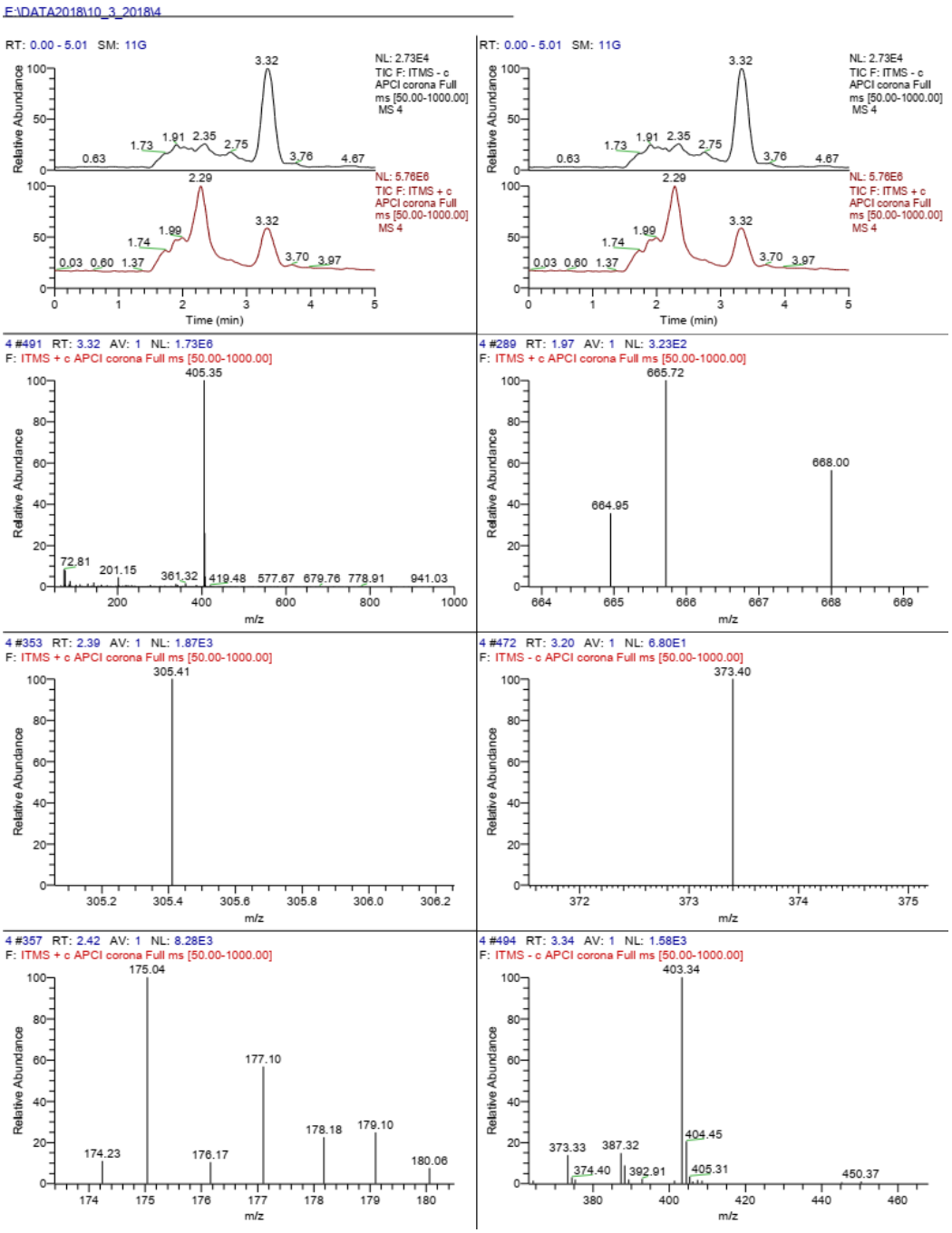

Figure. B2. Molecular mass spectra of intermediate products obtained from *P. Chrysosporium* on 5th day

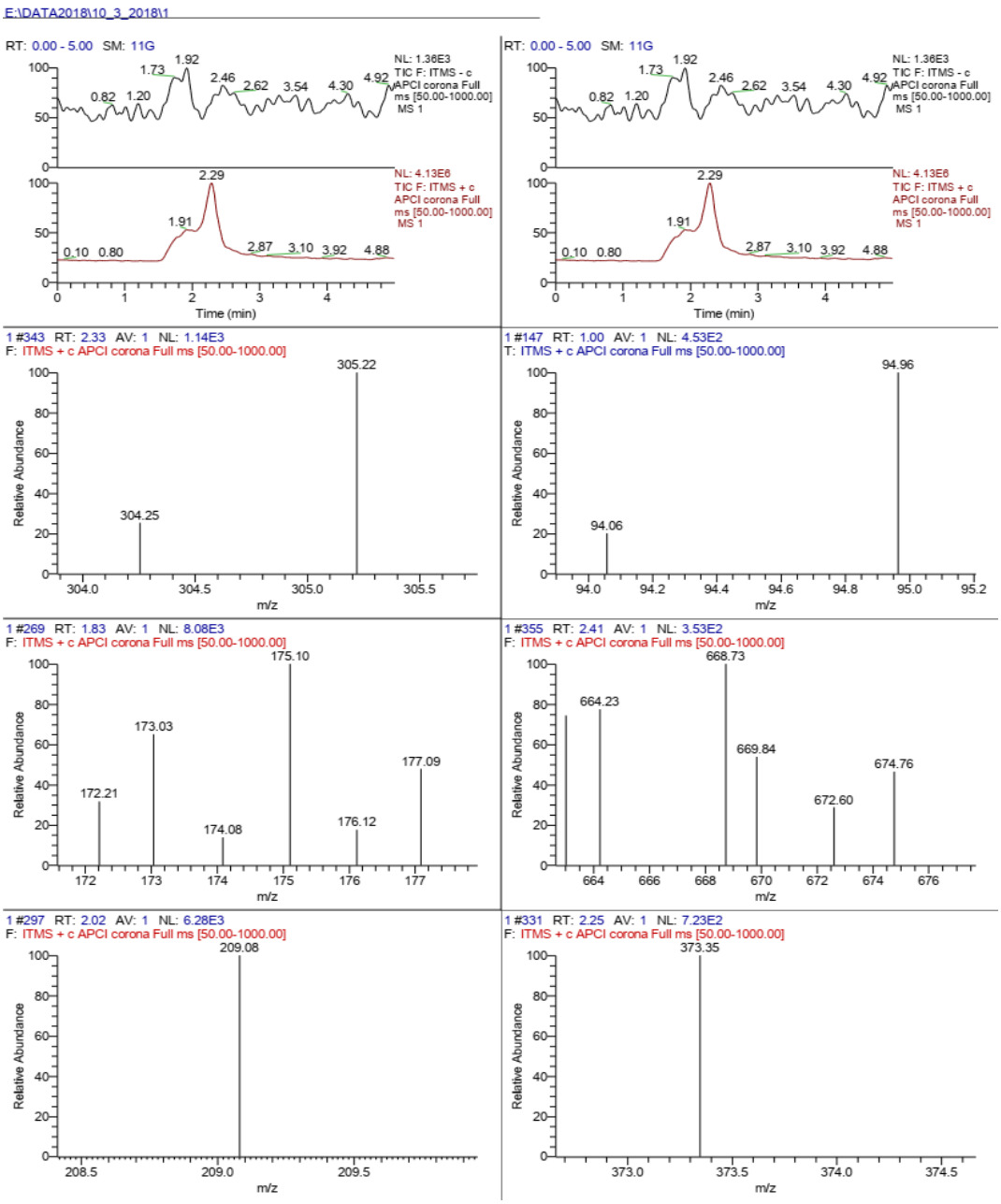

Table no B 1: Experimental parameter for RTD analysis for contactor 32.5 L and 65 L

For 32.5 L Reactor

Sr No	Number of disks(N)	Rotational speed (ω)	Recycle ratio (V_r / V_0)	Tau (min)	Mean (min)	Variance (min^2)	T/tau
1	2	10	9.75	730	371.6331	77765.228	0.50908643
2	2	10	9.75	730	395.4551	82370.138	0.54171931
3	2	20	9.75	730	404.6686	110580.5	0.55434054
4	2	20	9.75	730	454.63278	111662.5	0.62278463
5	3	10	9.75	730	402.0742	75215.2	0.550786575
6	3	10	9.75	730	416.5142	78524.61	0.570567397
7	3	15	9.75	730	440.782	99940.68	0.603810959
8	3	15	9.75	730	444.4928	100440	0.608894247
9	3	20	9.75	730	465.3611	101011.14	0.63748095
10	3	20	1.858	139.180	104.6232	5243.916	0.75171052
11	4	10	9.75	730	469.6293	122702.4	0.64332780
12	4	10	0.102	74.871	60.0505	1823.23	0.80204434
13	4	15	1	139.180	91.6439	4717.023	0.65845514
14	4	15	9.75	730	418.4767	85913.17	0.57325575
15	4	20	9.75	730	455.4066	94347.99	0.62384465
16	4	20	9.75	730	461.3141	105527.039	0.63193712
17	4	20	9.75	730	494.7383	382350.6	0.67772369
18	4	20	1.858	139.180	104.9417	6676.965	0.75399892

For 64 L Reactor

Sr no	No of paddles	Speed of rotation(ω) RPM	Recycle ratio	Tau	Mean Residence time(min)	Variance (min^2)	T/tau
1	4	6	9.75	730	371.6331	77765.2282	0.509086438
2	4	10	9.75	730	395.4551	82370.138	0.541719315
3	4	12	9.75	730	404.6686	110580.5	0.554340548
4	4	20	9.75	730	454.632785	111662.5	0.622784637
5	6	4	9.75	730	402.0742	75215.2	0.550786575
6	6	6	9.75	730	416.5142	78524.61	0.570567397
7	6	8	9.75	730	440.782	99940.68	0.603810959
8	6	10	9.75	730	444.4928	100440	0.608894247
9	6	12	9.75	730	465.3611	101011.14	0.637480959
10	6	10	1.858	139.18	104.6232	5243.916	0.751710526
11	6	20	9.75	730	469.6293	122702.4	0.643327808
12	6	6	0.102	74.871	60.0505	1823.23	0.80204434
13	6	6	1	139.18	91.6439	4717.023	0.65845514
14	8	6	9.75	730	418.4767	85913.17	0.57325575
15	8	10	9.75	730	455.4066	94347.99	0.62384465
16	8	15	9.75	730	461.3141	105527.03	0.63193712
17	8	20	9.75	730	494.7383	382350.6	0.67772369
18	8	10	1.858	139.18	104.9417	6676.965	0.75399892

APPENDICES

RESEARCH PUBLICATIONS

Patent:

Keyur Raval, **Rohit P. Kalnake**, and D. V. R. Murthy granted an Indian Patent having the title "ROTATING PACKED DISC BIOREACTOR". The application Number is 201841000694 and published dated 23rd November 2020.

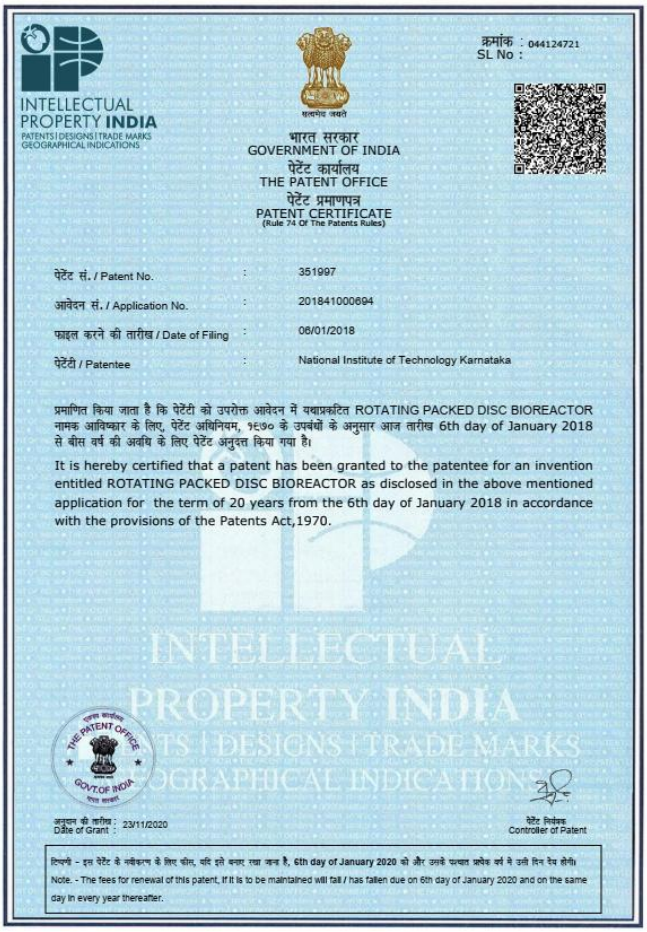

INTELLECTUAL PROPERTY INDIA
PATENTS | DESIGNS | TRADE MARKS
GEOGRAPHICAL INDICATIONS

क्रमांक : 044124721
SL No :

सत्यमेव जयते

भारत सरकार
GOVERNMENT OF INDIA
पेटेंट कार्यालय
THE PATENT OFFICE
पेटेंट प्रमाणपत्र
PATENT CERTIFICATE
(Rule 74 Of The Patents Rules)

पेटेंट सं. / Patent No.	:	351997
आवेदन सं. / Application No.	:	201841000694
फाइल करने की तारीख / Date of Filing	:	08/01/2018
पेटेंटी / Patentee	:	National Institute of Technology Karnataka

प्रमाणित किया जाता है कि पेटेंटी को उपरोक्त आवेदन में यथाप्रकटित ROTATING PACKED DISC BIOREACTOR नामक आविष्कार के लिए, पेटेंट अधिनियम, १९७० के उपबंधों के अनुसार आज तारीख 6th day of January 2018 से बीस वर्ष की अवधि के लिए पेटेंट अनुदत्त किया गया है।

It is hereby certified that a patent has been granted to the patentee for an invention entitled ROTATING PACKED DISC BIOREACTOR as disclosed in the above mentioned application for the term of 20 years from the 6th day of January 2018 in accordance with the provisions of the Patents Act,1970.

INTELLECTUAL PROPERTY INDIA
TS | DESIGNS | TRADE MARKS
OGRAPHICAL INDICATIONS

THE PATENT OFFICE GOVT.OF INDIA

अनुदान की तारीख : 23/11/2020
Date of Grant :

पेटेंट नियंत्रक
Controller of Patent

टिप्पणी - इस पेटेंट के नवीकरण के लिए फीस, यदि इसे बनाए रखा जाना है, 6th day of January 2020 को और उसके पश्चात प्रत्येक वर्ष में उसी दिन देय होगी।
Note. - The fees for renewal of this patent, if it is to be maintained will fall / has fallen due on 6th day of January 2020 and on the same day in every year thereafter.

Publications from this work:

1. **Kalnake, R. P**., Murthy, D. V. R., Achar, A., & Raval, K. (2020). Residence Time Distribution Studies in a Modified Rotating Packed Disc Contactor: Mathematical Modeling and Validation. *International Journal of Chemical Reactor Engineering, 1* ISSN-1542-6580 Vol.18- 4.

2. **Rohit. P. Kalnake**, D.V.R. Murthy, Keyur Raval. (2020). "Enhancement of the oxygen transfer rate in a modified rotating packed disc bioreactor. (Submitted)
3. **Rohit P. Kalnake**, Keyur Raval, John Robert, D. V. R. Murthy. "Enhanced degradation of azo dye using mixed cultures of white-rot fungi in a modified rotating packed disc bioreactor. (Submitted)

Conference:

1. **Rohit P. Kalnake,** John Robert, Keyur Raval, D. V. R. Murthy (2018). "A novel mixed culture method for total organic carbon reduction of synthetic dye waste water." Advances and challenges for sustainable ecosystem (ICACSE 6^{th} – 8^{th} December,2018), National Institute of Technology, Tiruchirappalli, India.
2. **Rohit P. Kalnake,** Keyur Raval, John Robert, D. V. R. Murthy (2018). "Continuous treatment of reactive black-5 using immobilized mixed culture in a rotating biological contactor"." National Symposium on Environmental Pollution Prevention and Control: Future perspective (EPPC: FP.:2019) to be held during 23-25 August 2019 at NITK Surathkal.

BIO-DATA

Rohit Purushottam Kalnake

Email ID: rohitkalnake@gmail.com

Contact no: +919096899826

Personal Details:

Name	**:** Rohit P. Kalnake
Father's name	**:** Purushottam Kalnake
Date of birth	**:** 7th November, 1989
Gender	**:** Male
Nationality	**:** Indian
Permanent Address	**:** Rohit P. Kalnake Behind Railway Station, Sausar Th: Sausar, Distt: Chhindwara Madhya Pradesh 480406

Educational qualification:

- **Pursuing PhD (July 2015 – December 2020)**
  National Institute of Technology Karnataka, Surathkal.
- **M. Tech (Chemical Engineering) 2013**
  Laxminarayan Institute of Technology, Nagpur, Maharashtra; 65.47%.
- **B. Tech (Chemical Engineering) 2011**
  Anuradha Engineering College, Maharashtra; 67.15%

Paper Publications – 4

Patent - 1

Declaration:

I hereby declare that the above written particular are true to the best of my knowledge.

Place: Surathkal **Rohit P. Kalnake**

Date: 00/07/2021